UNIVERSIDADE FEDERAL DO CEARÁ
CENTRO DE TECNOLOGIA
DEPARTAMENTO DE ENGENHARIA HIDRÁULICA E AMBIENTAL
PROGRAMA DE PÓS-GRADUAÇÃO EM ENGENHARIA CIVIL: SANEAMENTO AMBIENTAL

ANDRÉ MADSON ARAÚJO FROTA

PRODUCTION, CHARACTERIZATION AND ASSESSMENT OF SLUDGE-DERIVED BIOCHAR FOR WATER TREATMENT AS A SUSTAINABLE SOLUTION TOWARDS A CIRCULAR ECONOMY

FORTALEZA
2023

ANDRÉ MADSON ARAÚJO FROTA

PRODUCTION, CHARACTERIZATION AND ASSESSMENT OF SLUDGE-DERIVED BIOCHAR FOR WATER TREATMENT AS A SUSTAINABLE SOLUTION TOWARDS A CIRCULAR ECONOMY

Dissertação apresentada ao Programa de Pós-graduação em Engenharia Civil: Recursos Hídricos, do Departamento de Engenharia Hidráulica e Ambiental, da Universidade Federal do Ceará, como requisito parcial à obtenção do título de Mestre em Engenharia Civil. Área de concentração: Saneamento Ambiental.

Orientador: Prof. Dr. José Capelo Neto
Coorientadora: Profª. Dra. Tannaz Pak

FORTALEZA

2023

Dados Internacionais de Catalogação na Publicação
Universidade Federal do Ceará
Sistema de Bibliotecas
Gerada automaticamente pelo módulo Catalog, mediante os dados fornecidos pelo(a) autor(a)

F961p Frota, Andre Madson Araujo.
Production, characterization and assessment of sludge-derived biochar for water treatment as a sustainable solution towards a circular economy / Andre Madson Araujo Frota. – 2023.
107 f. : il. color.

Dissertação (mestrado) – Universidade Federal do Ceará, Centro de Tecnologia, Programa de Pós-Graduação em Engenharia Civil: Saneamento Ambiental, Fortaleza, 2023.
Orientação: Prof. Dr. Jose Capelo Neto.
Coorientação: Profa. Dra. Tannaz Pak.

1. Biochar. 2. Sludge. 3. Pyrolysis. 4. Water treatment. I. Título.

CDD 628

ANDRÉ MADSON ARAÚJO FROTA

PRODUCTION, CHARACTERIZATION AND ASSESSMENT OF SLUDGE-DERIVED BIOCHAR FOR WATER TREATMENT AS A SUSTAINABLE SOLUTION TOWARDS A CIRCULAR ECONOMY

Dissertação apresentada ao Programa de Pós-graduação em Engenharia Civil: Recursos Hídricos, do Departamento de Engenharia Hidráulica e Ambiental, da Universidade Federal do Ceará, como requisito parcial à obtenção do título de Mestre em Engenharia Civil. Área de concentração: Saneamento Ambiental.

Orientador: Prof. Dr. José Capelo Neto
Coorientadora: Profª. Dra. Tannaz Pak

Aprovado em: 07 / 02 / 2023

BANCA EXAMINADORA

_____

Prof. Dr. José Capelo Neto (Orientador)
Universidade Federal do Ceará (UFC)

_____

Profª. Dra. Tannaz Pak
Teesside University (TU)

_____

Prof. Dr. Erdin Ibraim
University of Bristol

AGRADECIMENTOS

À CNPq, pelo apoio financeiro com a manutenção da bolsa de auxílio.

À minha avó, Antônia Marlene Frota, por todo o amor, carinho e esforços dedicados a mim, sempre provendo da melhor maneira para que pudesse encarar e vencer os desafios diários desta jornada e à minha mãe, Lucina Alves de Araújo, por todo o auxílio, amor e compreensão investidos em mim.

Ao meu orientador, Prof. Dr. José Capelo Neto, por ter me orientado durante a produção deste trabalho, sempre de forma responsável, solícita e atenciosa, compartilhando de suas experiências e vivências nos âmbitos profissionais e acadêmicos, características fundamentais que o tornam um profissional exemplar.

À Profª. Dra. Tannaz Pak, pela colaboração para que este trabalho acontecesse, bem como pela oportunidade de fazer parte do MAGIC project, que foi uma experiência enriquecedora e bastante proveitosa para minha vida pessoal e acadêmica.

A todos os colaboradores Profª. Mona Lisa, Prof. Thiago, Profª. Cássia, Prof. Odair, Dra. Naiara, e profissionais da CAGECE. Todos nos auxiliaram em todas as etapas da pesquisa, tornando a execução deste trabalho possível.

Aos colegas do Selaqua por toda a ajuda durante os experimentos, em especial à Stefany e Kelly que sempre se prontificaram para ajudar nos experimentos e me ajudaram a tocá-los.

À Thaís e Kamila, amigas que me orientaram e colaboraram com o desenvolvimento do projeto, além das conversas e apoio dado durante tempos difíceis. À Karla Monique, por toda a ajuda, desde a preparação para o processo seletivo de ingresso até os dias atuais, compartilhando conhecimento e palavras de conforto nos momentos difíceis.

Ao Louis por toda a paciência e ajuda com a revisão dos artigos, pelo o apoio nos momentos difíceis e as palavras de incentivo.

À minha família e amigos que sempre me apoiaram e se esforçaram para que eu conquistasse meus objetivos durante essa jornada.

“Um passo a frente e você já não está mais no mesmo lugar.” (Chico Science).

RESUMO

Com o crescente aumento populacional e o aumento da poluição dos corpos hídricos, problemas relacionados à eutrofização tem se tornado mais comuns em todo o mundo. As florações de cianobactérias – organismos potencialmente capazes de liberar cianotoxinas prejudiciais aos ecossistemas aquáticos e à saúde humana – são um risco associado à esse fenômeno. Uma das tecnologias comumente utilizadas para remoção desses contaminantes é o carvão ativado. Entretanto, seu emprego encarece o processo de tratamento de água e aumenta a produção de lodo nas estações de tratamento de água – ETAs, logo, tal prática pode se tornar inviável sob o aspecto econômico e ambiental. Um material promissor para adsorção em meios líquidos é o biochar. Inicialmente, na primeira parte desta pesquisa, através de uma revisão sistemática, foi encontrado que propriedades como a área superficial, quando considerada sozinha, não é um bom indicador de capacidade de adsorção. É necessário avaliar uma combinação das propriedades do adsorvato, adsorvente e solução aquosa para a seleção correta de PAC ou biocarvão. No geral, embora carvão ativado tenha sido amplamente utilizado para a remoção de cianotoxinas, não há dados suficientes disponíveis e poucos estudos foram realizados para diferentes toxinas, uma vez que a maioria se concentra em MC-LR. Já para o biochar, as lacunas de conhecimento são ainda maiores. Na segunda parte desta pequisa, após a produção e caracterização do biochar derivado de lodo de ETA, foi encontrado que o aumento da temperatura afetou negativamente o rendimento do biochar, que diminuiu de 37,5 para 33,5 % conforme a temperatura aumentou de 450 para 600 ºC. A amostra de lodo seco apresentou pH 5,6 e, à medida que a temperatura de pirólise aumentou de 450 para 600 ºC, o pH do biochar aumentou de 6,6 para 6,9. O BC600, produzido a uma maior temperatura, apresentou uma área superficial maior (66,54 m^2/g) do que o BC450 (43,18 m^2/g). Após a ativação química, o biochar ativado (BC600A) apresentou um aumento substancial em sua área superficial, chegando a 2.000 m^2/g. Além disso, a ativação química resultou na diminuição do potencial zeta. A alta fração mineral no lodo resultou em um biochar rico em cinzas (61-71%) e com baixo teor de carbono (0,2-1,4%), atribuindo, assim, mais características inorgânicas do que orgânicas ao material. O biochar produzido em temperatura mais elevada apresentou uma estrutura carbonácea mais desenvolvida típica de materiais adsorventes. Por último, a aplicação do biochar no processo de tratamento se mostrou pouco eficiencte para o tratamento de águas naturais, tendo pouco contribuído para com o processo de coagulação e adsorção. Dessa forma, o uso de biochar derivado lodo de ETA deve ser estudado adiante, para uma melhor

compreensão de suas características e possíveis modificações químicas ou físicas que possam melhoras suas propriedades enquanto adsorvente.

Palavras-chave: Cianotoxinas. Lodo. Pirólise. Biochar. Tratamento de água

ABSTRACT

Due to increasing population growth and increased pollution of water bodies, problems related to eutrophication have become more common around the world. Cyanobacteria blooms – organisms capable of releasing cyanotoxins harmful to aquatic ecosystems and human health – are a risk associated with this phenomenon. One of the technologies commonly used to remove these contaminants is activated carbon. However, its use makes the water treatment process more expensive and increases the production of sludge in water treatment plants (WTPs), so this practice can become unfeasible from an economic and environmental point of view. A promising material for adsorption in aqueous media is biochar. Initially, in the first part of this research, it was found through a systematic review that properties such as surface area, when considered alone, are not a good indicator of adsorption capacity. It is necessary to evaluate a combination of adsorbate, adsorbent and aqueous solution properties for the correct selection of PAC or biochar. Overall, although activated carbon has been widely used for cyanotoxin removal, not enough data are available, and few studies have been performed for different toxins, as most focus on MC-LR. As for biochar, the knowledge gaps are even greater. In the second part of this research, after the production and characterization of the biochar derived from DWT sludge, it was found that the increase in temperature negatively affected the biochar yield, which decreased from 37.5 to 33.5% as the temperature increased from 450 to 600°C. The dried sludge sample had a pH of 5.6 and, as the pyrolysis temperature increased from 450 to 600 ºC, the pH of the biochar increased from 6.6 to 6.9. BC600, produced at a higher temperature, had a larger surface area (66.54 m^2/g) than BC450 (43.18 m^2/g). After chemical activation, the activated biochar (BC600A) showed a substantial increase in surface area, reaching 2,000 m^2/g. Furthermore, chemical activation resulted in a decrease in the zeta potential. The high mineral fraction in the sludge resulted in biochar rich in ash (61-71%) and low in carbon (0.2-1.4%), thus attributing more inorganic than organic characteristics to the material. The biochar produced at a higher temperature showed a more developed carbonaceous structure typical of adsorbent materials. Finally, the application of biochar in the treatment process proved inefficient for the treatment of natural waters, having little contribution to the coagulation and adsorption process. Thus, the use of DWT sludge biochar should be studied further to better understand its characteristics and possible chemical or physical modifications that could improve its properties as an adsorbent.

Keywords: Cyanotoxins. Sludge. Pyrolysis. Biochar. Water treatment

LIST OF FIGURES

CHAPTER I

CHAPTER II

CHAPTER III

LIST OF TABLES

CHAPTER I

CHAPTER II

CHAPTER III

TABLE OF CONTENTS

1 GENERAL INTRODUCTION

One of the consequences of the growing world population and its environmental impacts is the acceleration of N and P entry rates into the biosphere. Such nutrients are essential for maintaining aquatic food chains and can positively affect water bodies. However, the adverse effects of excessive input of nutrients by human activities (anthropogenic eutrophication) often outweigh the positive aspects, often causing a reduction in water quality (WURTSBAUGH; PAERL; DODDS, 2019).

Wastewater release, agriculture and other anthropogenic activities usually overwhelm natural processes and substantially increase N and P concentrations (CARPENTER et al., 1998). Cyanobacterial blooms have been considered the worst aspect of anthropogenic eutrophication. Nutrient-enriched water bodies are especially prone to harmful blooms if they also have long residence times (low flushing rates), water temperatures periodically exceeding 20 °C, calm surface waters, and persistent vertical stratification (PAERL; OTTEN, 2013), such as the Brazilian semiarid reservoirs.

Many cyanobacteria produce toxins that can cause severe acute intoxication in mammals (including humans), affecting the hepatopancreatic, digestive, endocrine, dermal, and nervous systems (PAERL; OTTEN, 2013). Blooms are a particular concern for water utilities concerning providing potable water to a satisfactory standard. Some of the most common problems in water treatment plants due to blooms are increased demand for coagulant, difficulty in operation due to pH changes, disturbances in flocculation - particularly by excreted organic matter, overloading of sedimentation tanks as a result of increased of the coagulant dose – leading to algae transport, filter penetration and clogging, formation of the trihalomethane precursor (THM) and increased demand for chlorine (HENDERSON et al., 2008).

Conventional water treatment technologies (coagulation, flocculation, clarification, and filtration) or their variations (direct or double filtration) are ineffective in removing dissolved compounds from water, especially cyanotoxins and other dissolved secondary metabolites. Instead, other water treatment processes are often needed to introduce another barrier to consumers' protection (ABBAS et al., 2020; CHOW et al., 1999). Conventional methods of remediating persistent pollutants from aqueous and gaseous phases mainly employ chemical precipitation, ion exchange, adsorption (i.e. activated carbon), and membrane separation processes, among other techniques. These costly methods

often generate considerable chemical residues, which have no economic value (OLIVEIRA et al., 2017).

Biochar can remove various contaminants from aqueous solutions but is still an unexplored technology for drinking water treatment. Most of the literature to date has focused on applying biochar as a soil amendment, carbon sequestration, and reduction of greenhouse gas emissions (GWENZI et al., 2017). Biochar has been considered a potential substitute for activated carbon in environmental remediation and water treatment due to its low cost, relative abundance, and adsorption capacity (INYANG; DICKENSON, 2015). Using such materials in water treatment plants is crucial in regions such as the Brazilian semi-arid region, where water scarcity is a severe problem and concern about the quality and quantity of water resources is constant. In this context, developing new, more economical and sustainable technologies that guarantee a safe water supply for the population is essential.

Firstly, this master's dissertation aims to understand the properties of powdered activated carbons (PACs) and biochars produced from different feedstocks and clarify which physical and chemical properties play a major role in the adsorption of three types of cyanotoxins (microcystin-LR, saxitoxin, and cylindrospermopsin) In order to achieve that, a systematic review was carried out. Secondly, this study proposes a new technique for using drinking water treatment sludge as a feedstock for manufacturing biochar via pyrolysis. The main objectives were to characterize the composition and structural properties of the biochar and assess how these properties can influence biochar application in water treatment. Lastly, a jar test study was conducted to develop and assess models for removing colour, turbidity, chlorophyll-*a*, and UV_{254} as responses to produce high-quality drinking water. This explored the application of sludge biochar as an adsorbent and its efficiency on water treatment processes.

This master's thesis is organised into the following six parts:

1 – General introduction
2 – Chapter I presents the first paper entitled "Understanding the properties of activated carbon and biochar for the adsorption and removal of cyanotoxins: a systematic review."
3 – Chapter II presents the second paper entitled "Production and characterization of biochar from drinking water treatment sludge via pyrolysis for water treatment purposes."
4 – Chapter III presents the second paper entitled "Application and assessment of sludge-derived biochar in water treatment systems as a potentially sustainable solution toward a circular economy."
5 – General conclusion
6 – References of the General Introduction

CHAPTER I

Understanding the properties of activated carbon and biochar for the adsorption and removal of cyanotoxins: a systematic review

Understanding the properties of activated carbon and biochar for the adsorption and removal of cyanotoxins: a systematic review

André Madson Araújo Frota[1], Thaís Lopes Pinheiro[1], Erdin Ibraim[2], Tannaz Pak[3], José Capelo Neto[1]

[1]Federal University of Ceará, [2]University of Bristol, [3]Teesside University

ABSTRACT

Cyanotoxins pose a health threat when present in the water supply. Conventional water treatment processes are not effective in removing extracellular toxins. In order to achieve a secure water supply, advanced treatment techniques are usually applied. Powdered activated carbon (PAC) has been shown to be an effective adsorbent for removing such toxins. However, due to its high cost, alternative adsorbent materials need to be developed. Biochar is a potential adsorbent material that could replace PAC for removing toxins. This paper aimed at investigating which PAC properties play key roles in cyanotoxin adsorption. To achieve that, a systematic review addressing the adsorption of toxins such microcystins-LR (MC-LR), cylindrospermopsin (CYL), and saxitoxins (STXs) was carried out. As a result, the review showed that some commonly adopted indices are not relevant to cyanotoxin adsorption, specially if appraised by themselves, *i.e.* total surface area. Along with a multi-barrier approach, PAC has be applied taking account of the complexity of the water system, which includes a better understanding of the characteristics of the adsorbent, the target toxin and the aqueous medium. The biochar systematic review showed that no studies have yet designed biochar specifically for the removal of toxins. Overall, it was found that most studies do not focus on understanding PAC properties in cyanotoxins. For biochar, the knowledge gap is even greater since it a newer material.

Keywords: Activated carbon. Biochar. Cyanotoxins. Systematic review

2 INTRODUCTION

Due to the increasing frequency and intensity of cyanobacterial blooms, researchers began investigating technologies for removing cyanotoxins from water supplies. Most cyanotoxins are water-soluble; thus, remediation measures involve chemical procedures which reduce or remove toxins entirely from water (HITZFELD; HOGER; DIETRICH, 2000). Conventional treatment can eliminate algal cells and, therefore, the cell-bound cyanotoxin (in the particulate form), but many studies (FALCONER et al., 1989; HIMBERG et al., 1989; HOFFMANN, 1976; KEIJOLA et al., 1988) have shown that conventional techniques such as coagulation, sedimentation, and filtration are inefficient in removing extracellular soluble toxins from water (ALBUQUERQUE JR. et al., 2008; CAMPINAS; ROSA, 2006). In such cases, it may be necessary to employ advanced treatment methods, such as activated carbon (AC), membrane filtration, or oxidants, as a part of a multi-barrier approach (PIVOKONSKY et al., 2021). Such advanced methods add significantly to both the cost and complexity of the water treatment process (VELZEBOER et al., 1995).

Activated carbon can be defined as a network of interconnected pores of varying sizes which are classified according to their diameter in micropores (<2.0 nm), mesopores (2-50 nm), and macropores (>50 nm). The pores provide a large internal surface area to activated carbon, typically ranging from 800 to 1200 $m^2.g^{-1}$, enabling them to adsorb various contaminants from water (DONATI et al., 1994). In drinking water treatment, activated carbon is employed in two forms: powdered (PAC) to perform adsorption simultaneously with clarification or granular (GAC) in columns or beds to perform adsorption in percolation units (WARHURST et al., 1997). While activated carbon does not have any impact on cyanobacteria and intracellular toxins, it can be successfully applied to remove extracellular cyanotoxins such as microcystins (MCs), cylindrospermopsin (CYL), and saxitoxins (STXs) (MEREL et al., 2013). Several countries, including Canada, the USA, Australia, Great Britain, China, and Brazil, have reported that MC-LR contamination has negatively affected human and animal health. The World Health Organization (WHO) has set the recommended level of MC-LR-equivalent in drinking water to 1.0 $\mu g.L^{-1}$ (DROGUI et al., 2012). Generally, PAC has demonstrated the removal of toxins to concentrations below WHO guidelines (LAMBERT; HOLMES; HRUDEY, 1996).

Among the advanced water treatment methods, adsorption is advantageous in contrast to alternative methods because of its affordability and design simplicity for cyanotoxins removal (ABBAS et al., 2020). For dealing with taste and odour problems, for example, PAC is commonly applied due to its lower price than GAC, without requiring significant adaptations (retrofitting) or additional costs. Another advantage of PAC is that it can be used sporadically at varying doses relative to the actual current treatment requirements (DONATI et al., 1994) since cyanobacterial problems are of a transient, intermittent nature (HO et al., 2011), making PAC a better cost-effective option as it could be applied exclusively to a sole situation. However, its effectiveness depends on using the correct dose for each characteristic case in the water treatment plant. For example, a PAC overdose could achieve water devoid of toxicity, but the cost would gradually become high. On the other hand, an under-dose could compromise its effectiveness and result in potentially toxic water to consumers (COOK; NEWCOMBE, 2008).

In developing countries, where activated carbon is usually imported, the high cost can be a considerable disincentive against using activated carbon in water treatment. There is enormous potential for activated carbons to be produced from agricultural and industrial wastes within these countries (WARHURST et al., 1997). In Brazil, in 2004, the activated carbon import values reached approximately 3.2 thousand tons, translating to a cost of US$ 6.5 million. In 2012, this value was close to US$ 20 million (6.5 thousand tons). In 2013 it reached approximately 23.2 million dollars accounting for 7.5 thousand tons of activated carbon, thus leaving Brazil with a deficit in the trade balance for activated carbon (NOBRE et al., 2015). In this context, the need to develop technologies for producing high-quality activated carbons, preferably from low-cost raw materials, is clear to substitute these importations (ALBUQUERQUE JR. et al., 2008).

Biochar is the solid product of pyrolysis, a material rich in carbon obtained when the biomass is heated in a closed vessel with little or no air available at relatively low temperatures (<700 ° C) and which can be used for carbon sequestration, soil conditioning and pollution remediation (LEHMANN; JOSEPH, 2009; YIN et al., 2017). Various carbonaceous materials such as agricultural residues, algal biomass, forest residues, manures, activated sludge, energy crops, digestate, etc., can be used to produce biochar (OLIVEIRA et al., 2017). Biochar has been considered a potential substitute for activated carbon in environmental remediation and water treatment due to its inexpensiveness, relative abundance, and adsorption capacity (INYANG; DICKENSON, 2015). Since it is a porous-carbonaceous material and abundant in functional groups, biochar has been widely studied

as an adsorbent for the remediation of contaminants, including inorganic (heavy metals, ammonia, nitrate, phosphate, sulfide, etc) and organic pollutants (agrochemicals, antibiotics, polycyclic aromatic hydrocarbons (PAHs), polychlorinated biphenyls (PCBs), volatile organic compounds (VOCs) and aromatic dyes) and gases (LI; JIANG, 2017; OLIVEIRA et al., 2017). Biochars have an excellent ability to remove various contaminants from aqueous solutions but are still an unexplored technology for the treatment of drinking water. Most of the body of literature to date has focused on applying biochar as a soil amendment, for carbon sequestration, and for reducing greenhouse gas emissions (GWENZI et al., 2017). Therefore, knowledge about the practical application of biochar in water treatment operations, such as drinking water, is limited (INYANG; DICKENSON, 2015).

This paper aims to understand the properties of PACs produced from different feedstocks and clarify which physical and chemical properties play a major role in the adsorption of three types of cyanotoxins (microcystin-LR, saxitoxin, and cylindrospermopsin). Furthermore, given the need for cheaper and more sustainable adsorption materials, we aim to understand how current research on biochar production and its application, specifically for cyanotoxins removal from water, has been developed in the last decade, as it is a promising porous-carbonaceous material for adsorption of contaminants in aqueous solutions. Covering this knowledge gap will help understand the development of PAC in water treatment, which will benefit the water industry, decision-makers, and water company managers, further enhancing biochar studies for cyanotoxin adsorption.

3 METHODOLOGY

To achieve the objectives of this study, a systematic review was carried out following the Preferred Reporting Items for Systematic Reviews and Meta-Analyses (PRISMA) protocol (Figures 1 and 2). A systematic review is a review of a well-formulated question that uses systematic and explicit methods to identify, select, and critically appraise relevant research, and to collect and analyze data from the studies that are included in the review (MOHER et al., 2009). This type of study can provide researchers with an in-depth view of the past, enabling an overview of future research opportunities by identifying knowledge gaps.

Figure 1 – PRISMA flow of information through the different phases for the systematic review of PAC

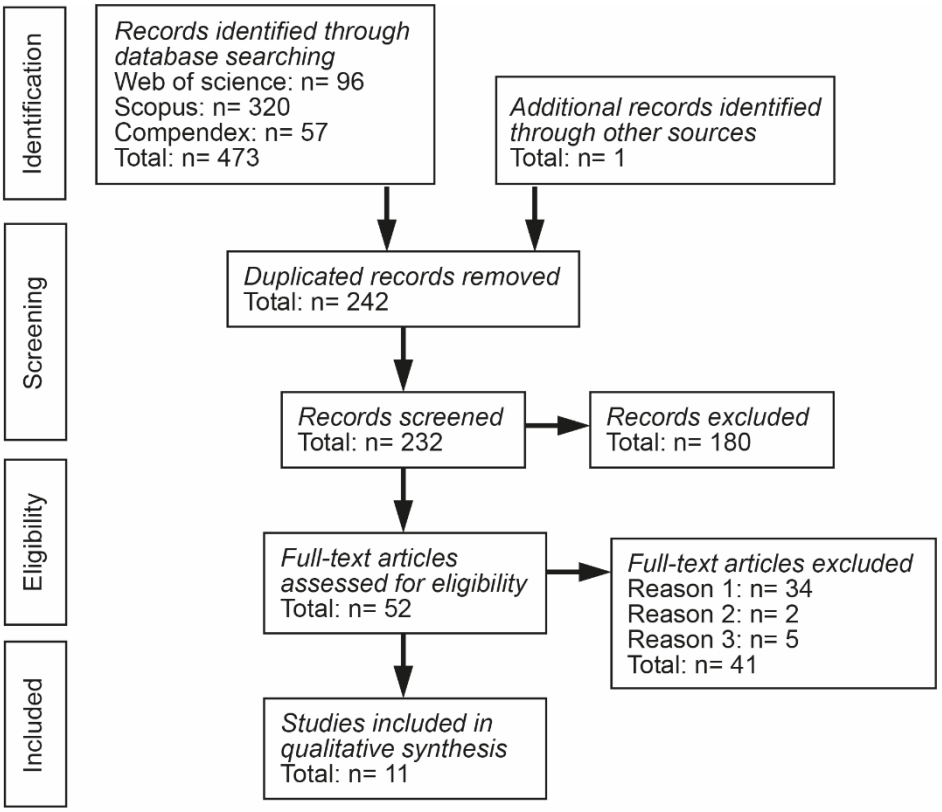

Different databases (Scopus, Web of Science, and Compendex) were searched using the combination of 8 keywords (cyanotoxin, algal toxin, MC-LR, saxitoxin, cylindrospermopsin, adsorption, activated carbon, and biochar) using the Boolean expressions AND and OR, so that the publications collected were on the specific topic of this research. The data were collected from August through September 2021, and only peer-reviewed journal papers written in English were considered. In the study eligibility phase, different criteria were considered: if the paper does not focus on the characteristics and properties of PAC and/or toxins (Reason 1), the paper is not available online (Reason 2), and it is a book chapter or review paper (Reason 3).

Figure 2 – PRISMA flow of information through the different phases for the systematic review of biochar

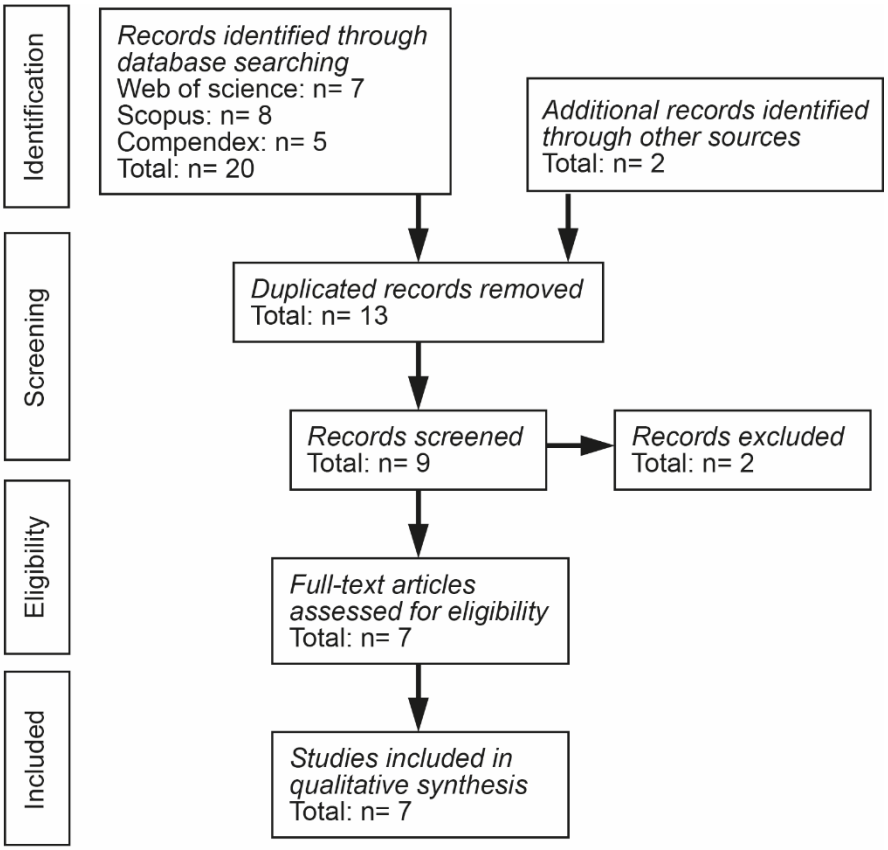

The PAC search retrieved a total of 473 studies, which were narrowed down to 13, as shown in the PRISMA flow diagram (Figure 1). As a systematic review is an iterative process, based on the references of the included studies, other papers not found in the search mechanisms mentioned above were added to this review under "Additional records identified through other sources". For the biochar search, filtering the search from 2010 to 2021, a total of 20 papers was obtained. These were then narrowed down to 7, as shown in the PRISMA flow diagram (Figure 2).

The quality assessment of all the papers found in this search was carried out using EndNote X9. Firstly, the duplicated papers were excluded from the retrieved results. Then, the title and abstract of the remaining papers were examined. After this, the papers that did not satisfy the inclusion criteria and/or were utterly unrelated studies were excluded (screening phase). In the final phase, the remaining studies were fully assessed for eligibility. The data was analysed, extracted, summarized, and discussed in the following sections.

4 ACTIVATED CARBONS

4.1 Starting material and PAC type

The internal structure of activated carbons and their pore size distribution depend on the starting material and the activation method. For example, wood-based carbon shows a regular system of pores, whereas coal-based carbon shows a random network of pores (DONATI et al., 1994). While studying the adsorption of microcystins onto activated carbon fibres (ACF), Albuquerque Jr. et al. (2008) found that the structures of activated carbon from macadamia nutshell, dried coconut shell endocarp, and unripe coconut mesocarp were more suitable for the production of microporous carbons, while sugar cane bagasse and pinewood residues were better suited to the production of mesoporous carbons (Table 1). Many authors have demonstrated in their studies that the type of PAC was shown to be an important factor for the efficient removal of geosmin and saxitoxins with a coal-based carbon shown to be superior to a wood-based carbon using waters from two different reservoirs (CAPELO-NETO; SILVA BUARQUE, 2016; COELHO et al., 2020; HO et al., 2009).

Many studies relating to the adsorption of cyanotoxins onto activated carbon have been carried out on microcystins, specially MC-LR (ALBUQUERQUE JR. et al., 2008; BAJRACHARYA; LIU; LENHART, 2019; COOK; NEWCOMBE, 2008; DONATI et al., 1994; HUANG; CHENG; CHENG, 2007; LEE; WALKER, 2006; ŞENGÜL; ERSAN; TÜFEKÇI, 2018). Some suggest that coal and wood-based carbons are the best options for microcystin adsorption due to their large mesopore volume (HO et al., 2011). Bajracharya et al. (2019), comparing the uptake of MC-LR to PAC versus time at pH of 8.5 in the presence of NOM, demonstrated that the wood and coal blend-based PAC showed significant differences in MC-LR adsorption. The adsorption rate onto the wood-based carbon was more rapid than that of the other PAC types. Their finding was consistent with previous studies (DONATI et al., 1994; HUANG; CHENG; CHENG, 2007), in which wood-based carbons reached equilibrium more rapidly than coal-based carbons due to the higher amount of mesopores in wood-based PACs compared to other PACs.

Albuquerque Jr. et al. (2008), comparing pore volume distribution results for coconut- and wood-based PAC (Table 1) to those obtained by Donati et al. (1994) and Pendleton et al. (2001), found that the pinewood PAC had a volume of secondary micropores of 0.35 $cm^3.g^{-1}$ and a volume of mesopores of 1.06 $cm^3.g^{-1}$, which represent an improvement in the group of available pores for the adsorption of complex molecules like MCs of about

93.15 %. As for the PAC obtained from the dried coconut shell endocarp, the material had a volume of secondary micropores of 0.28 $cm^3.g^{-1}$ and a volume of mesopores of 0.21 $cm^3.g^{-1}$, representing an increase of 172.22 % in the number of available pores compared to the studies above mentioned, showing, therefore, a correlation between the activated carbon porosity and the starting material.

Ho et al. (2009) found that coal-based PAC was shown to be the more effective carbon for removing saxitoxins. Again, this can be attributed to the different characteristics of the PACs, particularly the greater surface area and more microporous nature of coal-based PACs. Differences were observed in the adsorption of the individual saxitoxin variants, where the ease of adsorption of the variants by both PACs followed the trend: STX > GTX2 > GTX3 > C1 $\simeq$ C2. The adsorption trend also matches the toxicity; the most toxic variant (STX) is also the most easily removed by PAC, while the C-toxins are the most difficult to remove. The authors also present that a previous study reported similar adsorption trends using different PACs and attributed this to the variants' size, with greater removal for smaller molecular sizes. The authors also dismissed the notion that the charge of the variants may have influenced adsorption, with favourable adsorption using carbon with a high positive surface charge.

4.2 Particle size

In a study investigating the adsorption of cylindrospermopsin and microcystins from drinking water supplies, Ho et al. (2011) obtained results that suggested that the PACs used had a wide range of pores which could balance the influence of water quality, in particular the presence of natural organic matter (NOM). The most contrasting characteristic between the coal-based PACs was the effective particle size, ranging from 20-25 μm to 10 μm (Table 1). The authors also argued that, even though previous studies had shown that the adsorption equilibrium of a microcontaminant is not affected by particle size, the particle size can influence the adsorption kinetics, with faster adsorption in smaller particle sizes. As confirmed in their results, when both PACs were ground down to the same particle size, a negligible difference in the removal of the cyanotoxins was observed between the PACs.

4.3 Elemental composition

From the data obtained for eight PACs, Donati et al. (1994) suggested that no significant relationship exists between the starting material and the surface composition. In contrast, the starting material appeared to be related to the type of impurity on the carbons. The X-ray photoelectron spectroscopy (XPS) data also showed that while carbon-to-oxygen ratios varied, there was no apparent relationship to the level of MC-LR adsorption, assuming that trace levels of impurities did not influence MC-LR adsorption.

Studying the properties of activated carbon, Pendleton et al. (1997) found that the surfaces of coconut-based carbons are less hydrophilic than wood-based carbons. That means, for more hydrophilic surfaces, there is a stronger interaction between the water molecules and the surface, making it difficult the displacement of the water molecules by the target contaminant. Adsorption of the relatively hydrophobic molecule shows that the solvent molecules (water) are more readily displaced from low oxygen-content activated carbons than those with high oxygen content (PENDLETON; SCHUMANN; WONG, 2001). Therefore, wood-based carbons show lower adsorption energies and, consequently, lower adsorption capacity for the target contaminants, such as MIB (2-methylisoborneol). From this study, the authors also suggested that selecting an appropriate carbon depends on its surface hydrophilicity, which can be determined via water adsorption or elemental analysis.

Table 1 includes the bulk oxygen content for each carbon. The wood-based carbons contained more oxygen than coconut-based carbons. In the different PACs used by Shi et al. (2012) for STX adsorption, their oxygen content increased in the following order: bituminous coal < wood < lignite coal. In their study, the carbon's oxygen content trend was inconsistent with the three carbons' STX removal trend. In that sense, the authors concluded that different factors, such as pH, PAC type, dosage, contact time, and NOM concentration, play different roles in adsorption efficiency for STX removal using PAC.

4.4 Surface functional groups and surface charge

Donati et al. (1994) argue that while it is suggested that characteristics such as charge and functional groups on the carbon surface and functional groups of the toxin molecule do not affect the adsorption of MC-LR, they do, however, affect the adsorption of natural organic matter (NOM) which may also contribute to competitive adsorption. A study

by Pendleton et al. (2001) showed that both the adsorbent surface chemistry and the primary micropore volume have virtually no influence on the amount of MC-LR adsorbed from ultrapure water. On the other hand, Huang et al. (2007) demonstrated that the functional groups on the carbon surface were an essential factor in its ability to adsorb MC-LR. The most common oxygenated groups on activated carbons surface are carboxylic acids, carbonyls, quinones, phenolic hydroxyls, anhydrides, ethers, lactones, and lactols (TOLES; MARSHALL; JOHNS, 1999). To investigate the effects of surface chemistry on MC-LR adsorption, Huang et al. (2007) modified the surface chemistry of wood carbon by thermal reduction at 550 ºC and 950 ºC. The reduced activated carbons had 6.9% and 4.2% oxygen content, respectively, whereas virgin wood carbon had a higher oxygen content of 11.5% (Table 1). While the oxygen content was reduced, the micro and mesopores showed almost no change. Therefore, the toxin was exposed to activated carbons with increased hydrophobic character but with the same volume available for adsorption. It was also found that an increased amount of carboxylic groups on the surface leads to increased water cluster formation, which could result in weaker dispersion interactions with organic adsorbates. The authors assumed that the influence of surface chemistry (i.e., oxygen content) applies at low adsorptive concentrations; thus, the amount adsorbed in virgin carbon was considerably lower than the two treated carbons. Another chemical characteristic the authors obtained regarded the surface chemical groups according to their acid-base character. At a fixed pH of 7.5, the authors found a good correlation between these groups and MC-LR adsorption. The virgin carbon possessed more basic groups and was more effective than acid-washed carbons. Data from these carbons indicated that the raw carbons contained more hydroxyl groups than the acid-washed carbons.

Shi et al. (2012) findings agree with the later results discussed above, suggesting that activated carbon surface chemistry, including the type and number of functional groups and pore structure, have been shown to play an important role in removing organic compounds in drinking water treatment. Experimental results obtained by Shi et al. (2012) showed that the sorption capacity for STX followed the trend: lignite-coal based < bituminous-coal based < wood-ash based. While this order of removal and sorption capacity corresponds with the order of BET surface areas (Table 1), normalization of the removal data to BET surface area showed that BET surface area accounted only for a part of the performance trend noted. Another significant factor was hypothesized to be related to the surface charge. The pH_{PZC} for wood-ash and bituminous-coal-based ACs (4.9 and 6.1, respectively) are less than the solution pH; hence, both PACs would have a net negative

charge at pH 8.2. The pH_{PZC} for lignite-coal based, however, was 10.9, and greater than solution pH so that the surface of lignite-coal based would have a net positive charge at pH 8.2. Because STX is approximately 75% cationic and 25% neutral at a pH of 8.2, STX would be expected to be repulsed by the lignite-coal-based surface and attracted to the bituminous-coal-based and wood-ash-based surfaces, which is consistent with the observed trend of lignite-coal based having the least STX removal.

Activated carbon's surface can exhibit either acidic or basic character. The former may be due to the presence of functional groups (i.e. carboxyls, phenols, lactones, and acid anhydrides), which dissociate to produce a negative surface charge. At the same time, the latter can be attributed to delocalized π-electrons of the basal planes, nitrogen functionalities, and surface oxygen-containing groups (i.e. pyrones, chromenes, diketones, and quinones), which accept protons from the solution and are responsible for the positive surface charge (PIVOKONSKY et al., 2021). Most activated carbons show a negative surface charge at high pH values (alkaline solutions) due to the presence of negatively charged carboxylate and anhydride anionic surface functional groups on their surface (HUANG; CHENG; CHENG, 2007). Non-electrostatic adsorption mechanisms most often control the removal of neutral organics from water via carbon adsorption in water treatment. However, when an organic compound has a cationic or anion character, it becomes more polar and may be poorly adsorbed by activated carbon via non-specific physisorption, while electrostatic mechanisms could be enhanced. Infrared spectroscopy data obtained for the wood-based carbons showed that the oxygen content was present in the adsorbent as hydroxyl, phenol, or lactol groups as well as ethers, carbonyls, quinones, and lactones. Since these activated carbons were chemically activated with phosphoric acid (Table 1), a proportion of the oxygen content was also attributed to surface phosphate groups. The coconut-based activated carbons, however, contained only ethers, carbonyls, quinones, and lactones functional groups, and no surface OH groups (PENDLETON; SCHUMANN; WONG, 2001). Albuquerque Jr. et al. (2008) verified that carbons obtained from different raw materials also presented the acid groups mentioned above on their surfaces. They can become ionized in water solution, producing H^+ ions; consequently, the pore surface of the activated carbon obtains negative charges.

4.5 Surface area and pore size distribution

Differences in pore structure and size distribution result in different adsorption properties. As reported by Donati et al. (1994), previous researchers studied the effect of pore size distribution on the adsorption of small taste and odour (T&O) compounds, such as 2-methylisoborneol (MIB). They reported that competitive adsorption between these small molecules and naturally occurring humic material depended on pore size distribution. They concluded that there is no correlation between the tendency of activated carbons to adsorb a particular compound and the commonly used adsorption capacity indexes such as molasses number, iodine number, phenol number, and surface area. The results found by Donati et al. (1994) showed that pore volume was strongly dependent on the starting material. The wood-based carbons had a larger micropore and mesopore volume than other carbons. The coconut and peat moss-based carbons had low mesopore volume, and the coal-based carbons lay somewhere in between (Table 1). Nonetheless, one of the coal-based PACs, which possessed a relatively high micropore and mesopore volume compared to other coal-based PACs, did not follow this pattern, possibly because of a different activation mode, as suggested by the authors. Donati et al. (1994) also showed that the wide-ranging MC-LR adsorption maxima for the PACs are directly related to the pore volume in the mesopore region. The wood-based PACs, the most effective MC-LR adsorbents, had the most significant mesopore volume (Table 1) compared with less effective PACs. There was little correlation between micropore volume and MC-LR adsorption.

Lee & Walker's (2006) findings are in agreement with the previous study, confirming that pore size distribution plays a vital role in MC-LR adsorption because this toxin, with an estimated diameter of 3 nm, is too large to enter micropores (< 2.0 nm) but adsorbs in mesopores (2-50 nm). The wood-based PAC used in this study had significant mesopore volume, while micropores dominated the coconut-based PAC. The total available surface area was unimportant, given that the wood-based carbon had a slightly lower specific surface area than the coconut-based carbon (Table 1). Therefore, wood-based PAC was more effective at removing MC-LR than coconut-based carbon primarily due to greater mesopore volume. Similarly, Huang et al. (2007) analyzed different activated carbons used at a water treatment plant, showing that PACs with the largest volume of mesopores and macropores adsorbed MC-LR to the most considerable extent. Pivokonsky et al. (2021) include that the adsorption efficiency of algal metabolites is given by the combination of the pore size distribution of the activated carbon rather than by the absolute surface area value. Algal

metabolites preferentially become trapped in the pores corresponding to their size because plenty of contact points are available between the contaminants' molecules and the PAC surface.

Ho et al. (2011) found that the removal of a wide range of molecular weight compounds increased with PAC dose, which was attributed to the pore structure of the PACs. Therefore, due to this observation, they implied that the type of NOM might not significantly influence the cyanotoxins' adsorption when using the tested PACs (Table 1), as their adsorbents contained a broad pore size distribution. It is also important to highlight that there is a consensus amongst most suppliers that a high specific surface area is important for removing a particular contaminant. Still, this assumption must be made with caution. Although an adsorbent may possess a high specific surface area (usually measured by nitrogen adsorption), the surface area available for the adsorption of a particular toxin may be pretty small due to molecular sieve effects (PENDLETON; SCHUMANN; WONG, 2001).

4.6 Molecular size of cyanotoxins

The adsorption characteristics of an adsorbent-adsorbate system also depend on the size of the adsorbate compounds. As previously discussed, when an activated carbon has less volume in the mesopore region, it cannot adsorb as much MC-LR as a highly mesoporous carbon because of the larger size of this cyanotoxin, which prevents it from entering smaller micropores (DONATI et al., 1994). Huang et al. (2007) argue that by reducing the pH, the electrostatic repulsion between neighbouring negatively charged sites is also decreased and is responsible for stretching out the MC-LR molecules, thus, reducing MC-LR size due to its tendency to coil, reducing its overall molecular dimensions. The authors also suggested that besides the change in molecular dimensions, the formation of hydrogen bonds is also one of the main reasons for increasing adsorption at lower pH.

In a study by Ho et al. (2009) using two types of PAC (micro and mesoporous), it was observed that coal-based carbons contained a greater volume of micropores than wood-based, which are favourable for the adsorption of smaller molecular weight compounds. Smaller toxin molecules, such as STXs, can utilise surface areas within micropores and larger pores; thus, using microporous instead of mesoporous carbon is recommended for STX removal (NEWCOMBE; NICHOLSON, 2004). However, larger molecules, including much of the natural organic matter (NOM) and MC-LR (HUANG;

CHENG; CHENG, 2007), are generally too large to utilize the micropores. Usually, NOM can interfere with the sorption of smaller adsorbates via two mechanisms: direct competition for sorption sites and pore blockage (SHI et al., 2012). Although it is believed that the most significant adsorption competition would exist between compounds of similar size and shape, competitive adsorption is not only dependent upon the size of the competing compound but also highly dependent upon the pore volume distribution of the adsorbent (HO et al., 2011).

4.7 Effect of pH

As already discussed in previous sections, factors such as the charge and nature of functional groups on both the carbon surface and the adsorbate are also known to influence adsorption processes, turning parameters such as the pH and ionic strength of a system critical to consider and understand (DONATI et al., 1994). The solution's pH affects PAC adsorption due to adsorbent surface chemical group preferential polarization (Pendleton et al., 2001). Huang et al. (2007) reported that previous authors examined the effect of pH in the range of 5-7 on humic acid adsorption by activated carbon and demonstrated that the adsorption affinity for humic acid is indirectly proportional to pH increase. Full-scale drinking water treatment processes involve competitive adsorption between the target contaminant and many other dissolved species classified as humic substances or dissolved organic matter (DOM). Such mixtures make a complex system challenging to analyze and interpret, as commented by the authors.

A study conducted by Shi et al. (2012) demonstrated that pH significantly impacts the adsorptive efficiency of PAC for STX removal. At an intermediate pH of 8.2 for water treatment, the relative performances of three PACs (Table 1) were (from lowest to highest capacity): lignite-coal-based < bituminous-coal-based < wood-based. In their study, the adsorption efficiency of STX increased with increasing pH because of the electrostatic interactions between functional groups of STX (speciation) and PAC surface due to the ionization of surface groups present in the PAC, causing a reduction in the repulsive electrostatic interactions between the positively charged STX and the adsorbent. In contrast, MC adsorption was enhanced with decreasing pH because MC is predominantly negatively charged at a pH range of 3-12 (PIVOKONSKY et al., 2021). These results suggest that the choice of PAC should be closely matched to the objectives of the PAC treatment. Furthermore, they also reinforced that water quality conditions play a critical role in PAC

sorption performance and must be well understood or studied in laboratory or field experiments to optimize water treatment performance.

While considering MC-LR adsorption, when the pH is lowered from 6.5 to 2.5, a decrease in the MC-LR water solubility is expected. Therefore, an increase in MC-LR affinity for the carbon surface is predicted. At low pH, the toxin molecule may behave as a filament, while at high pH, the structure may become an open "net", offering larger dimensions or cross-sectional area. Thus, pH changes can modify MC-LR molecular shape (PENDLETON; SCHUMANN; WONG, 2001).

Huang et al. (2007) found that for all the different activated carbons tested (coconut shell, bituminous coal and wood-based ACs), the adsorption of MC-LR increased as pH was lowered from 8 to 3. At pH 3, all the carbons shifted from a positively charged surface to a neutral charge (pH_{pzc}) at 5.2 for coconut shell, 5.8 for bituminous coal, and 4.1 for wood-based PAC (Table 1), indicating an increase in the negative charges. The pH at the point of zero charge (pH_{pzc}) is the pH value at which the surface ionic groups are neutralized, providing the adsorbent with an uncharged surface (PENDLETON; SCHUMANN; WONG, 2001). Conversely, in high pH solutions, MC-LR is negatively charged, and as most activated carbons show negative charges at alkaline pH, repulsion forces between the surface of carbon and MC-LR occur. Another factor regarding MC-LR is that at low pH, the weak acidic functional groups are undissociated, presenting a hydrophobic nature, and therefore are better adsorbed to the carbon surface than dissociated acidic functional groups at high pH, as already discussed in the surface functional groups section.

Similarly, Bajracharya et al. (2019) reported that, in the absence of NOM and at a pH of 5.2, the adsorption of MC-LR to PAC increased with decreasing pH, with all four PAC types exhibiting their most extensive amounts of adsorbed MC-LR. On the other hand, in the presence of NOM, the quantity of MC-LR adsorbed by PAC tended to decrease with decreasing pH, except for the coconut-based PAC. In wood-based and coal blend-based PACs this trend was more significant, where the amount of adsorbed toxin decreased by 28 and 40%, respectively, as the pH decreased from 9.5 to 5.2. Therefore, the reduction in MC-LR adsorption with decreasing pH likely reflects an increase in the adsorption of NOM with decreasing pH.

4.8 Effect of NOM

Water quality strongly influences the removal of cyanotoxins by activated carbon since NOM can compete and limit their adsorption (DONATI et al., 1994; HUANG; CHENG; CHENG, 2007). Donati et al. (1994) found that the UV_{254} absorbance of river water decreased significantly over time, indicating adsorption of both NOM and MC-LR. Competition for adsorption sites results in a decrease in MC-LR adsorption in raw water compared to ultrapure water. This can be expected as MC-LR is of a similar size to a large proportion of NOM in natural waters. In the same study, the effect of competitive adsorption between MC-LR and NOM was inferior in the wood-based PAC compared to other carbons. Wood-based PACs are highly mesoporous, so they can more readily accommodate both MC-LR and NOM substances of similar size. However, in less mesoporous adsorbents, such as coal, coconut, and peat moss-based PAC, there is greater competition for the fewer mesoporous sites available, which results in a more significant decrease in MC-LR adsorption. Blockage of transport pores by large organic molecules can also contribute to this since wood-based carbons possess a regularly ordered structure, enabling easier passage to the adsorption pores than the random network of pores in coal, coconut, and peat moss-based carbons. The authors suggest that this could explain why MC-LR adsorption for coal-based was reduced by 46% in river water, despite having relatively high mesopore volume compared with the other non-wood-based carbons (CAMPINAS; VIEGAS; ROSA, 2013; DONATI et al., 1994).

The competitive effects of NOM and organic matter pre-loading on activated carbon were evaluated by Lambert et al. (1996), which showed that both decreased the ability of activated carbon to remove MC-LR. Although activated carbon can efficiently adsorb MC-LR, reaching a lower concentration of toxin would require a high and unusual amount of PAC to compensate for the presence of NOM in both water and the adsorbent (MEREL et al., 2013). Bajracharya et al. (2019) found that the type of NOM also seemed to impact PAC performance, with NOM associated with algal bloom conditions exhibiting more of an impact on MC-LR adsorption than did NOM associated with terrestrial sources. The magnitude of the impact of NOM on MC-LR adsorption varied with PAC type, and it followed, from highest to lowest, this order: wood, coal blend, bituminous coal, and coconut shell (BAJRACHARYA; LIU; LENHART, 2019).

Huang et al. (2007) evaluated the competitive effect of NOM on MC-LR adsorption using wood-based activated carbon by conducting adsorption isotherm

experiments with both natural water containing NOM and ultrapure water. The maximum adsorbed capacity (Q_{max}) was observed to be much lower in the competitive isotherm compared with the ultrapure water. MC-LR removal decreased from 12% to 65%. Due to its characteristics (high in hydrophilic organics and more polar than MC-LR), NOM in the natural water competed with MC-LR for sorption sites.

Ho et al. (2009) found that the effect of water quality on the adsorption of STXs was minor, with a negligible difference observed between the removals in reservoir waters. These results suggest that lower competitive effects were evident and may be due to the wide range of pores of the carbons. Contradictorily, Shi et al. (2012) evaluated the impact of competition with NOM using natural water collected from a local pond in which the dissolved organic carbon (DOC) concentration was very high (28 ± 2 mg.L^{-1}). The results showed that the most significant effects of NOM on STX adsorption occurred at pH 7.05, with much smaller amounts of STX removed when NOM was present, compared to DI water. The authors hypothesized that the STX–NOM solution-phase interactions might have been enhanced at this pH due to the increasingly cationic nature of the STX in the presence of the negatively charged NOM. These interactions may have inhibited the adsorption of STX on the carbon surface.

NOM competes with target contaminants for adsorption sites on the surface of PAC, and thus, in high concentration, NOM would result in greater competition and, consequently, reduce the adsorption of the target contaminant. Furthermore, NOM can also block pores, reducing the target contaminant's adsorption (HO et al., 2008). For these mechanisms, NOM molecular weight is critical as the small molecular weight fraction (<1000 Da) is more important in competitive adsorption because, once adsorbed, they reduce the capacity of PAC for the target compound. On the other hand, the large molecular weight fraction cause pore blockage/constriction, thus, reducing the rate of the adsorption of the target compound (BAJRACHARYA; LIU; LENHART, 2019).

The relative impact of the two mechanisms varies to some extent on the type of PAC. Bajracharya et al. (2019) analysed the presence of NOM and its impact on the rate and the amount of MC-LR adsorption in different types of PACs. For the wood-based PAC, the rate of MC-LR adsorption decreased to a greater quantity in the presence of NOM than the extent of adsorption, suggesting pore blockage was more important than direct competition for this type of PAC. The bituminous coal-based PAC demonstrated a higher reduction in adsorption capacity than the adsorption rate. Therefore, site competition was the most important mechanism for this PAC. On the other hand, the coal blend-based PAC showed

similar decreases in both the extent and rate, indicating neither mechanism dominated. The authors assumed these differences likely reflect the presence of different forms of porosity on the PAC types and the ability of the NOM molecules to access sites within these pores. Similarly, when testing PAC adsorption, results showed that the adsorption of MC-LR was reduced by 11.3% in the presence of NOM as both MC-LR and NOM compete for similar mesoporous sites due to the similar molecular size of the two compounds (LEE; WALKER, 2006).

4.9 Removal capacity and activated carbon limitations

Donati et al. (1994) found that the initial rate of MC-LR uptake from river water for both wood and coal-based PACs was slower than that observed in ultrapure water. The adsorbents showed a decrease in initial uptake of MC-LR of 36 and 42% for wood and coal-based PACs, respectively. The wood-based carbons were the most effective adsorbents, adsorbing 280 and 220 µg MC-LR.mg^{-1} carbon, respectively. The least effective adsorbents were the coconut-based, adsorbing 40 and 20 µg MC-LR .mg^{-1} carbon, and the peat moss-based, which adsorbed 20 µg MC-LR.mg^{-1} carbon (Table 1).

Sugarcane bagasse and pinewood-activated carbon fibres showed adsorption of 161.3 and 200.0 µg MC-LR.mg^{-1} carbon, respectively. When compared to other results available in the literature, these results give an idea of the profile of the carbon that should be used in water treatment plants to remove toxins like MCs, requiring a volume of secondary micropore above 0.35 $cm^3.g^{-1}$ and a volume of mesopore greater than 0.40 $cm^3.g^{-1}$ (ALBUQUERQUE JR. et al., 2008). The adsorption of MC-LR onto activated carbon fibres from pinewood and sugarcane bagasse showed the same tendency described in previous studies (DONATI et al., 1994; PENDLETON; SCHUMANN; WONG, 2001). The greater the volumes of secondary micropores and mesopores of the carbons, the greater their capacity to adsorb MC-LR. The authors also attribute the greater adsorption affinity for the cyanotoxin in the pinewood-based PAC compared to the sugarcane bagasse PAC due to the higher volumes of secondary micropores and mesopores in the former (Table 1).

Wood-based PAC achieved 84% of total microcystin removal with a 20 $mg.L^{-1}$ PAC dose when the initial concentration of microcystin was 30 $\mu g.L^{-1}$. The adsorption efficiency of microcystin did not show significant changes at higher doses. The pore size distribution was PAC's most important physical property for considering adsorption performance. It is also apparent that the kinetic rate of adsorbed microcystin increases by

increasing the adsorbent dose, but the maximum amount adsorbed was at a dose of 20 $mg.L^{-1}$ of PAC (SENGUL; ERSAN; TUFEKCI, 2018).

In another study, wood, coal blend, bituminous coal, and coconut shell-based PACs removed about 93, 46, 20, and 10%, respectively, of the initial 50 $\mu g.L^{-1}$ MC-LR concentration. The authors suggested that using PAC alone at a dose equal to or less than 5 $mg.L^{-1}$, regardless of source material, likely would not remove MC-LR below the WHO guidelines (BAJRACHARYA; LIU; LENHART, 2019). Therefore, while activated carbon can efficiently adsorb cyanotoxins, their complete adsorption would require a high amount of different adsorbent types. Consequently, activated carbon should not be considered as an individual remediation measure but as a part of a multi-barrier approach (MEREL et al., 2013).

5 BIOCHAR

5.1 Role of feedstocks

Due to their low surface area, some non-activated biochars can be inferior to commercially activated carbons in their sorption capacity for organic contaminants (INYANG; DICKENSON, 2015). Although biochars share some similarities with activated carbon, there is a consensus that they exhibit high physical-chemical and structural heterogeneities, depending on the feedstock and pyrolysis conditions. There is still a reluctance to use biochar as a low-cost, renewable alternative to activated carbon, a trend also reported for other adsorbents (GWENZI et al., 2017).

Li et al. (2018) found that biochar produced at higher temperatures (600ºC) had higher ash content compared to those produced at a lower temperature (300º), following this trend: chicken manure biochar > maize straw biochar > pine sawdust biochar (Table 3). Therefore, this suggests that biochars derived from animal wastes tend to contain higher mineral ash content than those from plant residues. The interaction of higher ash content with organic matter in biochars could influence the sorption characteristics of organic pollutants. Moreover, mineral ash content may provide additional cation and/or anion binding sites for ionizable organic compounds (IOCs) adsorption, such as MC-LR (Li et al., 2018). These authors also found that, depending on the feedstock type and temperature, the biochars varied significantly in their structural properties and capacity to adsorb MC-LR from water. They suggested that chicken manure-derived biochars have great potential as

low-cost sustainable sorbents to diminish MC-LR risks. In another study for the MC-LR adsorption, different feedstocks were tested, and the capacity of biochar for MC-LR removal was in the following order: Kentucky bluegrass biochar > coffee residue biochar > grape pomace biochar > rice husk biochar > microalgae biochar. MC-LR adsorption tended to improve with the increase in pyrolysis temperature (SONG et al., 2021).

Li et al. (2018) found that for plant residue-derived biochars, the organic carbon contents increased as temperatures are risen, implying a greater carbonization degree when pyrolysis is carried out at higher temperatures. Oppositely, the organic carbon content of biochars containing high ash mineral content varied inversely with increasing temperature. The authors believe this is primarily due to the higher ash content of animal waste-derived than plant residue-derived biochars. The authors also found that the bulk functionalities differed between the tested biochars (pine sawdust, maize straw, and chicken manure), which they attribute to being feedstock and pyrolysis temperature dependent. The study also suggested that the ash mineral naturally present in the biochar could enhance the sorption of MC-LR through mechanisms such as electrostatic interaction, pore-filling, and H-bonding effect, which are linked to the point of zero charges, mesoporosity, and total surface functionality, respectively.

5.2 Elemental composition and surface chemistry

Wei & Lu (2021) obtained biochar from rice straw pyrolyzed at different temperatures, and each biochar showed different elemental compositions (Table 3). As the pyrolysis temperatures increased from 300 to 700 ºC, the carbon (C) contents improved, whereas the hydrogen (H) and oxygen (O) contents declined. Meanwhile, the nitrogen (N) contents remained generally unchanged during the process. The H/C atomic ratio (aromaticity index) decreased with the temperature rising from 300 ºC to 700 ºC, indicating that the aliphatic carbon was pyrolyzed into aromatic carbon. With the increasing pyrolysis temperature, the molar O/C ratio (polarity index) significantly decreased, making the surface of rice straw biochar more hydrophobic. Meanwhile, the decrease of the [(O + N)/C] ratio (polarity index) indicated a reduction of the surface polar functional groups. The temperature had a significant correlation with the indexes mentioned above. The authors found that for rice straw biochar pyrolyzed at 300 ºC, the surface functional groups had almost no changes, whereas for other biochars, the intensity of the adsorption peaks decreased, and the O-H bond stretching vibrations in the region of 3,683 cm^{-1} disappeared. On the other hand, for

the biochars pyrolyzed at higher temperatures (500-700 ºC), the -NO_2 adsorption peak in the region of 1,591 cm^{-1} shifted to a higher wavelength after MC-LR adsorption. Therefore, the authors attribute these functional groups presented on the surface of rice straw biochars as the adsorption sites for MC-LR.

Song et al. (2021) produced biochar using Kentucky bluegrass as feedstock at different pyrolysis temperatures (Table 3). In their results, the C content increased during pyrolysis due to the loss of volatile substances while H and O contents decreased, consequently reducing the O/C (polarity) and H/C (aromaticity) indexes. In contrast, ash contents increased with the increase in pyrolysis temperature. The pH_{pzc} of the biochar slightly increased from 6.35 to 7.07 as the temperature increased. Moreover, the minerals, including P, K, Ca, Mg, and Fe, slightly increased with a rise in the pyrolysis temperature.

Zeng & Kan (2021) used bermudagrass as feedstock for biochar production. Their study compared raw biochar (non-activated) with iron-activated biochar for MC-LR removal (Table 3). The C content of activated biochar decreased due to the high iron content from the $FeCl_3$ activation. In addition, the O and H contents of the activated biochar were much lower than those of non-activated biochar, which indicates that the $FeCl_3$ activation favoured the elimination of O and H. Moreover, the lower H/C, O/C, and [(O+N)/C] in the activated biochar suggested that the aromaticity and hydrophobicity increased while the polarity decreased after the $FeCl_3$ activation.

As for the spent mushroom substrate, as the pyrolysis temperature rose from 300 to 600 °C, the C contents of the biochars increased, but the O and H contents declined. Consequently, the atomic ratios of [(O+N)/C], O/C, and H/C decreased significantly. The authors also found that the adsorption bands were weakened as the pyrolysis temperature was increased, which is in agreement with the decrease of O content at higher pyrolysis temperatures. This confirms a loss of O- containing functional groups (e.g. hydroxyl, carboxyl, and carbonyl) due to dehydration and decarboxylation (LIU et al., 2021). Interestingly, these authors also showed that biochar produced under the N_2 atmosphere showed slightly higher degrees of peak intensity than biochar produced under the CO_2 atmosphere. A higher pyrolysis temperature and CO_2 better developed the physical structure of biochars, while lower pyrolysis temperatures and N_2 generated more surface functional groups in biochars.

Based on recent literature, Li et al. (2018) suggested that polar surface groups might affect adsorption more than bulk polarity. In that sense, a more significant presence

of surface O- and H-containing polar groups can form more hydrogen bonds with the MC-LR molecule's H, N, and O atoms and readily facilitate MC-LR sorption.

5.3 Surface charge

Wei & Lu (2021) showed that, as pyrolysis temperature increased from 300 to 700 ºC, the pH_{pzc} of all rice straw biochars increased, ranging from 3.5 to 5.5, and the alkalinity increased as well. The authors attributed this due to two reasons: the oxygen-containing functional groups on the surface of the biochar (such as hydroxy) decreased with the increasing pyrolysis temperature (ZHANG; LIU; LIU, 2015), and, secondly, at 400 ºC carbonates would be formed (YUAN; XU; ZHANG, 2011). Regarding $FeCl_3$ activation, the pH_{PZC} of bermudagrass biochars increased from 4.19 to 7.36 after activation, implying that acidic functional groups were reduced under the activation conditions (ZENG; KAN, 2021).

5.4 Morphology and microstructures

In Wei & Lu's (2021) study, all rice straw biochars presented a porous structure and a large surface. The pore canals were narrow and sparse at lower temperatures with a smooth surface. However, the pores gradually became larger and denser with an increase in the pyrolysis temperature. Small and dense micropores existed in each pore canal, with an increasing quantity. Song et al. (2021) demonstrated that biochar generated at higher pyrolysis temperatures developed a crystallization structure due to concentrated minerals such as Ca, Si, Mg, P, K, etc.

5.5 Effect of pH

For the adsorption of MC-LR in rice straw biochar, all adsorbents demonstrated better adsorption capacity at a lower pH of 3, while there was no significant difference in MC-LR removal rates at pH 7 and 9. The pH_{pzc} of all the biochars was in the range of 3.5–5.5; their zeta potentials were positive at pH 3 while negative at pH 7 and 9. On the other hand, MC-LR has a negative charge when pH > 2.19; therefore, the electrostatic attraction explains why the rice straw biochar showed better adsorption capacity at a lower pH. Moreover, as previously discussed, MC-LR molecules become smaller at lower pH, reducing overall molecular dimensions. As a result, hydrogen bonds could be formed

between the coiled molecules and the biochar surface charges, promoting the improvement of the adsorption capacity (HUANG; CHENG; CHENG, 2007; WEI; LU, 2021). Comparably, Li et al. (2014) also found that adsorption significantly decreased as pH increased. The authors supposed that electrostatic attraction may occur between the positively charged biochar surface and the negatively charged MC-LR. Moreover, higher adsorption of MC-LR at lower pHs may be attributed to the positive charges on the carbon surface with decreasing pH, whereas at higher pHs, the similar electronegative nature results in the repulsion of MC-LR from the biochar surface.

Liu et al. (2021), using spent mushroom substrate as a starting material, found that the adsorption efficacy of MC-LR to biochar produced at a higher temperature (600ºC) was inversely correlated to the solution pH. Similarly, increasing the pH led to an increase in the negative charges of the biochar surfaces. Hence, electrostatic repulsion between the toxin and the adsorbent was expected, weakening the adsorption efficacy. As the pH of natural water usually stands between 6 and 8, at which the adsorption efficacy of the higher pyrolytic biochar reached 79.1–83.2%, the authors suggested that it could be a promising adsorbent for MCs removal from natural water. In line with the mentioned studies, at lower pH, higher adsorption was observed with the maximum MC-LR adsorption capacity at pH 3 (5,034 $\mu g.g^{-1}$) and pH 4 (3,676 $\mu g.g^{-1}$) for Kentuck bluegrass-biochar (750ºC). However, lower MC-LR adsorption capacities (2714−2964 $\mu g.g^{-1}$) were observed at higher pH (5–9) (SONG et al., 2021).

Zeng & Kan (2021) also found optimal pH values at pH 3 and 4, while the adsorption capacity decreased with higher pH. However, adsorption capacity values at pH 7-8 (8.36-9.03 $mg.g^{-1}$) were not significantly different from those at pH 3-4 (9.64-9.69 $mg.g^{-1}$), suggesting that iron-activated biochar has excellent potential for the treatment of MC-LR from natural water and wastewater with various pH values.

5.6 Surface area and pore distribution

Li et al. (2018) found in their study that all tested chicken manure biochars and maize straw biochar produced at higher pyrolysis temperature – both possessing high mesoporosity – demonstrated to be better sorbents compared to the other biochars tested, which contained a lower mesoporosity, even though some of these had greater total pore volume and/or microporosity (Table 2). The authors also suggested that the pore-filling effect could be one central mechanism that dominates MC-LR sorption and outweighs the

aromaticity or surface functionality roles for the biochars produced from specific feedstocks and pyrolysis temperatures.

Wei & Lu (2021) found that the average pore size of all rice straw adsorbents was within the mesopore range (2–50 nm). Thus, microcystins are easier and preferential to be adsorbed onto the biochars. With the increase of pyrolysis temperatures from 300 ºC to 700 ºC, the total pore volume and the micropore volume increased (Table 2). In addition, the specific surface area of the biochars improved significantly from 3.87 $m^2.g^{-1}$ to 360.9 $m^2.g^{-1}$. At the highest temperature, the surface area of the adsorbent was nearly 100 times higher than that of biochar produced at the lowest temperature, which the authors attributed to the carbonisation process of biomass.

Generally, the specific surface area of Kentucky bluegrass biochars improved with the increase in pyrolysis temperature, but this trend was the inverse at 550 ºC and 750 ºC. The porosity revealed a similar trend with the specific surface area, which the authors attributed to the destruction of the porous structure of biochar and the blocking of pores by tar (SONG et al., 2021). For biochar produced from bermudagrass, compared to non-activated biochar (85.82 $m^2.g^{-1}$), the iron-activated material showed a nearly ten times higher surface area (835.10 $m^2.g^{-1}$), suggesting the $FeCl_3$ activation can provide significant improvement in terms of surface area (ZENG; KAN, 2021).

The biochars produced at a higher temperature from peeled wood chips presented a significant amount of meso and macropores for MC-LR adsorption, as their micropore volume was almost half its total volume (Table 2). On the other hand, peeled wood chips biochars produced at a lower temperature presented no micropores. They possessed a much larger average pore diameter (Table 2), which indicated that their total surface area would be more suitable and available for MC-LR adsorption (LI et al., 2014). After coexisting with DOM, the adsorption capacity of MC-LR decreased, which means that DOM, such as tannic acid (TA), acted as a strong competitor by occupying the effective adsorption sites for MC-LR in the mesopore and macropore regions due to the larger molecule size of TA than MC-LR (LI et al., 2014).

To improve porosity in biochars, acid-soaking is an effective method, primarily due to mineral removal and the exposition of hidden and blocked pores. Another advantage of deashing could be the release of dissolved organic residues and removing carbon fragments from biochars, enabling a more porous structure. In their study, Liu et al. (2018) observed that deashing slightly increased the surface area and pore volume of low-temperature biochars (≤400 ºC) while significantly increasing the surface area in high-

temperature biochars (≥500 ºC). Therefore, deashing might influence the physicochemical properties of biochars, consequently affecting MC-LR sorption behaviour.

5.7 Pyrolysis temperature and other pyrolytic conditions

At the same pyrolysis temperature, compared to other feedstocks, chicken manure biochar exhibited the strongest sorption for MC-LR, contributed mainly by electrostatic attraction, pore-filling, and H-bonding effects, corresponding to their higher pH_{PZC}, mesoporous volume, and total surface functionality (LI et al., 2018). The studied rice straw biochars showed a significantly positive association of temperature to the specific surface area, total pore volume, and mesoporous volume, while temperature and average pore diameter distribution were negatively correlated. The higher the pyrolysis temperature, the better its adsorption capacity on MC-LR (Table 2), thus, indicating that the adsorption efficiency of rice straw biochars was positively related to the pyrolysis temperature. The biochar produced at 700 ºC exhibited the best adsorption capacity for MC-LR. The highest pyrolytic temperature provided the largest specific surface area (360.9 $m^2\ g^{-1}$), which can offer more effective binding sites for target contaminants. Moreover, the high pyrolysis temperature also provided better-developed structures than those at lower temperatures, meeting the size of MC-LR (WEI; LU, 2021).

The spent mushroom substrate biochars showed the greatest ash content when pyrolyzed at 600 ºC, decreasing as the pyrolysis temperature was lowered to 300 ºC. Both the S_{BET} and porosity of biochars were significantly improved as the temperature was raised from 300 to 600 ºC (Table 3). At the lowest temperature, the pore structures were less developed, while the porosity was better developed at 600 °C due to more water loss in the dehydration process, volatilization of organic matter, and fracture/collapse (LIU et al., 2021). In their study, Song et al. (2021) found that the relationship between the adsorption capacities of different biochars and H/C ratio associated with the pyrolytic temperature as an indicator of hydrophobic value had a high correlation in all tested biochars. The result indicated that the highest pyrolytic temperature was observed as the optimal condition (Table 3), and hydrophobic interaction revealed one of the possible MC-LR adsorption mechanisms. Generally, these phenomena deduced that the biochar produced at higher pyrolysis temperature could influence the adsorption of contaminants due to an increase in the surface area, higher hydrophobicity, and concentration of specific elements (i.e., P, K, Ca, Mg, and Fe, etc.). In another study, high-temperature (700 °C) peeled wood chips

biochar showed a high carbon content, low H/C ratio (Table 3), and high specific surface area (Table 2), which implies the formation of a highly carbonized aromatic structure. By contrast, low-temperature biochar (300 ºC) exhibited low carbon content, high H/C ratio, and low specific surface area, indicating that some organic residues from the feedstock remain on its structure after incomplete carbonization (LI et al., 2014).

5.8 Influence of ions on MC-LR adsorption

Evaluating the adsorption capacity in water from a river and a lake, Song et al. (2021) observed a considerable decrease in MC-LR adsorption compared to DI water results. The adsorption capacities from the river and lake water were 1,000 $\mu g.g^{-1}$ and 1,421 $\mu g.g^{-1}$, respectively, while in DI water, it was 2,769 $\mu g.g^{-1}$. The authors suggested that the decrease in the adsorption capacity could be due to the cationic and anionic metal ions, as they found a higher amount of metal ions such as Na^{+}, Mg^{2+}, K^{+}, Ca^{2+}, Cl^{-}, NO_3^{-}, and SO_4^{-} in the natural waters. This phenomenon is likely due to the rapid absorption of ions Mg^{2+}, Ca^{2+}, and NO_3^{-} onto the biochar surface, resulting in the removal of the metal ions, rather than MC-LR.

Zeng & Kan (2021) also investigated the use of biochar in natural water. The iron-activated biochar was tested with the MC-LR spiked with environmentally relevant concentrations (5, 25, and 50 $\mu g.L^{-1}$) in DI water and lake water. For both experiments, the final MC-LR concentration was lower than 1 $\mu g.L^{-1}$, which can meet the World Health Organization (WHO) guideline. The authors also suggested that because the adsorbent could be magnetically removed, iron-activated biochars appear applicable to the treatment of lake waters containing MC-LR due to their effective adsorption, magnetic separation, and regeneration.

5.9 Activated biochar

Zeng & Kan (2021) found that, compared with the control (no activation), the $FeCl_3$ activation led to a significant increase in MC-LR adsorption capacity. Depending on the impregnation rate, the adsorption capacity was affected. In their study, MC-LR adsorption capacity was greatly improved (from 0.76 to 9.00 $mg.g^{-1}$) when the iron impregnation ratio rose from 0 to 2; but at a ratio of 3, the adsorption capacity was decreased. The authors argue that a high dose of ferric activator could cause hyperactivation while

deteriorating pore structure, causing blockage of pores with aggregated iron and lowering surface area.

6 CONCLUSIONS

The current work provides an understanding that the general indexes adopted by water companies and decision-makers appear to lack a deepened knowledge of key factors on absorbents for toxin removal. One such factor is the specific surface area which by itself is a poor indicator of adsorption capacity. Thus, water companies have to appreciate a combination of detailed knowledge of the adsorbate, adsorbent and aqueous solution properties for the correct selection of PAC or biochar. Overall, this systematic review has shown that although activated carbon has been widely used for cyanotoxin removal, not enough data is available and fewer studies have been carried out for different toxins since most focus on MC-LR, leaving many knowledge gaps for other toxins such as saxitoxins and cylindrospermopsins. As for biochar, the knowledge gaps are even greater, especially since it is a newer technology and there are few studies for cyanotoxins adsorption. In addition, no studies have been found to tailor biochar specifically for cyanotoxins adsorption and assessed its impact on water quality. Therefore, biochar is not yet a reliable option for water treatment, especially on full-scale operations, due to the great diversity in feedstock options, manufacturing procedures and properties.

REFERENCES

ABBAS, T. et al. Recent advancements in the removal of cyanotoxins from water using conventional and modified adsorbents—a contemporary review. **Water (Switzerland)**, v. 12, n. 10, 1 out. 2020.

ALBUQUERQUE JR., E. C. et al. Removal of cyanobacteria toxins from drinking water by adsorption on activated carbon fibers. **Materials Research**, v. 11, n. 3, p. 371–380, 2008.

BAJRACHARYA, A.; LIU, Y.-L.; LENHART, J. J. The influence of natural organic matter on the adsorption of microcystin-LR by powdered activated carbon. **Environmental Science: Water Research & Technology**, v. 5, n. 2, p. 256–267, 2019.

CAMPINAS, M.; ROSA, M. J. The ionic strength effect on microcystin and natural organic matter surrogate adsorption onto PAC. **Journal of Colloid and Interface Science**, v. 299, n. 2, p. 520–529, 2006.

CAMPINAS, M.; VIEGAS, R. M. C.; ROSA, M. J. Modelling and understanding the competitive adsorption of microcystins and tannic acid. **Water Research**, v. 47, n. 15, p. 5690–5699, 2013.

CAPELO-NETO, J.; SILVA BUARQUE, N. M. Simulation of saxitoxins adsorption in full-scale GAC filter using HSDM. **Water Research**, v. 88, p. 558–565, 2016.

COELHO, J. A. et al. Modeling Geosmin removal in a full-scale filter. **Anais da Academia Brasileira de Ciencias**, v. 92, n. 3, p. 1–10, 2020.

COOK, D.; NEWCOMBE, G. Comparison and modeling of the adsorption of two microcystin analogues onto powdered activated carbon. **ENVIRONMENTAL TECHNOLOGY**, v. 29, n. 5, p. 525–534, 2008.

DONATI, C. et al. Microcystin-LR adsorption by powdered activated carbon. **Water Research**, v. 28, n. 8, p. 1735–1742, 1994.

DROGUI, P. et al. Removal of microcystin-LR from spiked water using either activated carbon or anthracite as filter material. **Environmental Technology**, v. 33, n. 4, p. 381–391, 2012.

FALCONER, I. R. et al. Using Activated Carbon to Remove Toxicity from Drinking Water Containing Cyanobacterial Blooms. v. 81, n. 2, p. 102–105, 1989.

GWENZI, W. et al. Biochar-based water treatment systems as a potential low-cost and sustainable technology for clean water provision. **Journal of Environmental Management**, v. 197, p. 732–749, 15 jul. 2017.

HIMBERG, K. et al. The effect of water treatment processes on the removal of hepatotoxins from Microcystis and Oscillatoria cyanobacteria: A laboratory study. **Water Research**, v. 23, n. 8, p. 979–984, 1989.

HITZFELD, B. C.; HOGER, S. J.; DIETRICH, D. R. Cyanobacterial Toxins: Removal

during Drinking Water Treatment, and Human Risk Assessment. **Environmental Health Perspectives**, v. 108, p. 113–122, 2000.

HO, L. et al. Optimizing PAC and chlorination practices for cylindrospermopsin removal. **Journal / American Water Works Association**, v. 100, n. 11, p. 88–96, 2008.

HO, L. et al. Optimising water treatment practices for the removal of Anabaena circinalis and its associated metabolites, geosmin and saxitoxins. **Journal of Water and Health**, v. 7, n. 4, p. 544–556, 2009.

HO, L. et al. Application of powdered activated carbon for the adsorption of cylindrospermopsin and microcystin toxins from drinking water supplies. **Water Research**, v. 45, n. 9, p. 2954–2964, 2011.

HOFFMANN, J. R. . Removal of Microcystis toxins in water purification processes. **Water SA**, v. 58, n. 2, 1976.

HUANG, W.-J.; CHENG, B.-L.; CHENG, Y.-L. Adsorption of microcystin-LR by three types of activated carbon. **Journal of Hazardous Materials**, v. 141, n. 1, p. 115–122, 2007.

INYANG, M.; DICKENSON, E. The potential role of biochar in the removal of organic and microbial contaminants from potable and reuse water: A review. **Chemosphere**, v. 134, p. 232–240, 1 set. 2015.

KEIJOLA, A. M. et al. Removal of cyanobacterial toxins in water treatment processes: Laboratory and pilot-scale experiments. **Toxicity Assessment**, v. 3, n. 5, p. 643–656, 1988.

LAMBERT, T. W.; HOLMES, C. F. B.; HRUDEY, S. E. Adsorption of microcystin-LR by activated carbon and removal in full scale water treatment. **Water Research**, v. 30, n. 6, p. 1411–1422, 1996.

LEE, J.; WALKER, H. W. Effect of process variables and natural organic matter on removal of microcystin-LR by PAC - UF. **Environmental Science and Technology**, v. 40, n. 23, p. 7336–7342, 2006.

LEHMANN, J.; JOSEPH, S. Biochar for Environmental Management: An Introduction. In: LEHMANN, J.; JOSEPH, S. (Eds.). . **Biochar for Environmental Management: Science and Technology**. 1. ed. London: Routledge, 2009.

LI, D. C.; JIANG, H. The thermochemical conversion of non-lignocellulosic biomass to form biochar: A review on characterizations and mechanism elucidation. **Bioresource Technology**, v. 246, p. 57–68, 1 dez. 2017.

LI, J. et al. Comparative study for microcystin-LR sorption onto biochars produced from various plant- and animal-wastes at different pyrolysis temperatures: Influencing mechanisms of biochar properties. **Bioresource Technology**, v. 247, p. 794–803, jan. 2018.

LI, L. et al. Mechanisms and Factors Influencing Adsorption of Microcystin-LR on Biochars. **Water, Air, & Soil Pollution**, v. 225, n. 12, p. 2220, 19 dez. 2014.

LIU, B.-L. et al. Adsorption of microcystin contaminants by biochars derived from contrasting pyrolytic conditions: Characteristics, affecting factors, and mechanisms. **Science of The Total Environment**, v. 763, p. 143028, 2021.

LIU, G. et al. Characteristics and mechanisms of microcystin-LR adsorption by giant reed-derived biochars: Role of minerals, pores, and functional groups. **Journal of Cleaner Production**, v. 176, p. 463–473, 2018.

MEREL, S. et al. State of knowledge and concerns on cyanobacterial blooms and cyanotoxins. **Environment International**, v. 59, p. 303–327, 2013.

MOHER, D. et al. Preferred reporting items for systematic reviews and meta-analyses: The PRISMA statement. **PLoS Medicine**, v. 6, n. 7, 2009.

NEWCOMBE, G.; NICHOLSON, B. Water treatment options for dissolved cyanotoxins. **Journal of Water Supply: Research and Technology - AQUA**, v. 53, n. 4, p. 227–239, 2004.

NOBRE, J. R. C. et al. Caracterização do carvão ativado produzido a partir de serragens de maçaranduba. **Scientia Forestalis/Forest Sciences**, v. 43, n. 107, p. 693–702, 2015.

OLIVEIRA, F. R. et al. Environmental application of biochar: Current status and perspectives. **Bioresource Technology**, v. 246, p. 110–122, dez. 2017.

PENDLETON, P. et al. Properties of activated carbon controlling 2-methylisoborneol adsorption. **Carbon**, v. 35, n. 8, p. 1141–1149, 1997.

PENDLETON, P.; SCHUMANN, R.; WONG, S. H. Microcystin-LR adsorption by activated carbon. **Journal of Colloid and Interface Science**, v. 240, n. 1, p. 1–8, 2001.

PIVOKONSKY, M. et al. Current knowledge in the field of algal organic matter adsorption onto activated carbon in drinking water treatment. **Science of the Total Environment**, v. 799, p. 149455, 2021.

SENGUL, A. B.; ERSAN, G.; TUFEKCI, N. Removal of intra- and extracellular microcystin by submerged ultrafiltration (UF) membrane combined with coagulation/flocculation and powdered activated carbon (PAC) adsorption. **Journal of Hazardous Materials**, v. 343, p. 29–35, 2018.

ŞENGÜL, A. B.; ERSAN, G.; TÜFEKÇI, N. Removal of intra- and extracellular microcystin by submerged ultrafiltration (UF) membrane combined with coagulation/flocculation and powdered activated carbon (PAC) adsorption. **Journal of Hazardous Materials**, v. 343, p. 29–35, fev. 2018.

SHI, H. et al. pH effects on the adsorption of saxitoxin by powdered activated carbon. **Harmful Algae**, v. 19, p. 61–67, 2012.

SONG, H. J. et al. Treatment of microcystin-LR cyanotoxin contaminated water using Kentucky bluegrass-derived biochar. **Journal of Water Process Engineering**, v. 41, n. April, p. 102054, 2021.

TOLES, C. A.; MARSHALL, W. E.; JOHNS, M. M. Surface functional groups on acid-

activated nutshell carbons. **Carbon**, v. 37, n. 8, p. 1207–1214, 1999.

VELZEBOER, R. et al. Release of geosmin by Anabaena circinalis following treatment with aluminium sulphate. **Water Science and Technology**, v. 31, n. 11, p. 187–194, 1995.

WARHURST, A. M. et al. Adsorption of the cyanobacterial hepatotoxin microcystin-LR by a low-cost activated carbon from the seed husks of the pan-tropical tree, Moringa oleifera. **SCIENCE OF THE TOTAL ENVIRONMENT**, v. 207, n. 2–3, p. 207–211, nov. 1997.

WEI, L.; LU, J. Adsorption of microcystin-LR by rice straw biochars with different pyrolysis temperatures. **Environmental Technology and Innovation**, v. 23, p. 101609, 2021.

YIN, Q. et al. Biochar as an adsorbent for inorganic nitrogen and phosphorus removal from water: a review. **Environmental Science and Pollution Research**, v. 24, n. 34, p. 26297–26309, 1 dez. 2017.

YUAN, J. H.; XU, R. K.; ZHANG, H. The forms of alkalis in the biochar produced from crop residues at different temperatures. **Bioresource Technology**, v. 102, n. 3, p. 3488–3497, 2011.

ZENG, S.; KAN, E. Adsorption and regeneration on iron-activated biochar for removal of microcystin-LR. **Chemosphere**, v. 273, p. 129649, 2021.

ZHANG, J.; LIU, J.; LIU, R. Effects of pyrolysis temperature and heating time on biochar obtained from the pyrolysis of straw and lignosulfonate. **Bioresource Technology**, v. 176, p. 288–291, 2015.

SUPPLEMENTARY MATERIALS

Table 1 – Data extracted from the studies included in the systematic review for PAC

Reference	Source material	Activation method	SA (m^2/g)	D_{avg} (µm)	V_{micro} (cm^3/g)	V_{meso} (cm^3/g)	V_{total} (cm^3/g)	O (%)	Toxin	Q_{max} (µg/mg)	pH	pH_{pzc}	Main results
(DONATI et al., 1994)	Coal	-	863-1,329	-	0.39-0.66	0.05-0.19	-	8.7-12.3	MC-LR	70-116[a] 43-63[b]	5.2-6.6	-	- Pore volume is dependent on the starting material - MC-LR adsorption is dependent on the volume of mesopores - Wood-based carbons were highly mesoporous and most effective - Surface areas and iodine numbers are not useful to evaluate the potential of MC-LR adsorption
	Coconut	-	991-1,067	-	0.42-0.45	0.02-0.03	-	9.8-10.3	MC-LR	20-40[a] 12-22[b]	5.2-6.6	-	
	Wood	-	1,197-1,366	-	0.60-0.72	0.27-0.49	-	6.6-13.1	MC-LR	220-280[a] 170-250[b]	5.2-6.6	-	
	Peat moss	-	493	-	0.23	0.06	-	7.9	MC-LR	20[a] 11[b]	5.2-6.6	-	
(PENDLETON; SCHUMANN; WONG, 2001)	Wood	Phosphoric acid	-	-	0.85[d]	0.4	-	14.9	MC-LR	189±10	6.5	3.4	- Low pH results in enhanced adsorption of MC-LR due either to precipitation or reduced solvency effect - To achieve effective MC-LR removal, the combination of secondary micropore and mesopore volumes should be considered
	Wood	Phosphoric acid	-	-	0.96[d]	0.38	-	9.2	MC-LR	200±16	6.5	3.4	
	Wood	Phosphoric acid	-	-	0.71[d]	0.26	-	11.4	MC-LR	161±12	6.5	3.4	
	Coconut	Steam	-	-	0.81[d]	0.05	-	3.1	MC-LR	22±2	6.5	6.2	
	Coconut	Steam	-	-	0.39[d]	0.07	-	5.7	MC-LR	7±2	6.5	6.2	
(LEE; WALKER, 2006)	Wood	-	640	17	D	D	-	-	MC-LR	20	7±0.2	3.02	- Total surface area was not an important factor - PAC surface chemistry does not play a significant role in MC-LR adsorption
	Coconut shell	-	752.8	9.6	D	-	-	-	MC-LR	5	7±0.2	2.04	

													- Wood-based carbon was more effective at removing MC-LR due to greater mesopore volume
(HUANG; CHENG; CHENG, 2007)	Coconut shell	-	950	1400[c]	0.812	0.089	-	3.5	MC-LR	16.1	7.5	5.2	- AC with more mesopores and macropores adsorbed more MC-LR
	Bituminous coal	-	950	1200[c]	0.689	0.175	-	4.3	MC-LR	17.5	7.5	5.8	- Surface functional groups were an important factor for MC-LR adsorption - Larger amounts of basic surface groups and higher pH_{pzc} provided a higher MC-LR adsorption
	Wood	-	1,050	1200[c]	0.242	0.76	-	11.5	MC-LR	83.3	7.5	4.1	- Competitive effects of NOM caused a reduction in adsorption capacity
(ALBUQUERQUE JR. et al., 2008)	Macadamia nutshell	Steam at ~900 ºC	1,079.50	-	0.37[d]	0.2	0.58	-	MC-LR	-	~6-8.5	-	- The structures from MNS, CS, and UCM produced microporous AC, while SCB and PWR produced mesoporous AC - The pine wood and sugarcane bagasse AC showed a variation in their adsorption capacities, dependent on the physical characteristics of the adsorbents, such as the volume of mesopore - The low efficiency for removing MCs from commercial AC used on WTPs of Brazilian hemodialysis centres is linked to the volume of mesopores
	Dried coconut shell endocarp	Steam at ~900 ºC	1,090.00	-	0.35[d]	0.21	0.57	-	MC-LR	-	~6-8.5	-	
	Sugar cane bagasse	Steam at ~900 ºC	1,174.30	-	0.33[d]	0.39	0.76	-	MC-LR	161.3	~6-8.5	-	
	Unripe coconut mesocarp	Steam at ~900 ºC	1,269.60	-	0.55[d]	0.12	0.67	-	MC-LR	-	~6-8.5	-	
	Pine wood residues	Steam at ~900 ºC	1,550.10	-	0.35[d]	1.06	1.40	-	MC-LR	200	~6-8.5	-	
(HO et al., 2008)	Coal	Steam	1,208	23	0.32	0.207	-	-	CYN	-	7.9	9.5	- The relatively high doses of PAC needed to remove CYN in the river water effectively can be attributed to the poor water quality (NOM)
	Wood	Phosphoric acid	519	21	0.098	0.173	-	-	CYN	-	7.9	3.0	

													- WTPs, along with water safety guidelines, should use multibarrier treatment options
(HO et al., 2009)	Coal	Stem	978	20	-	-	0.65	-	STXs	-	7.7-7.9	-	- PAC was an effective treatment barrier for the efficient removal of geosmin and saxitoxins - Coal-based carbon has shown to be superior in different reservoir waters
	Wood	Steam	926	20	-	-	0.67	-	STXs	-	7.7-7.9	-	
(HO et al., 2011)	Coal	Steam	1,289	20-25	-	-	-	-	CYN MCs	-	7.5-7.7	-	- CYN was shown to adsorb to a similar extent to MC-RR
	Coal	Steam	1,105	10	-	-	-	-	CYN MCs	-	7.5-7.7	-	
(SHI et al., 2012)	Lignite coal	-	507	-	0.14	0.386	0.638	10.9	STX	-	5.7-10.7	10.6	- pH has a significant impact on the adsorptive efficiency of PAC for STX treatment - The choice of PAC should be closely matched to the objectives of the PAC treatment - Water quality conditions also play a critical role in PAC sorption performance
	Bituminous coal	-	901	-	0.317	0.14	0.48	5.8	STX	-	5.7-10.7	6.1	
	Wood	-	1,464	-	0.391	0.807	1.22	9.4	STX	-	5.7-10.7	4.9	
(ŞENGÜL; ERSAN; TÜFEKÇI, 2018)	Wood	-	1,400	-	20%	80%	1.76	-	MC	-	8.07	-	- The adsorption efficiency is dependent on the PAC material, pore size distribution, initial MC concentration, PAC dose, and contact time
(BAJRACHARYA; LIU; LENHART, 2019)	Wood	Chemical	1,676	1-30	-	0.49	0.89	-	MC-LR	63.41	5.2-9.5	3.3	- Wood-based PAC had the best removal of MC-LR in systems with NOM - In the absence of NOM, the wood-based PAC and coal blend-based PAC performed similarly
	Coconut shell	Steam	703	5-76	-	0.04	0.35	-	MC-LR	-	5.2-9.5	6.2	
	Coal blend	Steam	644	2-65	-	0.09	0.35	-	MC-LR	40.74	5.2-9.5	6.6	

	Bituminous coal	Steam	950	2-56	-	0.15	0.56	-	MC-LR	-	5.2-9.5	6.1	- NOM associated with algal bloom conditions caused more impact on MC-LR adsorption - Competition with NOM varies depending upon the source of NOM and the solution pH

SA: surface area; D_{avg}: average pore diameter; V_{micro}, V_{meso}, and V_{total}: micropore, mesopore, and total pore volume; O: oxygen content; Q_{max}: maximum amount of toxin adsorbed; pH= solution pH; pH_{pzc}: solution pH at which the net surface charge of the adsorbent is zero; D: dominant pore type

[a] Adsorption in ultrapure water; [b] Adsorption in river water; [c] GAC; [d] Sum of primary and secondary micropores;

Table 2 – Data extracted from the studies included in the systematic review for biochar

Reference	Feedstock	PT (ºC)	RT (h)	Post	PS (mm)	SA (m^2/g)	D_{avg} (nm)	V_{micro} (cm^3/g)	V_{meso} (cm^3/g)	V_{total} (cm^3/g)	Toxin	Qe (µg/mg)	pH
(LI et al., 2014)	Peeled wood chips	300 700	6	-	< 0.154	4.094 392.1	27.3 2.43	0 0.136	-	0.028 0.238	MC-LR	0.74[c] 3.72[c]	7.5
(LIU et al., 2018)	Giant reed	300 350 400 500 600	2	-	< 0.125	2.69 2.12 3.02 2.56 58.8	20.0 21.0 17.3 21.3 8.09	0.00052 0.00046 0.00070 0.00078 0.0033	0.0128 0.0105 0.0120 0.0127 0.359	0.0135 0.0111 0.0130 0.0137 0.363	MC-LR	0.14 0.14 0.71 41.2 42.4	5
(LI et al., 2018)	Pine sawdust	300 600	3	0.1 M HCl for 24 h	< 0.149	1.39 371.24	9.94 1.64	0.0004 0.1201	0.0015 0.0022	0.0034 0.1518	MC-LR	~ 0.1 ~ 0.6	-
	Maize straw	300 600	3	0.1 M HCl for 24 h	< 0.149	3.78 353.55	13.25 1.88	0.0004 0.1112	0.0036 0.0070	0.0125 0.1659	MC-LR	~ 0.4 ~ 1.4	-
	Chicken manure	300 600	3	0.1 M HCl for 24 h	< 0.149	4.00 86.67	20.58 4.35	0 0.0225	0.0120 0.0317	0.0206 0.0942	MC-LR	~ 1.3 ~ 1.5	-
(WEI; LU, 2021)	Rice straw	300 400 500 600 700	6	1 M HCl for 12 h	-	3.87 31.06 163.8 174.7 360.9	18.70 16.71 6.331 5.464 5.223	0.000548 0.009174 0.04825 0.04721 0.1070	-	0.01282 0.03202 0.1012 0.1153 0.1947	MC-LR	~0.025 ~0.025 ~0.035 ~0.04 ~0.05	7
(LIU et al., 2021)	Spent mushroom substrate	300[a] 300[b] 600[a] 600[b]	4	-	< 0.15	0.96 1.05 4.02 2.78	9.52 9.04 22.0 20.5	-	-	0.0023 0.00238 0.0221 0.0142	MC-LR	~ 0.2 ~ 0.2 ~ 0.31 ~ 0.25	2-10
(SONG et al., 2021)	Kentucky bluegrass	350 550 750	2	Washed and dried at 60ºC	< 0.14	2.62 190 118	12.4 1.87 5.09	-	-	0.01 0.14 0.04	MC-LR	- - ~2.7	6

(ZENG; KAN, 2021)	Bermudagrass	800	2	-	< 0.106	85.82	-	-	-	-	MC-LR	-	6
	Bermudagrass[d]	800	2	$FeCl_3$ activation	< 0.106	835.1	-	-	-	-	MC-LR	10.12	

PT: pyrolysis temperature; RT: residence time; Post: post-treatment; PS: particle size; SA: surface area; D_{avg}: average pore diameter; V_{micro}, V_{meso}, and V_{total}: micropore, mesopore, and total pore volume; Q_e: adsorption capacity of toxin onto biochar at equilibrium time; pH: solution pH

[a] biochar produced under CO_2 atmosphere; [b] biochar produced under N_2 atmosphere; [c] adsorption at 25 ºC; [d] pre-treatment with iron impregnation;

Table 3 – Elemental composition and other biochar characteristics

Reference	Feedstock	PT (ºC)	Elemental composition (%)				Atomic ratio			Ash (%)	pH_{pzc}	Main results
			C	H	N	O	(N+O)/C	O/C	H/C			
(LI et al., 2014)	Peeled wood chips	300	70.1	3.63	0.89	25.38	0.283	0.272	0.617	-	8.5	- Multiple bindings (e.g., electrostatic interaction, hydrogen bonding) between MC-LR and biochar surface may cause the resistant desorption of MC-LR, resulting in the prolonged environmental fate of toxin
		700	80.4	1.21	0.78	17.61	0.173	0.164	0.179		9.7	
(LIU et al., 2018)	Giant reed	300	65.3	4.51	0.65	21.0	0.25	0.24	0.82	7.69	-	- Mesopores were predominant - High-temperature biochars (HBC) (≥ 500 ºC) had more mesopores than the low-temperature biochars (≤ 400 ºC) - HBCs exhibited greater adsorption capacity and affinity for MC-LR
		350	67.0	4.46	0.64	21.7	0.25	0.25	0.79	7.73		
		400	72.3	4.09	0.69	18.7	0.20	0.19	0.67	8.45		
		500	73.1	3.01	0.63	11.5	0.13	0.12	0.49	10.7		
		600	78.6	2.22	0.55	11.2	0.11	0.11	0.34	11.3		
(LI et al., 2018)	Pine sawdust	300	73.78	4.59	0.23	20.30	0.278	0.275	0.062	1.10	6.14	- Biochars produced from different feedstocks and at different pyrolysis temperatures varied significantly in their structural properties and MC- LR adsorption - At the same pyrolysis temperature, chicken manure biochars exhibited the most substantial MC-LR adsorption
		600	90.81	1.92	0.40	4.95	0.059	0.055	0.021	1.91	5.93	
	Maize straw	300	62.06	3.93	1.23	19.08	0.327	0.308	0.063	13.69	6.85	
		600	72.84	1.50	0.86	7.44	0.113	0.102	0.021	17.36	8.22	
	Chicken manure	300	39.07	2.95	3.52	17.96	0.550	0.460	0.076	36.50	8.00	
		600	32.30	0.93	1.86	15.42	0.535	0.478	0.029	49.99	9.22	
(WEI; LU, 2021)	Rice straw	300	60.09	6.07	2.00	12.14	0.24	0.20	0.10	19.70	3.5-5.5	- The higher the pyrolysis temperature, the better its adsorption capacity on MC-LR - The biochars had better adsorption capacity on MC-LR at lower pH, mainly due to the electrostatic interactions and the formation of hydrogen bonds
		400	61.39	4.65	1.93	7.71	0.16	0.13	0.08	24.33		
		500	63.03	3.84	2.28	1.95	0.07	0.03	0.06	28.90		
		600	63.62	3.51	2.06	0.29	0.04	0.004	0.06	30.46		
		700	63.83	1.82	1.80	0.19	0.03	0.003	0.03	32.36		
(LIU et al., 2021)	Spent mushroom substrate	300[a]	56.3	4.67	1.48	29.2	54.5	51.8	8.29	12.4	-	- The adsorption efficacy varied substantially with the solution pH and temperature, MC congeners, and pyrolytic conditions - Higher temperature and CO_2 favour the development of the physical structures of biochars, providing more adsorption sites
		300[b]	59.2	4.66	1.39	26.6	47.3	45.0	7.87	14.3		
		600[a]	65.3	2.14	1.35	14.0	23.5	21.4	3.28	19.7		
		600[b]	67.0	2.62	1.45	15.2	24.9	22.7	3.90	17.0		
(SONG et al., 2021)	Kentucky bluegrass	350	64.0	0.21	2.66	17.5	0.32	0.27	0.07	11.6	6.35	- MC-LR adsorption tends to improve with increasing pyrolysis temperature - Biochar formed at higher temperatures developed a crystallization structure due to concentrated minerals
		550	68.7	2.35	2.54	8.75	0.16	0.13	0.03	17.7	6.99	
		750	69.0	0.94	2.16	6.38	0.12	0.09	0.01	21.6	7.07	

(ZENG; KAN, 2021)	Bermudagrass	800	68.02	1.58	3.37	12.94	0.185	0.143	0.279	14.04	4.19	- $FeCl_3$ activation promoted a significant increase in MC-LR adsorption capacity and surface area - After adsorption, the biochar could be magnetically separated, making it practically applicable for treating natural lake waters
	Bermudagrass*	800	55.34	0.9	1.93	8.17	0.141	0.111	0.195	33.66	7.36	

PT: pyrolysis temperature; pH_{pzc}: solution pH at which the net surface charge of biochar is zero
[a] biochar produced under CO_2 atmosphere; [b] biochar produced under N_2 atmosphere; * iron-activated biochar

CHAPTER II

Production and characterization of biochar from drinking water treatment sludge via pyrolysis for water treatment purposes

Production and characterization of biochar from drinking water treatment sludge via pyrolysis for water treatment purposes

André Madson Araújo Frota[1], Naiara Cipriano Oliveira[1], Mona Lisa Moura de Oliveira[2], Thiago Padovani Xavier[3], Erdin Ibraim[4], Tannaz Pak[5], Odair Pastor Ferreira[1], José Capelo Neto[1]

[1] Federal University of Ceará, [2] State University of Ceará, [3] Federal University of Espírito Santo, [4] University of Bristol, [5]Teesside University

ABSTRACT

A key concern regarding the direct discharge from water treatment waste residuals to water bodies is the potential toxicity of iron and aluminium – chemicals customarily used as primary coagulants in the flocculation-sedimentation stage. Pyrolysis is a mature heat treatment method in bio-energy production, solid waste management, and preparation of carbon-based materials. Due to the advantages of pyrolysis, this study proposes a new technique based on drinking water treatment sludge as a feedstock for manufacturing porous biochar and its application in the treatment of contaminated waters. Different techniques were used to characterize the samples: proximate and ultimate analysis, Fourier-transform infrared spectroscopy (FT-IR), Raman spectroscopy, X-Ray diffraction analysis (XRD), zeta potential, adsorption-desorption isotherms, thermogravimetric analysis (TGA/DTG), and scanning electron microscopy (SEM). The analyses of the physicochemical properties of biochar from this study were carried out to provide information on the potential application of this material to water treatment. High ash mineral content affected biochar properties such as pH and zeta potential, which impact its application. Also, biochar produced at a higher temperature showed better structural properties for its use as an adsorbent. Overall, sludge-derived biochar showed limited application for water treatment purposes.

Keywords: Circular economy. Pyrolysis. Sludge. Characterization. Water treatment

7 INTRODUCTION

Conventional water treatment technologies (coagulation, flocculation, clarification, and filtration) or their variations (direct or double filtration) are ineffective in removing dissolved compounds from water, especially cyanotoxins and other dissolved secondary metabolites. Instead, additional water treatment processes are often needed to introduce another barrier to consumers' protection (ABBAS et al., 2020; CHOW et al., 1999). Conventional methods of remediating persistent pollutants from aqueous and gaseous phases mainly employ chemical precipitation, ion exchange, adsorption (i.e. activated carbon), and membrane separation processes, among other techniques. These methods are costly and often generate considerable chemical residues, which have no economic value (OLIVEIRA et al., 2017).

Water treatment processes generate solid and liquid residues (i.e. sludge) as a result of the concentration of particles and organic matter (OM) from raw water (PESTANA et al., 2016). A concern regarding the direct discharge of untreated water treatment plant sludge (WTPS) into water bodies is, along with an enormous load of OM, the potential toxicity to the biota from iron or aluminium-based coagulants such as Alum (Al_2 $(SO_4)_3.18H_2O$) and ferric chloride ($FeCl_3.6H_2O$). WTPS may also contain pathogens (bacteria, viruses, and protists), organohalogen contaminants, and other metals (SOTERO-SANTOS; ROCHA; POVINELLI, 2005). In developed countries, water treatment sludges are dewatered and/or treated before disposal. The final disposal of WTPS may include disposal into surface water, sanitary sewers, landfills, regeneration, reuse, and mechanical or chemical treatment. Depending on its physical, chemical, and microbiological quality, it is possible to utilize these WTPS in agriculture and silviculture, brick manufacture, recovery of alum for reuse as a coagulant, or to control phosphorus, in the case of wastewater treatment plants sludge (SOTERO-SANTOS; ROCHA; POVINELLI, 2005). Therefore, due to its aluminium content, DWTP sludge cannot be considered inert solid waste, so using this sludge as feedstock for other applications to solve its final disposal issue could be a sustainable alternative (CREMADES; CUSIDÓ; ARTEAGA, 2018).

Pyrolysis is a mature heat treatment method in bio-energy production, solid waste management, and preparation of carbon-based materials (LI; JIANG, 2017). Nowadays, pyrolysis has been seen as an effective management and disposal alternative for a range of biomasses and wastes because this process can reduce weight, volume, and waste foul odour, making it easier to handle. Biochar has been studied as a low-cost sorbent, as a soil amendment, and as a means of mitigating global warming by carbon sequestration (OH et al., 2012). Biochar

is the solid product of pyrolysis, a material rich in carbon obtained when the biomass is heated in a closed vessel with little or no air available at relatively low temperatures (<700 °C) (LEHMANN; JOSEPH, 2009; YIN et al., 2017). Biochar can be produced from different materials such as agricultural residues, algal biomass, forest residues, manures, sewage sludge, energy crops, digestate, etc. (OLIVEIRA et al., 2017), all readily available in large quantities and at a low or no cost. Moreover, it could be seen as a way of resource utilization to convert waste biomass into valuable adsorbents (WEI; LU, 2021). Biochars can remove various contaminants from aqueous solutions but are still a new technology for the treatment of drinking water (GWENZI et al., 2017).

Due to the advantages of pyrolysis, this study proposes a new technique based on drinking water treatment sludge as a feedstock for manufacturing biochar via pyrolysis. The choice of sludge as a feedstock was due to its availability in large quantities, attractive characteristics for resource recovery, and because, under current Brazilian legislation, it is considered an environmental liability. The study was designed with the principal objectives: to characterize the composition and structural properties of the biochar and assess how these properties can influence biochar application in water treatment. The results may shed light on the management and use of waste materials, such as drinking water treatment sludge, and be valuable for developing biochar as low-cost sustainable adsorbents for natural waters and water treatment systems.

8 MATERIALS AND METHODS

8.1 Sludge sampling and biochar production

8.1.1 Biochar production

Samples for biochar production were collected at the Oeste WTP, which uses polyaluminium chloride (PACl) and cationic polymer as a coagulant and coagulant aid, respectively. The Oeste WTP, supplied by the Gavião reservoir (Fortaleza metropolitan Region, Ceará, Brazil) (Figure S1), operates with an average flow of 1.1 m^3/s, producing 10 tons of sludge per day. The annual cost to dispose of this waste in landfills is around $ 31,000. The Gavião reservoir has a storage capacity of 33.30 hm^3 and an area of 5.9 km^2 (equivalent to more than 814 football stadiums) and was chosen for this study for its importance to the State of Ceará since it supplies water to more than 4 million inhabitants in the metropolitan region of

Fortaleza. The Trophic State Index (TSI) of the reservoir can be classified as eutrophic, indicating waters with high productivity, mainly affected by human activities (BARROS et al., 2020).

Before pyrolysis, the sludge was dried in an oven at 110 ± 5 ºC to a constant weight. All dried material was then ground into fine particle size and stored in desiccators until further use. The starting material was then pyrolyzed via slow pyrolysis under oxygen-limited conditions at 450 ºC and 600 ºC in a bench-scale pyrolysis unit using a quartz tubular reactor installed in a bipartite tubular oven (FT-1200/H/V, Fortlab) under a heating rate of 30 ºC/min and a residence time of 30 min since Agrafioti et al. (2013) observed that pyrolysis reactions are completed within 30 min for sludge. According to their pyrolysis temperature, the biochars in this study were designated as BC450 and BC600. Part of the BC600 biochar has also been activated (item 2.1.3) and will be identified as BC600A throughout this paper.

8.1.2 Biochar yield

Biochar yield was determined as the ratio of the final weight of the produced biochar to the dry weight of sludge subjected to pyrolysis:

$$\text{Biochar yield (\%)} = \frac{B}{A} \text{x } 100 \qquad (1)$$

where A is the dry weight of the sludge sample before pyrolysis and B is the biochar weight.

8.1.3 Biochar activation

Several studies have reported the effectiveness of KOH-activated carbon in the adsorption of various organic chemicals such as phenol, dyes, heavy metals, and pesticides (HEIDARINEJAD et al., 2020). For the activation, 4.0 g of KOH was dissolved in 10 ml of ultrapure water under an ice bath, and 1.0 g of sample (BC600) was added. The suspension was mixed using a magnetic stirrer for 30 minutes and then dried at 105 °C for 12 h. The resulting material was carefully ground and transferred to an aluminium container. Heat treatment was carried out in a tube furnace (EDG, model FTHI/20) under a moderate nitrogen flow. The sample was treated at 700 °C for 1 h, with a heating rate of 10 ºC.min^{-1}. After cooling, the sample was washed with 0.5 mol.l^{-1} HCl and ultrapure water until the pH was close to 7. The resulting solid (BC600A) was dried at 70 °C for 24 h.

8.2 Biochar characterization

Physical and chemical analyses were conducted to provide the basic properties of both raw sludge and biochar samples. Since some previous results of BC600 showed potentially better adsorption characteristics, some characterizations were performed only for this biochar.

8.2.1 Proximate and ultimate analysis

Proximate analysis was carried out using a conventional oven and a balance with a resolution of 0.1 mg. The final values presented are the calculated average. Based on ASTM-D-2216-98 (1998), the moisture content of the sludge was determined by oven-drying it at 110 ºC until constant weight. The wet-basis moisture is determined as follows (BASU, 2010):

$$\text{Moisture (\%)} = \frac{\text{A} - \text{B}}{\text{A} - \text{C}} \text{x } 100 \quad (2)$$

where A is the weight of the wet sample and the crucible, B is the weight of the dried sample and crucible, and C is the weight of the crucible.

The volatile matter was determined according to Standard Methods (2540G) (APHA, 2017). Briefly, a dried sample of sludge was placed in a pre-weighed crucible, heated in a muffle furnace at 550 ± 50 ºC for 1 h, then cooled in a desiccator and weighed. (AGRAFIOTI et al., 2013). The percentage of the volatile matter was determined as follows:

$$\text{Volatile matter (\%)} = \frac{\text{A} - \text{C}}{\text{A} - \text{B}} \text{ x } 100 \quad (3)$$

where A is the weight of the dried sample and crucible, B is the weight of the crucible, and C is the weight of residue and crucible after ignition.

To determine the ash content, 2 g of dried sample was placed in a pre-weighed crucible. The sample and the crucible were weighted together and then heated in a muffle furnace at 600 ºC. After cooling in a desiccator, the crucible and ash were weighted (ASTM E1534−93, 2019). The percentage of ash was determined as follows:

$$\text{Total ash (\%)} = \frac{\text{A} - \text{C}}{\text{B} - \text{C}} \quad (4)$$

where A is the weight of the ash and the crucible, B is the weight of the sample and crucible, and C is the weight of the crucible.

The fixed carbon content can be determined by difference (ZHAO; TA; WANG, 2017):

$$\text{Fixed carbon (\%)} = 100 - \text{ASH} - \text{VM} \quad (5)$$

where ASH stands for total ash content and VM for the volatile matter content.

Carbon (C), hydrogen (H), and oxygen (O) contents were through the following equations (CARNEIRO et al., 2020; YANG et al., 2021):

$$C = 0.637\ FC + 0.455\ VM\ (wt\%) \quad (6)$$

$$H = 0.052\ FC + 0.062\ VM\ (wt\%) \quad (7)$$

$$O = 0.304\ FC + 0.476\ VM\ (wt\%) \quad (8)$$

8.2.2 Zeta potential, pH, and pH_{pzc}

For zeta potential measurements, 5 mg of each sample were initially added to 10 mL of ultrapure water, resulting in a suspension with a concentration of 0.5 mg/mL. Subsequently, the suspensions were sonicated in an ultrasonic bath (Cole-Parmer, IL, USA) for 5 min, and pH measurements were performed using a Quimis Q400AS benchtop pH meter. At the end of the pH measurements, the samples were suspended again for 3 min in an ultrasonic bath, and soon after, the zeta potential was measured. For such measurements, an aliquot of each suspension (900 µL) was pipetted into a DTS 1070 capillary (Malvern) and placed in a Zetasizer Nano ZS equipment (Malvern). It is essential to mention that the zeta potential measurements were performed in triplicate for all analyzed samples.

The pH_{pzc} of the samples was determined by the salt addition method (BAKATULA et al., 2018; LIU et al., 2012). The initial pH values (pH_i) of a series of conical flasks with 50 mL of 0.1 M $NaNO_3$ solution were adjusted with 0.1 M HNO_3 or 0.1 M NaOH as needed to obtain the appropriate pH range of 2 to 11. Then, 0.2 g of biochar was added to the solutions and shaken for 24h using an orbital shaker at 120 rpm. After separation by centrifugation, the solution's final pH (pHf) was measured, and the pH_{pzc} was found at ΔpH=0 from a plot of ΔpH ($pH_f - pH_i$) vs pH_i.

8.2.3 Specific surface area

The textural properties of the samples were analyzed using N_2 adsorption-desorption isotherms (Belsorp, Belsorp Mini II model). Samples were degassed at 150 °C for 15 hours under nitrogen flow before analysis. The determination of the specific surface area was performed from isotherms using the Brunauer-Emmet-Teller (BET) method, and the pore volume and diameter were obtained by the Barrett-Joyner-Halenda (BJH) method.

8.2.4 Thermogravimetric analysis

Thermogravimetric analysis (TGA) of the BC600 and BC600A samples was performed using the Netzsch STA 449 F3 Jupiter® equipment. Approximately 38 mg of sample BC600 and 7 mg of sample BC600A were used, packed in an alumina (Al_2O_3) crucible. Analyzes were performed in the temperature range of 30 to 900 ºC, with a heating rate of 10 ºC/min under synthetic air flow (20 mL/min).

8.2.5 Chemical composition analysis

The structural evaluation of the samples was performed by spectroscopy in the infrared region using a Bruker model VERTEX 70v. The solid samples were dispersed in KBr (Merck, spectroscopic grade), pastilled with a press (Poente Brasil), and then analyzed. The spectra were obtained in the region of 4000-350 cm^{-1}, in transmittance mode, with a resolution of 2 cm^{-1} and 128 scans.

The X-ray diffractograms of the samples were obtained using a Bruker model D8 Advanced, using $K\alpha_1$ radiation from Cu (λ = 0.154 nm). The measurements were performed under a current of 40 mA and a voltage of 40 kV. Scanning was performed between angles of $5º < 2\theta < 65º$ and an angular velocity of 0.02º/s. Phase identification was performed using the X'pert Highscore Plus software.

The Raman spectra were recorded through a Jobin Yvon T64000 triple spectrometer equipped with a charge-coupled device detector. The spectrometer allowed a 2 cm^{-1} resolution. As the excitation source it was used a laser He\\Ne emitting at λ=488 nm, two 45-sec accumulation each.

8.2.6 Scanning electron microscopy

The morphological properties of samples BC600 and BC600A were analyzed by scanning electron microscopy. The micrographs were obtained on an FEI Quanta 450 FEG microscope. The samples were prepared by placing them on carbon tape. Subsequently, they were metalized with gold (a film approximately 20 nm thick). A secondary electron detector (SE) was used for the morphological analysis, and the images were obtained with an electron beam acceleration voltage of 10 kV.

9 RESULTS AND DISCUSSION

9.1 Biochar production and properties

The operational parameters strongly influence the reaction conditions, biochar characteristics, and properties. Temperature, pressure, reaction time, particle size, and heating rate are some of the parameters that control the biochar yield and the final quality of the pyrolysis products, all of which significantly influence the capacity of biochar to adsorb various contaminants (BACH; CHEN, 2017; TRIPATHI; SAHU; GANESAN, 2016; YIN et al., 2017).

The temperature increase negatively affected the biochar yield, which decreased from 37.5 to 33.5 % as the temperature increased from 450 to 600 ºC (Table 4). The increase in temperature allows the thermal cracking of heavy hydrocarbon compounds, leading to an increase in liquid and gas production and a decrease in the solid fraction yield (AGRAFIOTI et al., 2013; TRIPATHI; SAHU; GANESAN, 2016). The results in the present study are similar to those of Agrafioti et al. (2013), which showed yields varying from 28.5 to 27.3 % when the temperature was increased from 400 to 500 ºC. Oh et al. (2012) also obtained a decrease in yield from 89.7 to 83 % when the pyrolysis temperature increased from 300 to 700 ºC. Hossain et al. (2011) observed an even higher yield decrease from 63.7 to 52.4 % with temperatures increasing from 400 to 700 ºC.

The biochar yield is also dependent on the feedstocks used. The low yield obtained in our work (37.5 to 33.5 %) is a consequence of the high mineral fraction present in the sludge, as observed by its high ash and low carbon contents (Table 5), therefore, generating biochar with more inorganic than organic characteristics (FIGUEREDO et al., 2017). High biochar yields must be carefully considered since feedstocks with high ash content, such as our sludge, lead to biochar mainly composed of ash (WEBER; QUICKER, 2018).

The dried sludge sample showed a pH of 5.6, and as the pyrolysis temperature increased from 450 to 600 ºC, biochar pH increased from 6.6 to 6.9 (Table 4). During the pyrolysis process, predominantly acidic functional groups are detached, i.e. carboxyl, hydroxyl, or formyl groups, and the remaining solid becomes more basic. Moreover, the ash content, which is also basic in nature, is increased during the process (Table 5). Therefore, a higher pH value is expected and can be seen as a direct outcome of the increasing degree of carbonization (WEBER; QUICKER, 2018) and progressive loss of the acid surface functional groups (FIGUEREDO et al., 2017).

Table 4 – Summary of biochar yield and properties

Source	PT (ºC)	Yield (%)	S_{BET} (m^2/g)	pH	pH_{pzc}	ZP (mV)
Sludge	-	-	-	5.6	-	-14.9 ± 4.19
BC450	450	37.5	43.18	6.6	7.5	+16.3 ± 5.04
BC600	600	33.5	66.54	6.9	8.0	+21.7 ± 6.06
BC600A	600	-	2,000	-	-	+5.4 ± 5.23

PT = pyrolysis temperature; S_{BET} = surface area; ZP = zeta potential

In the present study, BC600 showed a higher surface area (66.54 m^2/g) than BC450 (43.18 m^2/g), as shown in Table 4. These values are inferior by almost two and three-fold compared to results found by other authors. At a temperature of 600 ºC, Chen et al. (2021) obtained a surface area of 114.6 m^2/g for biochar derived from sewage sludge. Similarly, Oh et al. (2012) found a surface area of 119.7 m^2/g (mean of S_{BET} at 400 and 500 ºC) and 114.4 m^2/g at 600 ºC for biochar derived from water treatment sludge. Such difference could be due to the different nature of the sludge as well as the dewatering methods used (XU et al., 2018). The raw material's surface area changes due to the escaping of volatile gases during the carbonization process. Generally, increasing pyrolysis temperatures (> 500°C) results in a higher surface area (OLIVEIRA et al., 2017; WEBER; QUICKER, 2018), and, despite differing from some results found in the literature, the results obtained in this study followed this general trend.

After chemical activation, BC600A showed a substantial increase in the surface area, reaching 2,000 m^2/g, a thirty-fold increase from its original form (BC600). As illustrated in Figure S2, the non-activated biochar (BC600) had a total pore volume of 0.14 cm^3/g and an average pore diameter (D_{avg}) of 8.69 nm (Figure S2c), a textural characteristic of mesoporous materials, which provides a better understanding of which target molecule sizes will be able to diffuse and be adsorbed. After the KOH activation, BC600A had a total pore volume of 1.69 cm^3/g, indicating an increase of twelve-fold. The average pore diameter, however, was reduced to 3.38 nm (Figure S2d). These changes are attributed to the intrusion of KOH into the internal structure of biochar, where it reacted with carbon, enabling the formation of pores and contributing to the change in pore distribution (JIN et al., 2014).

A developed porous structure and high specific surface area provide a large space for the adsorption of contaminants and ensure a sufficient interaction between the adsorbent

and adsorbate (YIN et al., 2017). However, it is essential to note that knowledge of the total surface area alone may not be sufficient for some biochar applications. Despite possessing a large surface area, biochar with a surface composed mainly of very small pores, for example, does not necessarily imply that adsorption sites will be easily accessible to large target contaminants (PENDLETON; SCHUMANN; WONG, 2001; WEBER; QUICKER, 2018).

The data obtained by the salt addition method indicated that the point of zero charge (pH_{pzc}) – the pH below which the adsorbent surface is positive, while above this value, the surface charge is negative (LI et al., 2018) – is at pH of 7.5 and 8.0, for BC450 and BC600 respectively, as represented in Figure S3. This variable is crucial for water treatment because the charges of the adsorbate and the adsorbent must be opposite to occur a more significant electrostatic interaction between them; otherwise, if the charges are equal, the adsorption process will be hindered by electrostatic repulsion (BAUTISTA-TOLEDO et al., 2005).

Figure 3 – Zeta potential for the (a) sludge, biochars (BC450 and BC600) and (b) the comparison between non-activated (BC600) and activated biochar (BC600A)

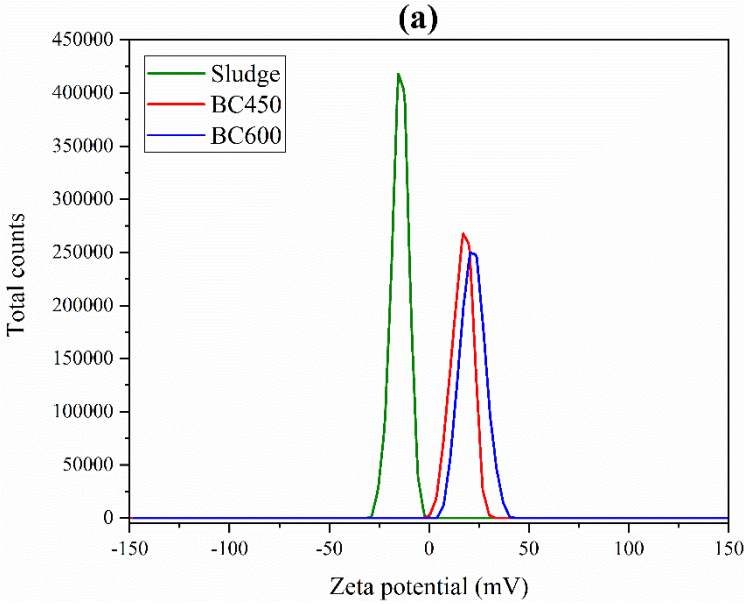

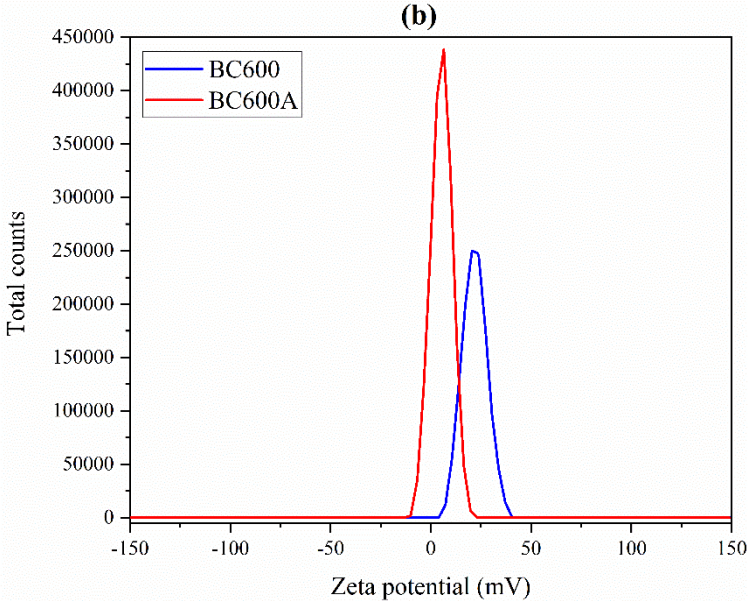

The zeta potential is the potential in the slipping plane of colloidal particles, and its value and sign are related to the surface charge of the particles and, in the water treatment context, it means how easy or difficult it is to coagulate the particles or colloids. Protonation and deprotonation of functional groups can create a net charge on the surfaces of the solid particle, which can form an electrical double layer in the solution phase near the surface (YUAN; XU; ZHANG, 2011). For most activated carbons, the surface charge at high pH values is negative, corresponding to the presence of negatively charged carboxylate and anhydride anionic surface functional groups. As shown in Table 4, after pyrolysis, the zeta potential of the sludge, initially negative, shifted to a positive surface charge for the biochar (Figure 3a). The zeta potential of biochar increases gradually with increasing temperature, indicating that the negative charge of the biochar surface gradually decreases, thus lowering the electronegativity. This phenomenon is related to the oxygen-containing functional groups on the surface of biochar (HONG; ZHANG; TAN, 2019; YUAN; XU; ZHANG, 2011). Such groups (i.e., COH, – COOH, etc.) have an important influence on the surface charge of biochar, and the content of oxygen-containing functional groups on the surface of biochar is closely related to the pH. The ash content plays a role in the pH, influencing the deprotonation of oxygen-containing functional groups, leading to changes in zeta potential. The pH of biochar increases with increasing pyrolysis temperature, while the oxygenated functional groups (–COH and – COOH) undergo different hydrolytic deprotonation (–CO– and –COO–) as the pH changes, thereby showing different electronegativity. Several studies have shown that the content of H and O gradually decreases with increasing temperature, and similar results were found in this study

(Table 5). As a result, the H/O functional groups also decrease. Therefore, the electronegativity of the biochar surface decreases with increasing pyrolysis temperature (HONG; ZHANG; TAN, 2019). Regarding the BC600A, due to chemical activation, the oxides (which carried more positive charges) were removed, thus resulting in a decrease in the zeta potential of the biochar (Figure 3b).

9.2 Proximate and ultimate analyses

Biomass containing more than 30 % moisture content is unsuitable for pyrolysis because it will inevitably lead to a low mass yield. For a better yield, dry biomass is advisable (TRIPATHI; SAHU; GANESAN, 2016; WEBER; QUICKER, 2018). During pyrolysis, while the water is wholly driven off, the ash content, on the other hand, largely remains in the solid product. It is crucial to determine the ash content of the biochar because the amount and type of inorganics can establish the possible applications. A high ash content may inhibit its use in high-grade industrial applications (WEBER; QUICKER, 2018).

As shown in Table 5, the ash content increased when the pyrolysis temperature increased. This behaviour agrees with most biochar studies since biochar ash content largely depends on the feedstock. As a large part of the ash content remains in the solid product, while water and volatile matter are released, the ash content inevitably increases with increasing temperature (WEBER; QUICKER, 2018). The ash content found in this study for the sludge feedstock (32 %) was lower than those found by Oh et al. (2012) and Carneiro et al. (2020), which ranged from 76 % to 68.9 %, respectively, but similar to those found in sewage sludge by Hossain et al. (2011) and Agrafioti et al. (2013), which ranged from 34 % to 25.9 %, respectively. The ash content in the sludge-derived biochar ranged from 61.3 to 71.1 % (Table 5) as temperature increased from 450 ºC to 600 ºC, a similar range (63.3 to 72.5 %) found by Hossain et al. (2011) at 400-700 ºC. However, Oh et al. (2012) found a higher biochar ash content, ranging from 83.8 to 90.6 % at 400-700 ºC. This high ash content seems a common trend amongst biochar groups of sludge and animal waste, whereas biochars made from herbaceous feedstocks show lower ash content. High ash content is undesirable due to the significant presence of inorganic minerals, which may cause the blockage of available pores and limit sorption sites' accessibility. Biochar usually needs to be washed using weak acid or deionized water to remove the ash content and expose more sorption sites (LI et al., 2018, 2019).

After the release of volatiles, the remaining carbon in biochar is identified as fixed carbon. High fixed carbon indicates a great extent of carbonization and low volatile content

(AHMED; HAMEED, 2020). The volatile matter and fixed carbon content present in the sludge (Table 5) differed from those obtained by Carneiro et al. (2020) (25.1 % and 6.0 %, respectively) and also from those observed by Hossain et al. (2011) (50.2 % and 8.2 %, respectively). As for the biochars, the volatile matter content was similar to those observed by Hossain et al. (2011), from 25.7 to 15.8 %, but differed significantly in fixed carbon content as it varied from 6.8 to 8.3 % as temperature increased from 400 to 700 ºC in their study.

Table 5 – Ultimate and proximate analysis of sludge and non-activated biochar

Source	Proximate analysis (wt%)				Ultimate analysis (wt%)			Atomic ratios	
	M[a]	VM	Ash	FC	C	H	O	H/C	O/C
Sludge	84	67.6	32.0	0.4	31.0	4.2	32.3	0.1358	1.0415
BC450	-	37.3	61.3	1.4	17.9	2.4	18.2	0.1335	1.0178
BC600	-	28.7	71.1	0.2	13.2	1.8	13.7	0.1357	1.0407

[a] wet-basis; M = moisture; VM = volatile matter; FC = fixed carbon;

When producing biochar, one of the main goals is to increase the stoichiometric carbon content in its chemical composition compared to that of the raw feedstock. An increase in reaction temperature should lead to a relative increase in carbon content while resulting in a lower relative content of hydrogen and oxygen due to the detachment of functional groups containing the latter elements (WEBER; QUICKER, 2018). However, as the pyrolysis temperature was increased, the C, H, and O content in our samples decreased in the same proportion (Table 5). This may be due to the high ash content present in the raw sludge (LI et al., 2018). Similarly, other studies found that when biosolids were used to produce biochar, the C content decreased with the increase of pyrolysis temperature because the C content was vulnerable to rapid thermal decomposition (LI et al., 2019). Some authors also suggest that charcoals produced from residues generally result in biochar with high ash content, which may be a result of the silica and other minerals present in the raw material and the gradual loss of C, H, and O during processing (FIGUEREDO et al., 2017).

The atomic ratios of O/C and H/C in biochar correlate directly with aromaticity, biodegradability, and polarity, which are highly desirable properties for removing organic pollutants (OLIVEIRA et al., 2017). As shown in Table 5, such atomic ratios remained almost the same despite the increase in the pyrolytic temperature to 450 ºC. Changes in the number of functional groups alter the material's affinity to water. A further increase in pyrolysis temperature possibly could result in more hydrophobic biochar due to the removal of more polar

surface functional groups. Thus aromaticity would be increased (WEBER; QUICKER, 2018), which would be noted by the decrease in the O/C ratio. However, as the temperature increased to 600 ºC, the hydrophilicity and aromaticity indexes, O/C and H/C, respectively, for BC600 increased (Table 5), showing similar values to those initially found in the sludge feedstock, indicating a less hydrophobic character.

Similarly, different authors (LI et al., 2018; ZORNOZA et al., 2016) have observed that treating biochar at higher temperatures may again reduce the hydrophobic character of the adsorbent (WEBER; QUICKER, 2018). Zornoza et al. (2016) produced biochar from pig manure, crop residues, and municipal solid waste at temperatures ranging from 300 to 700 °C. At 300 ºC all the biochars were classified as highly hydrophobic, likely due to the presence of labile aliphatic compounds, however, hydrophobicity disappeared totally in all biochars produced over 500 ºC. Li et al. (2018) produced biochar from chicken manure and observed a similar trend in the O/C ratio when the temperature increased from 300 to 600 ºC. All the biochars previously mentioned also had a high ash content. These results, therefore, corroborate those found in the present study for sludge-derived biochar.

9.3 Thermogravimetric analysis

After thermogravimetric (TG) analysis up to 900 ºC, the sludge, BC600, and BC600A lost 55.79 %, 36.91 %, and 79.59 % of their initial mass, respectively (Figure 4). The weight loss of biochar BC600 was lower than that of sludge due to the lower moisture and volatile matter content (HAO; YANG; JAHNG, 2018). Sludge thermal decomposition is a complicated process in which drying, devolatilization, heterogeneous reaction, ignition, and burnout occur (HAO; YANG; JAHNG, 2018).

As shown in Figure 4a, the derivative thermogravimetric (DTG) curve for the feedstock demonstrates a three-step mass loss. Dewatering generally occurs in a temperature range of 30 to 105 °C, but depending on the force of arrangement between water molecules and organic or inorganic compounds, the water may be removed at higher temperatures (CARNEIRO et al., 2020). Compared to lignocellulosic biomasses, the thermal decomposition temperature of DWT sludge is substantially lower, which indicates inferior thermal stability (CHOI et al., 2019). The second mass loss occurred at a temperature of 200 to 365 ºC, when the volatiles were released and/or burned, indicating that approximately 20.5 % of the initial mass was lost within this temperature range. The third mass loss occurred at a temperature range of 365 to 580 ºC, with a weight loss of 17.3 %. Similarly, Choi et al. (2019) found that most

mass decay of DWTS occurs from 120 to 580 °C, which is attributed to volatilization of the organic mass fraction in DWTS in line with dehydration of $Al(OH)_3$ (i.e. $2Al(OH)_3 \rightarrow Al_2O_3 + 3H_2O$). Therefore, the main decomposition in the sludge occurred between 200 to 580 ºC. It was also observed that mass loss by thermal decomposition was lower at temperatures > 600 ºC, as shown in the TG curve (HAO; YANG; JAHNG, 2018). It is generally stated that low pyrolysis temperatures (< 400 ºC) are linked to the decomposition of easily-degradable compounds like carbohydrates, simple lipids, and amino acids. In comparison, the high-temperature region (400–600 ºC) is responsible for decomposing compounds with high molecular weight, like aromatic compounds and polyphenols (XU et al., 2018). Many authors found similar results (CABALLERO et al., 1997; CARNEIRO et al., 2020; HAO; YANG; JAHNG, 2018; LI et al., 2014). On the other hand, slow thermal degradation rates at temperatures > 600 °C are likely attributed to char formation (carbonization) in line with dehydrogenation (CHOI et al., 2019).

Figure 4 – TG-DTG curves for the (a) sludge, (b) BC600, and (c) BC600A

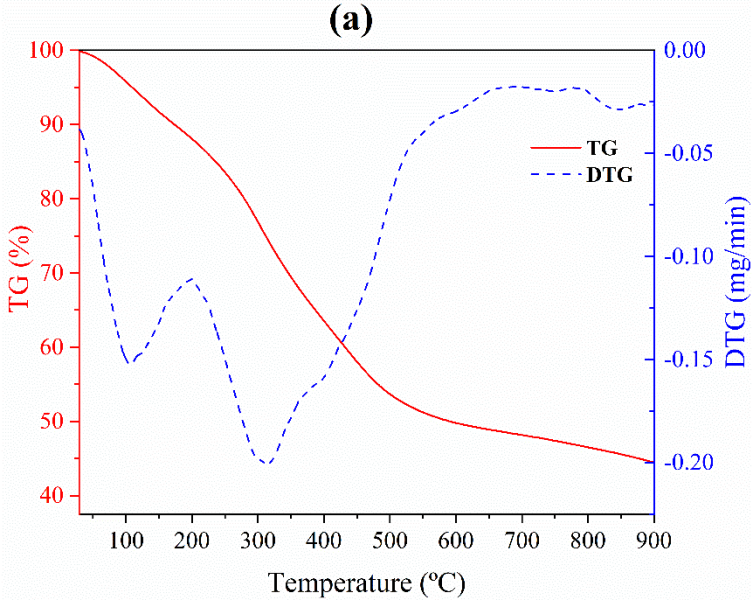

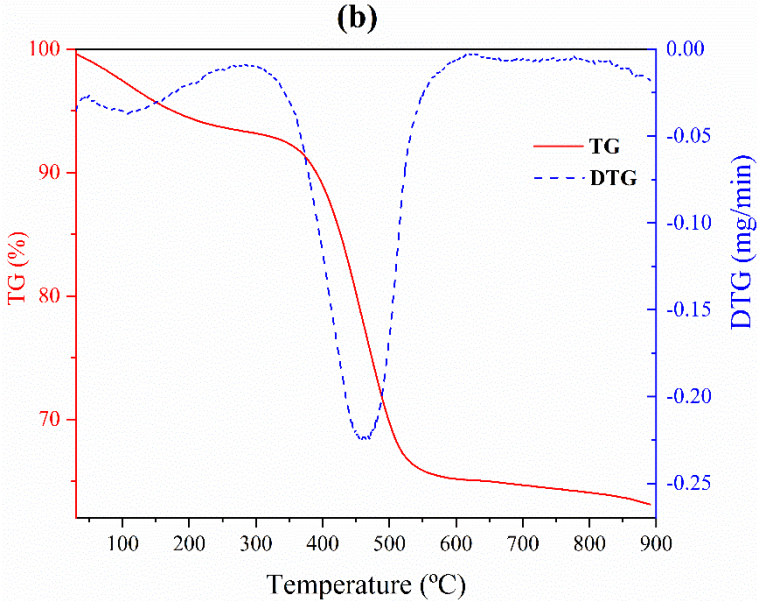

For the BC600, the DTG curve (Figure 4b) demonstrates a two-step mass loss. The first one is related to dehydration, going up to 150 ºC and causing a mass loss of 4.28 %. The second and main one occurred at a temperature range of 350 to 600 ºC, with a weight loss of 27.1 %. As previously observed, mass loss by thermal decomposition was nearly finished when the temperature reached 600 ºC. Activated biochar BC600A (Figure 4c) showed a mass loss of 5 % due to dehydration at 107 ºC. From 107 ºC to 387 ºC, the material had a mass loss of 8.06%, a range in which the volatiles were released and/or burned. From 387 ºC to around 605 ºC, the activated biochar lost around 60.72 % of its mass, presumably due to the organic/inorganic ratio modification caused by the chemical activation, thus allowing a higher presence of carbon in the material. From 605 ºC to 900 ºC, the activated biochar showed a mass loss of 5.11 % and

thermal decomposition was nearly finished within that temperature range. Comparing the TG-DTG data for different types of sludge, Carneiro et al. (2020) observed that drinking water treatment sludge may possess higher levels of mineral material in their composition, as their mass loss was much lower compared to other types of sludge, as observed in our experiment.

9.4 Chemical composition

The main chemical composition of sludges, in which PACl is used as a coagulant, comprises oxides of aluminium, silica, and iron (Table 6). The higher concentration of aluminium oxide in the sludge might occur because of the coagulant added to water treatment processes (OH et al., 2012), which is used to settle down suspended solids like clay and sand from water. As for the presence of SiO_2 in DWT sludge, it likely originated from clay minerals and free silica particles (YAZDANI et al., 2019).

Table 6 – Principal chemical compositions of drinking water treatment sludge

Source	SiO_2	Al_2O_3	Fe_2O_3	CaO	K_2O	TiO_2	SO_3	P_2O_5	MnO	Total (wt%)
Sludge	40.0	49.9	5.6	1.4	1.4	0.6	0.4	0.4	0.3	100

Source: Adapted from Oh et al. (2012)

The Fourier transform infrared spectroscopy (FT-IR) determines the functional groups on the biochar surface. Surface functional groups mainly include oxygen, nitrogen, hydrogen, halogen, etc., amongst which the oxygen and nitrogen groups significantly affect the adsorptive property of biochar (AHMED; HAMEED, 2020). Differences in infrared spectra are reflected by water loss, organic matter combustion, and an increase in mineral component ratio resulting from heat-induced mass loss (OH et al., 2012). FT-IR analysis of the samples was performed from 400 cm^{-1} to 4000 cm^{-1}; the spectra are shown in Figure 5. Usually, the broad and strong absorption peaks, seen in the range of 3300–3425 cm^{-1}, derive from the stretching vibration of –OH (CHEN et al., 2021). In the sludge feedstock and biochar spectra, the broadband occurred in the 3647- 3096 cm^{-1} range due to O–H stretching in –OH groups. The peak at 1085 cm^{-1} was due to C–O stretching of carbohydrate and alcohol functions. The bands below 600 cm^{-1} are due to metal–halogen stretching vibrations in both organic and inorganic halogen compounds. The presence of functional groups, such as the hydroxyl groups, suggests that the biochar could potentially be used as an adsorbent. The presence of the alkane group

was confirmed by C–H stretching at 2930 cm^{-1}. Also, the intensity of the peak observed in BC600 at 3416 $cm^{-1,}$ and 1456 cm^{-1} significantly decreased compared to the raw feedstock and BC450, reiterating the release of volatile content. (GHODKE et al., 2021; OH et al., 2012).

Figure 5 – FT-IR spectra showing the changes in the sludge and biochar

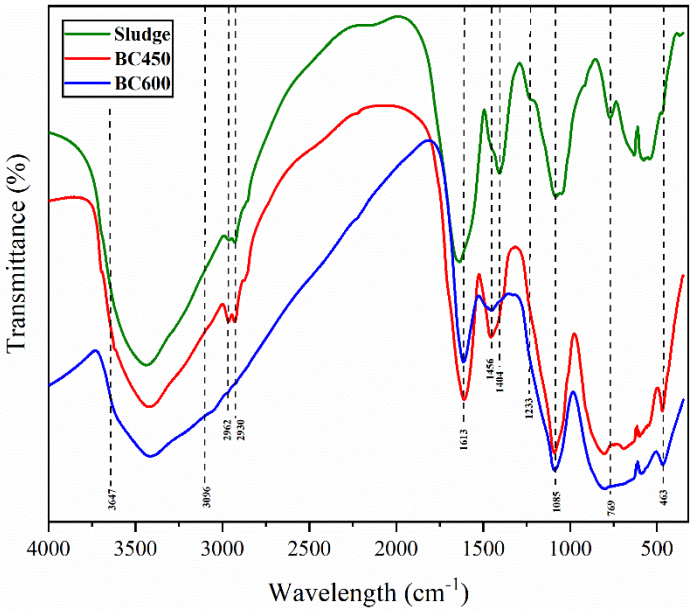

As previously discussed and reported by other authors, pyrolysis of sludge between 300 and 600 ºC resulted in considerable weight loss. It generated a char with an amorphous carbon matrix due to the conversion of the organic matter present in the sludge during thermal decomposition (FIGUEREDO et al., 2017).

Raman spectroscopy was used to analyse further the carbonaceous material's structure and degree of graphitization (Figure 6). The curve exhibited two bands at 1365 and 1597 cm^{-1}, corresponding to the D-band and G-band, respectively. The D-band could be labelled as the amorphous or disordered graphite, while the G-band could be regarded as indicative of the presence of graphitic crystallites (CHEN et al., 2021; ZHANG et al., 2015).

Figure 6 – Raman spectra for the non-activated biochar

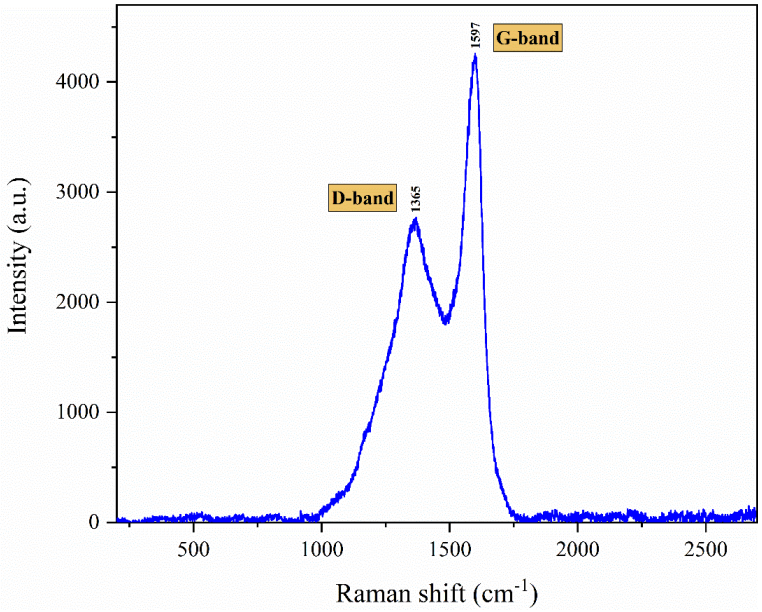

As shown in Figure 7, XRD data indicate the presence of quartz (Q) and gypsum (G), which were the most recognizable crystallographic structures in the BC600 sample. Gypsum structures probably originated from the aluminium-based coagulant agent applied in conventional water treatment, and quartz may be originated from suspended sediments and discharge of domestic or industrial effluent contribution (CARNEIRO et al., 2020). Similarly, Chiang et al. (2009) found that, in DWT sludge, silica is the principal crystalline phase present, and relatively low-intensity peaks corresponding to those for Al_2O_3 and Fe_2O_3 were also detected in their study.

Figure 7– XRD spectrum for the crystalline phases of the sludge and the sludge-derived biochar

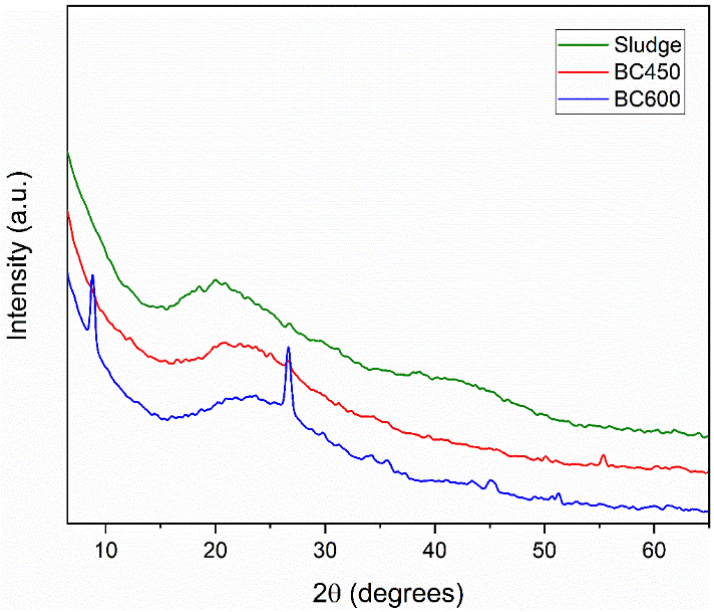

9.5 Scanning electron microscopy

Scanning electron microscopy (SEM) images are very useful for obtaining accurate details about the surface structure of biochar, showing the nature of biochar surface, and clarifying the development of pores (AHMED; HAMEED, 2020) as the comparison of the images between materials might enable a better understanding of the morphological changes due to pyrolysis (OH et al., 2012). Figure 8 shows SEM micrographs of biochar and activated biochar. Figures 8(a-b) show a poor structure that is smoothly compacted and covered with impurities. Contrastingly, after alkali activation (Figures 8(c-d)), the biochar sample presented a rougher surface with a more developed surface, showing a more intense presence of porous structures (JIN et al., 2014). The structural difference may reflect the specific surface area and the adsorption capacity as an environmental and cost-effective adsorbent for nutrients or pollutants (OH et al., 2012).

Figure 8 – SEM micrographs for the (a-b) biochar and (c-d) chemically activated biochar

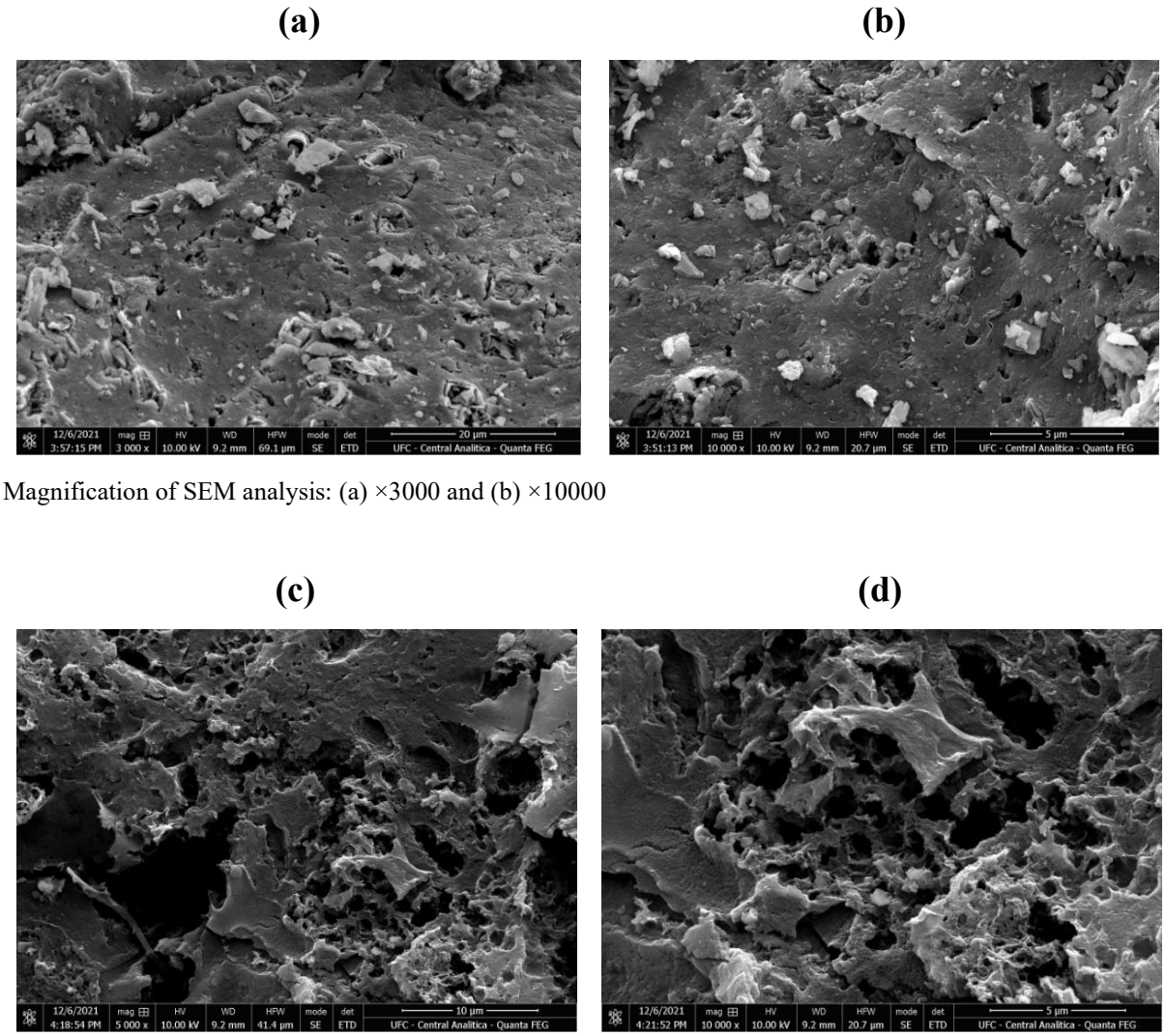

Magnification of SEM analysis: (a) ×3000 and (b) ×10000

Magnification of SEM analysis: (c) ×5000 and (d) ×10000

10 CONCLUSIONS

The high mineral fraction in the DWT sludge resulted in ash-rich and low-carbon-content biochar, thus, attributing more inorganic than organic characteristics to the material. As the ash content plays a significant role in the biochar's pH, it directly influences the zeta potential, which is crucial for water treatment performance. Chemical activation resulted in both an increase and development in the surface area and a decrease in the zeta potential. The biochar produced at a higher temperature showed a more developed carbonaceous structure typical of adsorbent materials, and the presence of functional groups, such as hydroxyl, suggests that the sludge biochar could potentially be used as an adsorbent. We conclude that such sludge

biochar production and properties complexity may limit its adsorption capacity as an environmental and cost-effective adsorbent for water treatment or high-grade applications.

REFERENCES

ABBAS, T. et al. Recent advancements in the removal of cyanotoxins from water using conventional and modified adsorbents—a contemporary review. **Water (Switzerland)**, v. 12, n. 10, 1 out. 2020.

AGRAFIOTI, E. et al. Biochar production by sewage sludge pyrolysis. **Journal of Analytical and Applied Pyrolysis**, v. 101, p. 72–78, 2013.

AHMED, M. J.; HAMEED, B. H. Insight into the co-pyrolysis of different blended feedstocks to biochar for the adsorption of organic and inorganic pollutants: A review. **Journal of Cleaner Production**, v. 265, p. 121762, 2020.

APHA. **Standard Methods for the Examination of Water and Wastewater**. 23rd. ed. Washington, DC: American Public Health Association, 2017.

ASTM-D-2216-98. Standard Test Method for Laboratory Determination of Water (Moisture) Content of Soil and Rock by Mass. **ASTM International**, n. January, p. 1–5, 1998.

ASTM E1534−93. Standard Test Method for Determination of Ash Content of Particulate Wood Fuels. **ASTM International**, p. 1–2, 2019.

BACH, Q. V.; CHEN, W. H. Pyrolysis characteristics and kinetics of microalgae via thermogravimetric analysis (TGA): A state-of-the-art review. **Bioresource Technology**, v. 246, p. 88–100, 1 dez. 2017.

BAKATULA, E. N. et al. Determination of point of zero charge of natural organic materials. **Environmental Science and Pollution Research**, v. 25, n. 8, p. 7823–7833, 2018.

BARROS, M. U. G. et al. Icyano: A cyanobacterial bloom vulnerability index for drinking water treatment plants. **Water Science and Technology: Water Supply**, v. 20, n. 8, p. 3517–3530, 2020.

BASU, P. **Biomass gasification and pyrolysis: practical design and theory**. Burlington: Elsevier, 2010.

BAUTISTA-TOLEDO, I. et al. Bisphenol A removal from water by activated carbon. Effects of carbon characteristics and solution chemistry. **Environmental Science and Technology**, v. 39, n. 16, p. 6246–6250, 2005.

CABALLERO, J. A. et al. Characterization of sewage sludges by primary and secondary pyrolysis. **Journal of Analytical and Applied Pyrolysis**, p. 433–450, 1997.

CARNEIRO, M. et al. Sludge and scum blends from water and sewage treatment plants for energy recovering toward a circular economy perspective. **International Journal of Environmental Science and Technology**, v. 17, n. 9, p. 3847–3856, 2020.

CHEN, W. et al. Effect of hydrothermal pretreatment on pyrolyzed sludge biochars for tetracycline adsorption. **Journal of Environmental Chemical Engineering**, v. 9, n. 6, p. 106557, 2021.

CHIANG, K. Y. et al. Lightweight bricks manufactured from water treatment sludge and rice husks. **Journal of Hazardous Materials**, v. 171, n. 1–3, p. 76–82, 2009.

CHOI, D. et al. Valorization of alum sludge via a pyrolysis platform using CO2 as reactive gas medium. **Environment International**, v. 132, n. July, p. 105037, 2019.

CHOW, C. W. K. et al. The impact of conventional water treatment processes on cells of the cyanobacterium microcystis aeruginosa. **Water Research**, v. 33, n. 15, p. 3253–3262, 1999.

CREMADES, L. V.; CUSIDÓ, J. A.; ARTEAGA, F. Recycling of sludge from drinking water treatment as ceramic material for the manufacture of tiles. **Journal of Cleaner Production**, v. 201, p. 1071–1080, 2018.

FIGUEREDO, N. A. DE et al. Characterization of biochars from different sources and evaluation of release of nutrients and contaminants. **REVISTA CIÊNCIA AGRONÔMICA**, v. 48, n. 3, p. 395–403, 2017.

GHODKE, P. K. et al. Pyrolysis of sewage sludge for sustainable biofuels and value-added biochar production. **Journal of Environmental Management**, v. 298, n. January, 2021.

GWENZI, W. et al. Biochar-based water treatment systems as a potential low-cost and sustainable technology for clean water provision. **Journal of Environmental Management**, v. 197, p. 732–749, 15 jul. 2017.

HAO, Z.; YANG, B.; JAHNG, D. Combustion characteristics of biodried sewage sludge. **Waste Management**, v. 72, p. 296–305, 2018.

HEIDARINEJAD, Z. et al. Methods for preparation and activation of activated carbon: a review. **Environmental Chemistry Letters**, v. 18, n. 2, p. 393–415, 2020.

HONG, M.; ZHANG, L.; TAN, Z. Effect mechanism of biochar's zeta potential on farmland soil's cadmium immobilization. **Environmental Science and Pollution Research**, n. 26, p. 19738–19748, 2019.

HOSSAIN, M. K. et al. Influence of pyrolysis temperature on production and nutrient properties of wastewater sludge biochar. **Journal of Environmental Management**, v. 92, n. 1, p. 223–228, jan. 2011.

JIN, H. et al. Biochar pyrolytically produced from municipal solid wastes for aqueous As(V) removal: Adsorption property and its improvement with KOH activation. **Bioresource Technology**, v. 169, p. 622–629, out. 2014.

LEHMANN, J.; JOSEPH, S. Biochar for Environmental Management: An Introduction. In: LEHMANN, J.; JOSEPH, S. (Eds.). . **Biochar for Environmental Management: Science and Technology**. 1. ed. London: Routledge, 2009.

LI, D. C.; JIANG, H. The thermochemical conversion of non-lignocellulosic biomass to form biochar: A review on characterizations and mechanism elucidation. **Bioresource Technology**, v. 246, p. 57–68, 1 dez. 2017.

LI, J. et al. Comparative study for microcystin-LR sorption onto biochars produced from various plant- and animal-wastes at different pyrolysis temperatures: Influencing mechanisms

of biochar properties. **Bioresource Technology**, v. 247, p. 794–803, jan. 2018.

LI, L. et al. TG-MS analysis of thermal behavior and gaseous emissions during co-combustion of straw with municipal sewage sludge. **Journal of Thermal Analysis and Calorimetry**, v. 118, n. 1, p. 449–460, 2014.

LI, S. et al. Predicting biochar properties and functions based on feedstock and pyrolysis temperature: A review and data syntheses. **Journal of Cleaner Production**, v. 215, p. 890–902, 2019.

LIU, Y. et al. Characterization of bio-char from pyrolysis of wheat straw and its evaluation on methylene blue adsorption. **Desalination and Water Treatment**, v. 46, n. 1–3, p. 115–123, 2012.

OH, T. K. et al. Characterization of biochar derived from three types of biomass. **Journal of the Faculty of Agriculture, Kyushu University**, v. 57, n. 1, p. 61–66, 2012.

OLIVEIRA, F. R. et al. Environmental application of biochar: Current status and perspectives. **Bioresource Technology**, v. 246, p. 110–122, dez. 2017.

PENDLETON, P.; SCHUMANN, R.; WONG, S. H. Microcystin-LR adsorption by activated carbon. **Journal of Colloid and Interface Science**, v. 240, n. 1, p. 1–8, 2001.

PESTANA, C. J. et al. Fate of cyanobacteria in drinking water treatment plant lagoon supernatant and sludge. **Science of the Total Environment**, v. 565, p. 1192–1200, 2016.

QI, X. et al. Combustion performance and slagging characteristics during co-combustion of Zhundong coal and sludge. **Journal of the Energy Institute**, v. 91, n. 3, p. 397–410, 2018.

SOTERO-SANTOS, R. B.; ROCHA, O.; POVINELLI, J. Evaluation of water treatment sludges toxicity using the Daphnia bioassay. **Water Research**, v. 39, n. 16, p. 3909–3917, 2005.

TRIPATHI, M.; SAHU, J. N.; GANESAN, P. Effect of process parameters on production of biochar from biomass waste through pyrolysis: A review. **Renewable and Sustainable Energy Reviews**, v. 55, p. 467–481, mar. 2016.

WEBER, K.; QUICKER, P. Properties of biochar. **Fuel**, v. 217, n. December 2017, p. 240–261, abr. 2018.

WEI, L.; LU, J. Adsorption of microcystin-LR by rice straw biochars with different pyrolysis temperatures. **Environmental Technology and Innovation**, v. 23, p. 101609, 2021.

XU, Q. et al. Pyrolysis kinetics of sewage sludge and its biochar characteristics. **Process Safety and Environmental Protection**, v. 115, p. 49–56, 2018.

YANG, H. et al. Effect of pyrolysis conditions on food waste conversion to biochar as a coagulant aid for wastewater treatment. **Journal of Water Process Engineering**, v. 41, n. February, 2021.

YAZDANI, M. et al. Improvement of biogas production from slaughterhouse wastewater using biosynthesized iron nanoparticles from water treatment sludge. **Renewable Energy**, v.

135, p. 496–501, 2019.

YIN, Q. et al. Biochar as an adsorbent for inorganic nitrogen and phosphorus removal from water: a review. **Environmental Science and Pollution Research**, v. 24, n. 34, p. 26297–26309, 1 dez. 2017.

YUAN, J. H.; XU, R. K.; ZHANG, H. The forms of alkalis in the biochar produced from crop residues at different temperatures. **Bioresource Technology**, v. 102, n. 3, p. 3488–3497, 2011.

ZHANG, J. et al. Multiscale visualization of the structural and characteristic changes of sewage sludge biochar oriented towards potential agronomic and environmental implication. **Scientific Reports**, v. 5, p. 1–8, 2015.

ZHAO, S. X.; TA, N.; WANG, X. D. Effect of temperature on the structural and physicochemical properties of biochar with apple tree branches as feedstock material. **Energies**, v. 10, n. 9, 2017.

ZORNOZA, R. et al. Stability, nutrient availability and hydrophobicity of biochars derived from manure, crop residues, and municipal solid waste for their use as soil amendments. **Chemosphere**, v. 144, p. 122–130, 2016.

SUPPLEMENTARY MATERIALS

Figure S1 – Location of the Gavião reservoir in the State of Ceará, Brazil

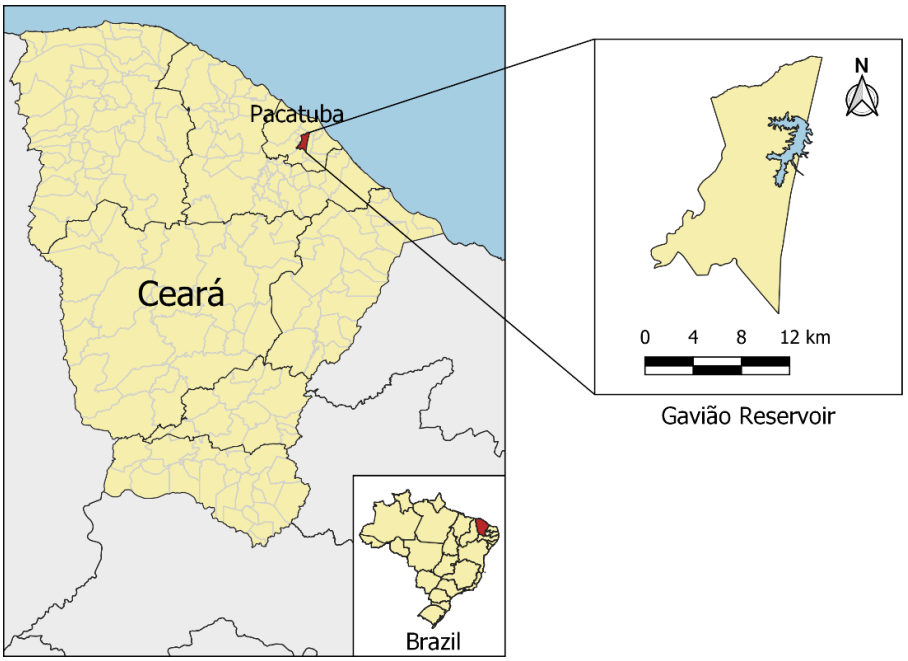

Figure S2 – Nitrogen adsorption-desorption isotherms for the (a) BC600 and (b) BC600A and pore size distribution for (c) BC600 and (d) BC600A

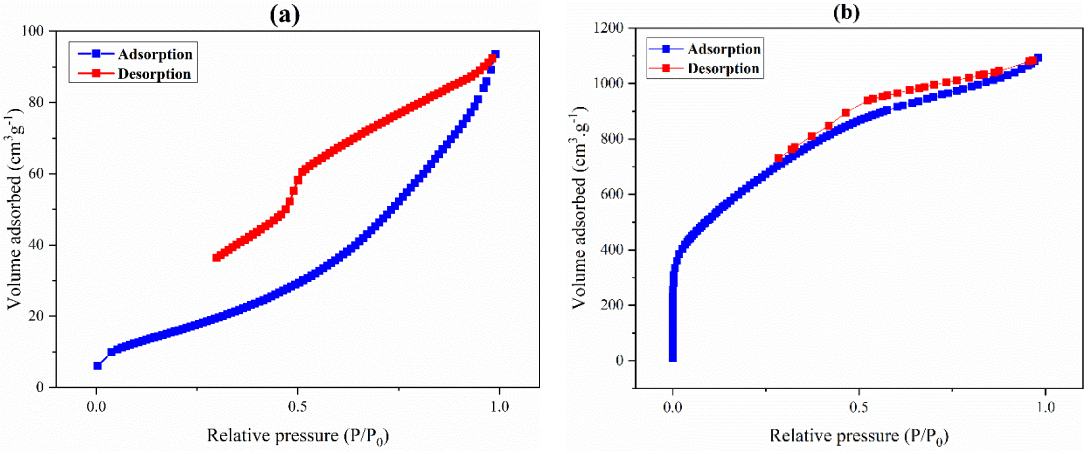

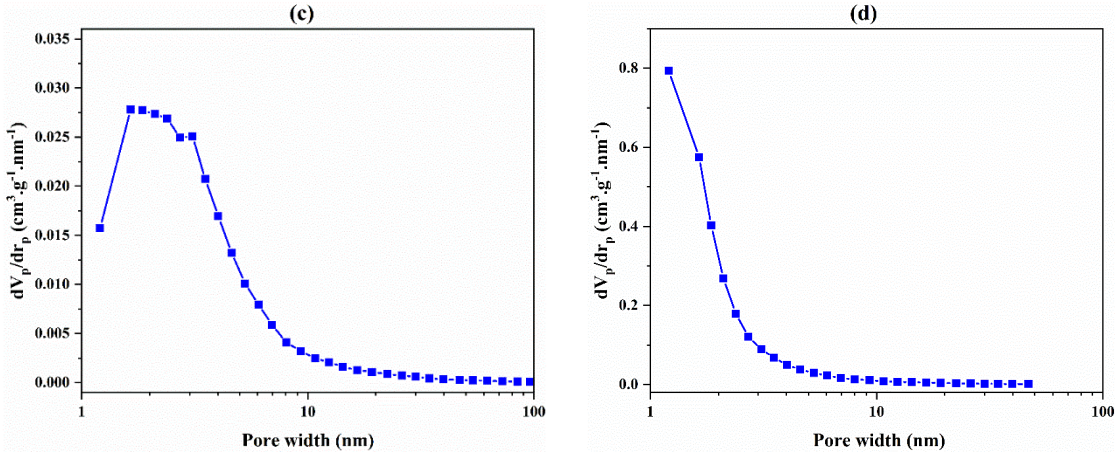

Figure S3 – pH_{pzc} curves for (a) BC450 and (b) BC600

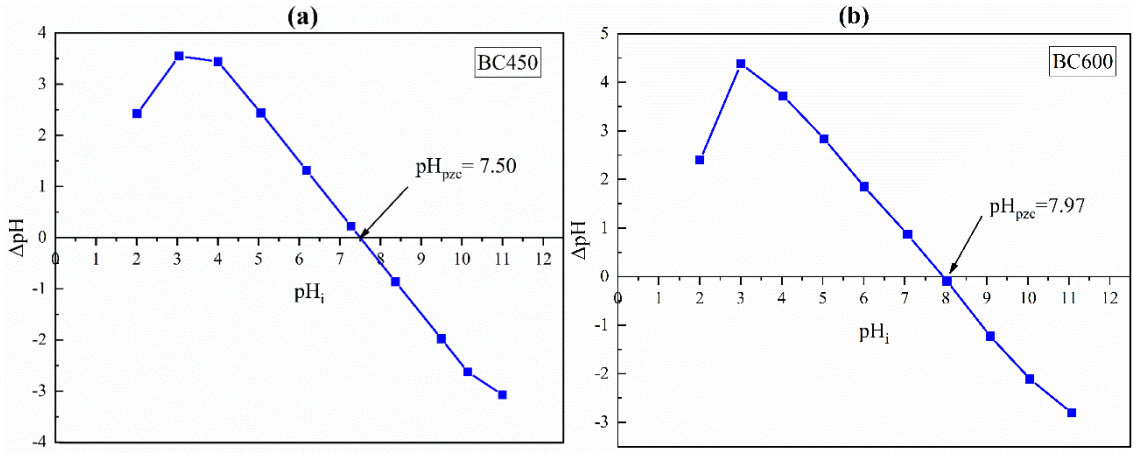

CHAPTER III

Application and assessment of sludge-derived biochar in water treatment systems as a potentially sustainable solution toward a circular economy

Application and assessment of sludge-derived biochar in water treatment systems as a potentially sustainable solution toward a circular economy

André Madson Araújo Frota[1], Thaís Lopes Pinheiro[1], Stefany Lobo Almeida[1], Erdin Ibraim[2], Tannaz Pak[3], José Capelo Neto[1]

[1]Federal University of Ceará, [2]University of Bristol, [3]Teesside University

ABSTRACT

Biochar has mainly been used for soil amendment, carbon sequestration, and reducing greenhouse gas emissions, but knowledge about the practical application of biochar in water treatment operations, such as drinking water or wastewater systems, is limited. Due to its adsorptive properties and lower cost, biochar has been considered a potential substitute for activated carbon in environmental remediation and water treatment. This research explored the application of drinking water treatment sludge-derived biochar as an adsorbent material for natural water treatment. Central composite design (CCD) and response surface methodology (RSM) were used to design the experiment, optimise the effective parameters with a minimum number of experiments, and analyse the interaction effects between the operating parameters. The main objective of this study was to develop and assess models for the removal of colour, turbidity, chlorophyll-*a*, and UV_{254} as responses to produce high-quality drinking water. This research demonstrated that DWT sludge biochar failed to improve water quality. The inorganic nature of the biochar might impact its performance; However, its addition did not significantly affect the water quality negatively, showing potential for its application in water treatment given its possible enhancement via a post-treatment process.

Keywords: Biochar. Sludge. Pyrolysis. Response surface methodology. Eutrophic water.

11 INTRODUCTION

Eutrophication is one of the most common causes of water quality impairment in inland and marine waters (LE MOAL et al., 2019). It produces several undesirable effects, among which we can highlight: recreational and aesthetic problems, loss of oxygen, occasional fish kills, loss of biodiversity, changes in the quality and quantity of fish of commercial value, and release of algal toxins, in addition to higher costs and more severe difficulties in water treatment regarding the removal of algae, colour, taste, and odour compounds, as well as greater consumption of chemicals and more frequent backwashing of filters, amongst other issues (CARPENTER et al., 1998; CHEUNG; LIANG; LEE, 2013; LE MOAL et al., 2019; PAERL; OTTEN, 2013; PAERL; PAUL, 2012; YIN et al., 2017). In aquatic ecosystems, cyanobacterial blooms are the most common problem linked to eutrophication. There are several indications that they have been occurring more frequently in freshwaters due to climate change and anthropic eutrophication, along with their ability to adapt and thrive in adverse or changing environmental conditions (BOTANA, 2016; LEHMAN et al., 2017; LÜRLING; VAN OOSTERHOUT; FAASSEN, 2017; PAERL; OTTEN; JOYNER, 2016; WELLS et al., 2015). Some cyanobacteria can produce toxins, tastes, and odours, significantly impairing water quality (CHOW et al., 1999).

In north-east Brazil, a semiarid region, cyanobacteria dominance and blooms are quite recurrent due to several factors, namely, high temperature, long photoperiods, alkaline pH, and abundant nutrient availability (LINS et al., 2016). Water scarcity and poor water quality are linked because contamination reduces the water supply and increases the costs of treating water for use (CARPENTER et al., 1998). Therefore, this poses a severe problem for a semiarid region because, in addition to the problems with the availability of water resources in terms of quantity, it is also necessary, more than ever, to maintain and guarantee the quality of the water supply (CIRILO; MONTENEGRO; CAMPOS, 2017).

Most literature has focused on applying biochar for soil amendment, carbon sequestration, and reducing greenhouse gas emissions (GWENZI et al., 2017). Therefore, knowledge about the practical application of biochar in water treatment operations, such as drinking water or wastewater systems, is limited. Biochar has been considered a potential substitute for activated carbon in environmental remediation and water treatment due to its low cost, relative abundance, and adsorption capacity (INYANG; DICKENSON, 2015). Since it is a porous carbonaceous material and abundant in functional groups, biochar has been widely

studied as an adsorbent in the remediation of contaminants, including inorganic and organic pollutants and gases (LI; JIANG, 2017).

The main objective of this study was to develop and assess models for the removal of colour, turbidity, chlorophyll-*a*, and UV_{254} as responses to produce high-quality drinking water exploring the application of sludge biochar as an adsorbent and its impact on water treatment processes. Such investigations are required to evaluate the feasibility of sludge-derived biochar application in water treatment works.

12 MATERIALS AND METHODS

12.1 Biochar and natural water sampling

Sludge-derived biochar was produced from sludge in which polyaluminium chloride (PACl) and cationic polymer are used as a coagulant and coagulant aid, respectively, from the Oeste Water Treatment Plant (WTP) in Caucaia, Ceará, Brazil. The dried sludge was pyrolysed at 600 ºC at a heating rate of 30 $ºC.min^{-1}$ to produce biochar. For the jar test experiments, natural eutrophic water samples were taken from the intake of the Oeste WTP and used in experiments immediately. Table 7 shows the water quality characteristics of the Gavião reservoir.

Table 7 – Water quality characteristics of the Gavião reservoir

Parameters	Reservoir water[a]	Unit
pH	7.75 ± 0.03	-
Turbidity	2.85 ± 0.29	NTU
Colour	28.23 ± 17.23	Pt-Co
UV_{254}	0.211 ± 0.0078	cm^{-1}
Chlorophyll-*a*	5.34 ± 5.41	$\mu g.L^{-1}$

[a] Mean ± standard deviation

12.2 Experimental design and data analysis

The central composite design (CCD) and response surface methodology (RSM) were used for designing the experiment, optimising the effective parameters with a minimum

number of experiments, and analysing the interaction effects between the operating parameters (MA et al., 2016). In RSM experiments, the independent variables or factors are varied over a continuous range. The goal is to determine the factor settings that produce a maximum or minimum response or to map the relationship between the response and the factor settings over this contiguous factor space (LAWSON, 2015). In this study, the effects of three independent factors, i.e., pH (A), coagulant dose (B), and biochar dose (C), were varied in the ranges of 6-9, 25-70 $mg.L^{-1}$, and 15-40 $mg.L^{-1}$, respectively. The corresponding ranges and levels of the experiment were determined according to previous experiments (not shown) and data available in the literature. The main objective of this study was to develop models for the removal of colour (Y_1), turbidity (Y_2), chlorophyll-*a* (Y_3), and UV_{254} (Y_4) as responses, as well as to assess optimum treatment models to produce high-quality drinking water applying biochar within the treatment plant. Three kinds of runs are required for CCD: factorial runs (2^k), axial runs (2k) and centre runs (6), where k is the number of parameters. Therefore, based on the parameters we chose for this study, the number of experiments required is: $N = 2^k + 2k + n_c = 2^3 + 2 \times 3 + 6 = 20$ (AZARGOHAR; DALAI, 2008).

Centre runs include six replications which are performed by setting all factors at their midpoints to estimate the residual error. They can be considered a barometer to evaluate the variability in the system. In this method, each parameter is coded to the ± 1 interval, reflecting low and high levels of the parameter. Each parameter is varied over five levels: ± α (axial points), ± 1 (factorial points), and the centre points (0). The distance of the axial points from the centre is equal to $(2^k)^{0.25}$ (AZARGOHAR; DALAI, 2008). Based on these coded factors, the list of experiments required for our study is shown in Table 8. The independent variables' levels are presented in their original units of measurement ($mg.l^{-1}$) and in their equivalent coded levels in parentheses. Experimental results are shown as removal percentage (%) of colour, turbidity, chlorophyll-*a* and UV_{254}. RSM was used to investigate the variables that significantly influence the analytical response, while analysis of variance (ANOVA) was used to determine the significance of the independent variables on the output responses. Design-Expert 13 was used for the experiment's statistical design and data analysis. The coefficient of determination R^2 expressed the polynomial model's goodness of fit, and its statistical significance was checked by Fisher's F-test using the same software. The *p*-value was used to evaluate models' terms at the 95% confidence level (GHAFARI et al., 2009). 3D surfaces and their respective contour plots were generated for the responses based on the effects of the factors varied at five levels.

Table 8 – Experimental design and actual vs predicted results for the CCD responses

Run	Factors			Responses							
				Y_1 (%)		Y_2 (%)		Y_3 (%)		Y_4 (%)	
	A	B[b]	C[b]	Act.	Pred.	Act.	Pred.	Act.	Pred.	Act.	Pred.
1	6.0 (-1)	25.0 (-1)	15.0 (-1)	74.9	76.5	41.0	41.7	50.0	11.1	50.2	47.5
2	7.5 (0)	47.5 (0)	27.5 (0)	88.1	90.2	49.8	53.2	50.0	100	57.3	58.9
3	7.5 (0)	47.5 (0)	27.5 (0)	95	90.2	48.7	53.2	83.3	100	57.8	58.9
4	9.0 (1)	25.0 (-1)	40.0 (1)	61.7	65.1	28.7	32.1	0.00	0.00	27.5	29.8
5	7.5 (0)	85.3 (α)	27.5 (0)	88.1	94.8	43.8	44.3	66.7	97.6	55.9	63.1
6	5.0 (-α)	47.5 (0)	27.5 (0)	88.1	87.4	14.3	15.2	50.0	97.6	49.3	55.1
7	6.0 (-1)	70.0 (1)	40.0 (1)	93	93.3	10.1	12.3	83.3	98.9	69.2	63.0
8	7.5 (0)	9.7 (-α)	27.5 (0)	74.9	82.5	12.2	12.5	16.7	10.6	28.4	28.5
9	7.5 (0)	47.5 (0)	27.5 (0)	88.1	90.2	55.7	53.2	100	100	59.7	58.9
10	10.0 (α)	47.5 (0)	27.5 (0)	61.7	68.8	60.0	59.3	33.3	12.9	32.2	33.8
11	6.0 (-1)	70.0 (1)	15.0 (-1)	88.1	87.9	14.3	11.0	66.7	0.10	65.9	63.0
12	9.0 (1)	70.0 (1)	40.0 (1)	88.1	80.5	68.0	64.7	50.0	58.0	59.2	56.1
13	9.0 (1)	70.0 (1)	15.0 (-1)	88.1	86.1	57.8	61.6	66.7	30.9	59.7	56.1
14	7.5 (0)	47.5 (0)	6.5 (-α)	74.9	75.2	47.7	51.5	0.00	0.00	56.9	58.9
15	7.5 (0)	47.5 (0)	48.5 (α)	74.9	79.1	49.8	47.0	66.7	0.30	57.8	58.9
16	7.5 (0)	47.5 (0)	27.5 (0)	95	90.2	48.4	53.2	100	100	58.3	58.9
17	6.0 (-1)	25.0 (-1)	40.0 (1)	88.1	86.3	35.4	33.6	83.3	79.4	48.8	47.5
18	7.5 (0)	47.5 (0)	27.5 (0)	88.1	90.2	56.8	53.2	66.7	100	59.2	58.9
19	7.5 (0)	47.5 (0)	27.5 (0)	93	90.2	59.6	53.2	100	100	58.3	58.9
20	9.0 (1)	25.0 (-1)	15.0 (-1)	74.9	73.5	43.8	40.1	50.0	1.00	32.7	29.8

[b] dosage in $mg.L^{-1}$; coded factors in parenthesis.

A jar test with variable speed and six paddle gang stirrers was used to perform a treatability study to simulate a conventional coagulation/flocculation process. Before the experiment, the amount of polyaluminium chloride (PACl) and polymer required to achieve the optimum dose was determined using a standard jar test method. Then, the natural water samples were divided into six jars (1.5 L each) and placed on the gang stirrer. The pH for each run was adjusted using either 0.1 M HCl or 0.1 M NaOH. The water treatment procedure (Figure 9)

consisted of a 1 min rapid mix (200 rpm), a 15 min slow mix (30 rpm), and a 30 min settling period (Table 9).

Figure 9 – Experimental jar test setup for experiments

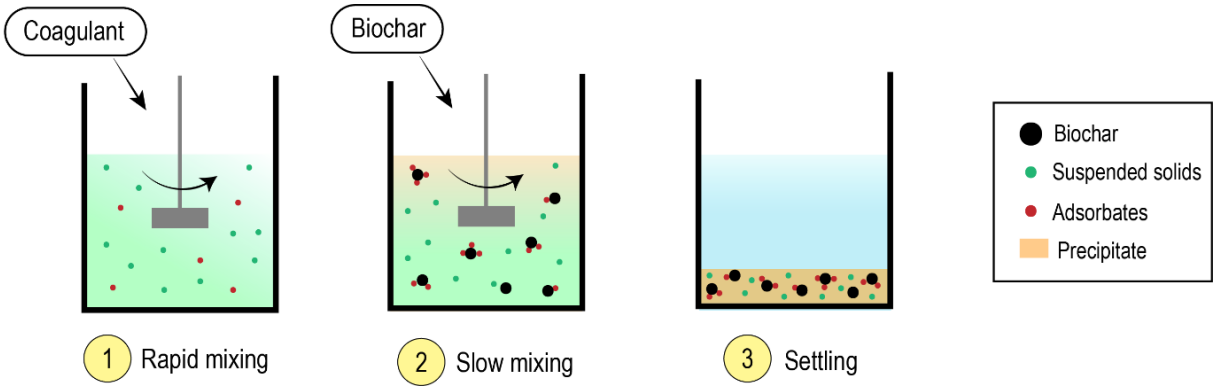

Table 9 – Jar test conditions

	Speed (rpm)	Time (min)	G[a] (s^{-1})
Rapid mix	300	1	762
Slow mix	20	20	20
Settling	-	30	-

[a] velocity gradient

12.3 Analytical methods

After settling, the supernatants were collected to measure residual turbidity using a turbidimeter. Finished pH values were measured with a pHmeter. The filtrates were tested for chlorophyll-*a* (spectrophotometric method – 10200 H) and colour (spectrophotometric single-wavelength method – 2120 C) as proposed by APHA (2017). Conventional treatment is very effective in removing particulate organic matter; on the other hand, dissolved organic matter (DOM) is one of the significant concerns in drinking water treatment due to its difficulty in removal (LIU et al., 2015). Thus, absorbance at the 254 nm wavelength, a helpful indicator for the relative levels of dissolved organic carbon (DOC) in natural waters, was measured with a UV/Vis spectrophotometer (DONATI et al., 1994). Samples for colour and UV_{254} were filtered through a 0.45 µm membrane filter before measurement readings.

13 RESULTS AND DISCUSSIONS

13.1 Statistical analysis

The CCD shown in Table 8 provided a basis for the development of mathematical equations where predicted results (Y_1, Y_2, Y_3, Y_4) were assessed as a function of pH (A), coagulant dose (B), and biochar dose (C) and calculated as the sum of a constant, first and second-order effects and interaction effects. Then, the goodness of fitness was assessed by ANOVA, by which statistically insignificant equation terms (p-value > 0.05) were removed (model reduction), aiming at improving the model R^2 coefficients (LIU et al., 2020; MA et al., 2016; PEI et al., 2014). Equations 2–5 represent the final modified equations in terms of coded factors. Data in Tables 10–13 show that all the models were significant at the 5% confidence level ($p < 0.05$), except the chlorophyll-*a* removal model.

The lack of fit F-test describes the variation of the data around the fitted model. No significant lack of fit (which is a double negative) is good since we want the model to fit the data. Lack of fit will be significant if the model does not fit the data well. The high p-values for lack of fit (>0.05) presented in Tables 10–12 show that the F-statistic was insignificant for the models, implying a significant model correlation between the variables and process responses, except for equation 4 regarding UV_{254} removal (Table 13). The R^2 coefficient gives the proportion of the total variation in the response predicted by the model, indicating the ratio of the sum of squares due to regression to the total sum of squares. A high predicted R^2 value, close to 1, is desirable and a reasonable agreement with adjusted R^2 is necessary**,** i.e., their difference is less than 0.2. A high R^2 coefficient ensures a satisfactory model adjustment to the experimental data (GHAFARI et al., 2009). All models indicated that the predicted R^2 is in reasonable agreement with the adjusted R^2, except the chlorophyll-*a* removal model (Table 12). A negative predicted R^2 implies that the overall mean may better predict the response than the current model. Additionally, even though chlorophyll-*a* lack of fit p-value was greater than 0.05, the correlation coefficients were all much lower than 0.90; thus, the model could not be used to simulate this response; that is, there are no significant terms and interactions between the independent variables and chlorophyll-*a* removal as observed in Table 12 (MA et al., 2016). It is also important to note that the R^2 for colour removal was not very high but the data still had a good fit.

Adequate precision measures the signal-to-noise ratio. A ratio greater than 4 is desirable as indicative of good model discrimination (GHAFARI et al., 2009; PEI et al., 2014).

The colour, turbidity and UV_{254} removal models demonstrated adequate signal, thus confirming they can be used to navigate the design space defined by the CCD. Chlorophyll-*a* removal model, on the other hand, indicated inadequate signal and should not be used to navigate the design space (Tables 10–13).

Before accepting a model as statistically correct, it is essential to validate the model. Diagnostic plots help judge a model's satisfactoriness. The models' validity was assessed by normal probability plots (see supplementary material), which indicates whether the residuals follow a normal distribution (follow the straight line). Normally distributed data has to be scattered randomly around the zero line with no characteristic pattern (GUYO et al., 2015; SHARMA; MALIK; SATYA, 2009). Figure S1a-S4a show that the residuals were close to the straight line and scattered randomly around it with no particular pattern. Except for UV_{254} removal, the residuals vs predicted values plots (Figure S1b-S4b) showed no outliers for any residuals since there were no data points outside the limit lines. It can also be seen that the residuals (difference between the experimental and the predicted value) were randomly distributed, therefore, indicative of well-behaved residuals (GUYO et al., 2015). Overall, diagnostic plots indicated a good agreement between actual data and models' predictions except for chlorophyll-a logit data.

13.2 Process analysis

The responses for removal efficiency were bound by 0 and 100 as lower and upper limits, respectively, to ensure that the predicted responses would be strictly within this range since 100% is the maximum removal possible. For that, Logit transformation was used based on Equation 1 (PEI et al., 2014; WANG et al., 2021):

$$Y' = ln\left(\frac{Y - 0\%}{100\% - Y}\right) \quad (1)$$

where Y' is the Logit response output and Y is the actual response input.

The response surface graphs and contour plots for colour removal are shown in Figure 10. The plots indicated that a reduction in pH and an increase in biochar dose would increase colour removal response as the optimum conditions lay within the centre of the concentrically closed curves (GHAFARI et al., 2009). Figure 10 also shows the response to a coagulant dose at the centre point (47.5 $mg.L^{-1}$), where optimum colour removal (~91%) occurred at a pH of 6.4 and a biochar dose of 32.2 $mg.L^{-1}$. Increasing the coagulant dose to its highest level (70 $mg.L^{-1}$) only increased efficiency to ~93%. This implies that adding biochar

to the water treatment process did not improve colour removal or reduce coagulant demand. Sludge-derived biochar has a high ash content due to its inorganic salt-rich feedstock (WEBER; QUICKER, 2018). High ash content may cause pore blockage and limit sorption sites' accessibility. Biochar usually needs to be washed using weak acid or deionized water to remove the ash content and expose more sorption sites (LI et al., 2018, 2019). Depending on its pyrolysis temperature, biochar can still show organic matter in its structure, being then diffused to the aqueous solution, worsening colour and reducing coagulant efficiency. To the authors' best knowledge, it is essential to note that no study has yet mentioned the impact that the release of organic matter present in biochars has on water quality when it is aimed at water purification.

Table 10 – ANOVA analysis and fit statistics for the colour removal response

Source	Sum of squares	DF	Mean square	F-value	*p*-value
Model	7.29	6	1.22	5.42	0.0052
A-pH	1.60	1	1.60	7.13	0.0192
B-Coagulant dose	2.18	1	2.18	9.71	0.0082
C-Biochar dose	0.0563	1	0.0563	0.2510	0.6247
AC	0.5564	1	0.5564	2.48	0.1393
A^2	1.33	1	1.33	5.94	0.0299
C^2	1.83	1	1.83	8.15	0.0135
Residual	2.92	13	0.2243		
Lack of fit	1.81	8	0.2268	1.03	0.5117
Pure error	1.10	5	0.2204		
Cor Total	10.21	19			
$R^2 = 0.7144$					
Adjusted $R^2 = 0.5826$					
Predicted $R^2 = 0.4030$					
Adeq precision = 8.1018					

Figure 10 – Contour and surface response plots for colour removal

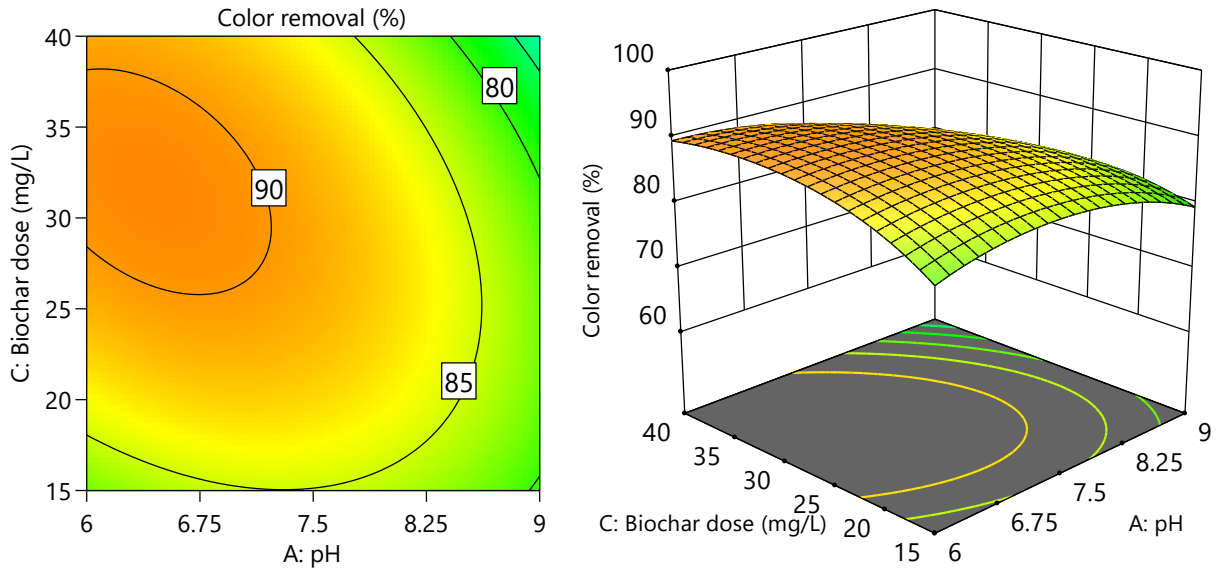

Equations 2–5 quantitatively describe the interaction relationship and contribution of pH, coagulant dose and biochar dose in removing colour, turbidity, and UV_{254}. The models, in coded factors, are:

$$Y_n = \frac{100K_n}{K_n + 1} \quad (2)$$

where K_1, K_2, and K_4, for colour (Y_1), turbidity (Y_2) and UV_{254} removal (Y_4), respectively, are:

$$K_1 = \text{antilog}\,[+2.22 - 0.3423A + 0.3995B + 0.0642C - 0.2637AC - 0.3027A^2 - 0.3543C^2] \quad (3)$$

$$K_2 = \text{antilog}\,[0.1267 + 0.6245A + 0.5127B - 0.0534C + 0.6569AB + 0.1198BC - 0.2824A^2 - 0.4305B^2 - 0.0553C^2 - 0.6127A^2B] \quad (4)$$

$$K_4 = \text{antilog}\,[0.3611 - 0.2606A + 0.4334B + 0.1185AB - 0.2104A^2 - 0.1954B^2] \quad (5)$$

The models' equations in coded factors can be used to predict the response for given levels of each factor (MOHAMED; EL-TAYEB, 2014). It is also helpful for identifying the relative impact of the factors by comparing the factor coefficients (PETER et al., 2021). From Equations 2–5 and the data provided in Tables 10–13, we can see that the pH (A) and coagulant dose (B) had the highest relative effects for the removal of the parameters evaluated, whereas the addition of biochar (C) played little to no significance in the removal of colour, turbidity and UV_{254}.

Table 11 – ANOVA analysis and fit statistics for the turbidity removal response

Source	Sum of squares	DF	Mean square	F-value	*p*-value
Model	14.01	9	1.56	32.82	< 0.0001
A-pH	5.33	1	5.33	112.31	< 0.0001
B-Coagulant dose	1.49	1	1.49	31.35	0.0002
C-Biochar dose	0.0390	1	0.0390	0.8224	0.3858
AB	3.45	1	3.45	72.81	< 0.0001
BC	0.1148	1	0.1148	2.42	0.1507
A^2	1.15	1	1.15	24.25	0.0006
B^2	2.67	1	2.67	56.34	< 0.0001
C^2	0.0440	1	0.0440	0.9287	0.3579
A^2B	1.24	1	1.24	26.23	0.0004
Residual	0.4742	10	0.0474		
Lack of fit	0.2869	5	0.0574	1.53	0.3254
Pure error	0.1872	5	0.0374		
Cor total	14.48	19			
$R^2 = 0.9673$					
Adjusted $R^2 = 0.9378$					
Predicted $R^2 = 0.8533$					
Adeq precision = 17.5059					

Figure 11 illustrates the interaction between different significant parameters for turbidity removal and their respective performance. In Figure 11a it is observed that the best turbidity removal conditions were achieved at both a high pH and coagulant dose. In Figure 11b it can be seen that in increasing both biochar and coagulant dose, the turbidity removal is also increased, but still to a small, limited removal range.

Figure 11 – Contour and surface response plots for turbidity removal for factors interactions: (a) pH and biochar dose and (b) coagulant dose and biochar dose

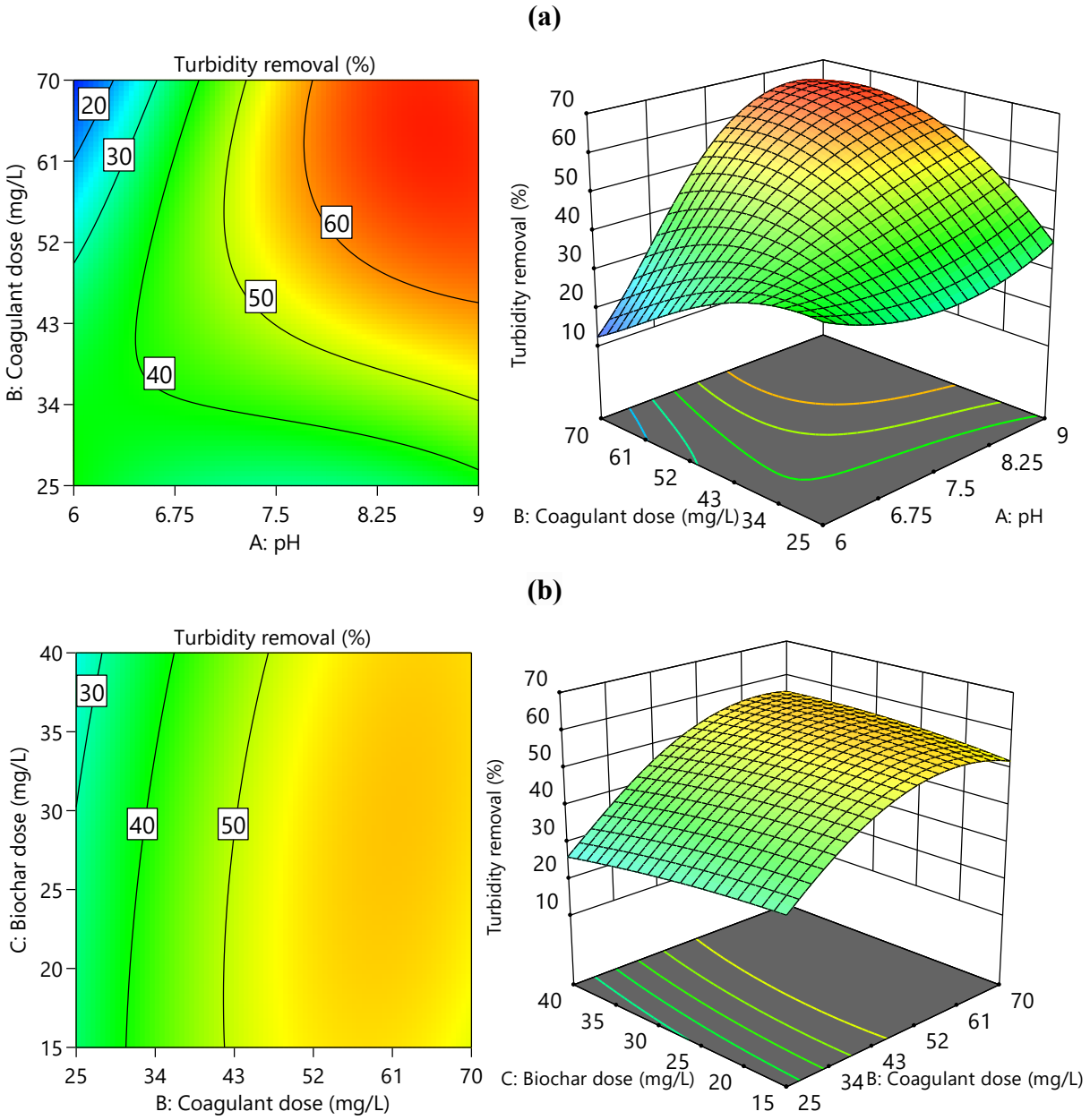

Table 12 – ANOVA for quadratic model and fit statistics for chlorophyll-*a* removal response

Source	Sum of squares	DF	Mean square	F-value	*p*-value
Model	812.51	9	90.28	1.40	0.3017
A-pH	38.07	1	38.07	0.5918	0.4595
B-Coagulant dose	41.06	1	41.06	0.6382	0.4429
C-Biochar dose	17.71	1	17.71	0.2753	0.6113
AB	42.42	1	42.42	0.6592	0.4357
AC	58.51	1	58.51	0.9093	0.3628

BC	36.26	1	36.26	0.5635	0.4701
A^2	100.66	1	100.66	1.56	0.2395
B^2	103.62	1	103.62	1.61	0.2332
C^2	460.64	1	460.64	7.16	0.0233
Residual	643.41	10	64.34		
Lack of Fit	288.64	5	57.73	0.8136	0.5868
Pure Error	354.77	5	70.95		
Cor Total	1455.93	19			
$R^2 = 0.5581$					
Adjusted $R^2 = 0.1603$					
Predicted $R^2 = -0.9020$					
Adeq precision = 3.5929					

Regarding UV_{254} removal, Figure 12 shows that the pH range of 6 to 8.5 and coagulant doses higher than 45.7 $mg.L^{-1}$ showed the best removal values, as observed by the more intense red colour in the graphs. As illustrated in Table 13, adding biochar to the treatment was not significant, therefore, it was not part of the model's equation in order to improve the model. Tables 10–13 show that the biochar dose (term C) was insignificant for almost all responses. On this basis, it can be concluded that, overall, adding biochar to water treatment failed to improve the effect of PACl, when it slightly increased the need for coagulant dose (Figure 11b).

Table 13 – ANOVA for reduced quadratic model and fit statistics for UV_{254} removal

Source	Sum of squares	DF	Mean square	F-value	*p*-value
Model	4.71	5	0.9413	38.33	< 0.0001
A-pH	0.9277	1	0.9277	37.77	< 0.0001
B-Coagulant dose	2.57	1	2.57	104.44	< 0.0001
AB	0.1124	1	0.1124	4.57	0.0506
A^2	0.6446	1	0.6446	26.25	0.0002
B^2	0.5558	1	0.5558	22.63	0.0003
Residual	0.3438	14	0.0246		
Lack of fit	0.3372	9	0.0375	28.19	0.0009
Pure error	0.0066	5	0.0013		
Cor total	5.05	19			
$R^2 = 0.9319$					
Adjusted $R^2 = 0.9076$					
Predicted $R^2 = 0.7426$					
Adeq precision = 16.9827					

Figure 12 – Contour and surface response plots for UV_{254} removal

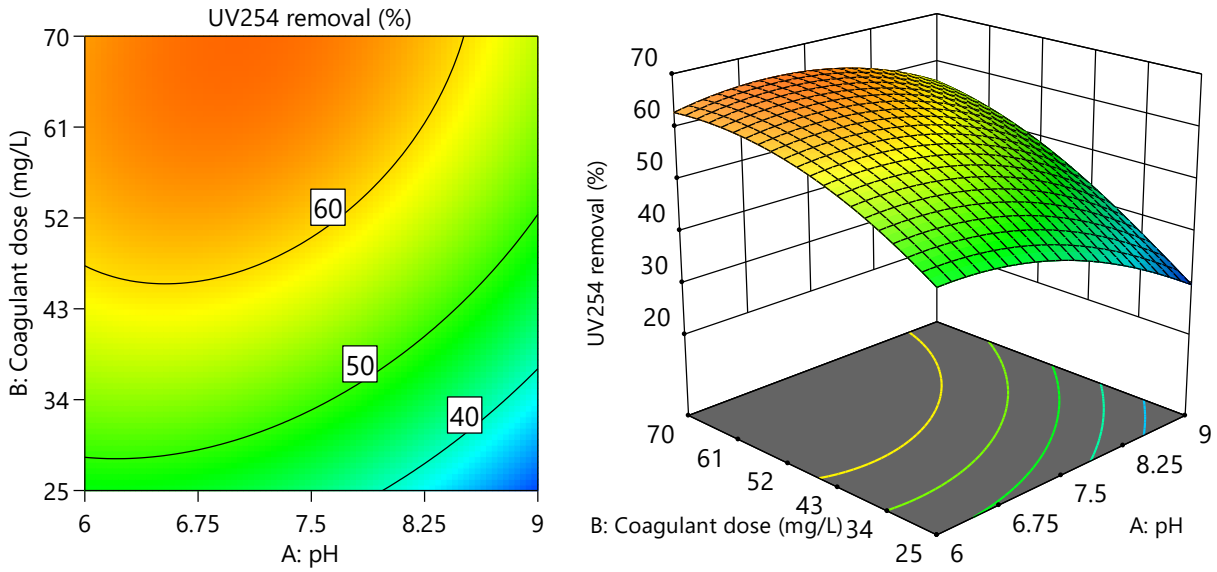

14 CONCLUSIONS

Pyrolysis is undoubtedly a great route to manage waste disposal to reduce waste volume and generate high-added-value products. However, considering that DWT sludge-derived biochar showed an insufficient advantage in improving water quality, its application in water treatment processes has to be further investigated to underline the mechanisms behind sludge-derived biochar. The inorganic nature of the biochar might have impacted its performance. It is important to note that even though biochar did not improve the parameters evaluated, its addition did not significantly affect the water quality negatively, showing potential for its application in water treatment given its possible enhancement via a post-treatment process.

REFERENCES

APHA. **Standard Methods for the Examination of Water and Wastewater**. 23rd. ed. Washington, DC: American Public Health Association, 2017.

AZARGOHAR, R.; DALAI, A. K. Steam and KOH activation of biochar: Experimental and modeling studies. **Microporous and Mesoporous Materials**, v. 110, n. 2–3, p. 413–421, 2008.

BOTANA, L. M. A Toxicological Perspective on Climate Change: Aquatic Toxins. **Chemical Research in Toxicology**, v. 29, n. 4, p. 619–625, 18 abr. 2016.

CARPENTER, S. R. et al. Nonpoint pollution of surface waters with phosphorus and nitrogen. **Ecological Applications**, v. 8, n. 3, p. 559–568, 1998.

CHEUNG, M. Y.; LIANG, S.; LEE, J. Toxin-producing cyanobacteria in freshwater: A review of the problems, impact on drinking water safety, and efforts for protecting public health. **Journal of Microbiology**, v. 51, n. 1, p. 1–10, fev. 2013.

CHOW, C. W. K. et al. The impact of conventional water treatment processes on cells of the cyanobacterium microcystis aeruginosa. **Water Research**, v. 33, n. 15, p. 3253–3262, 1999.

CIRILO, J. A.; MONTENEGRO, S. M. G. L.; CAMPOS, J. N. B. The Issue of Water in the Brazilian Semi-Arid Region. In: DE MATTOS BICUDO, C. E.; GALIZIA TUNDISI, J.; CORTESÃO BARNSLEY SCHEUENSTUHL, M. (Eds.). . **Waters of Brazil**. Cham: Springer International Publishing, 2017. p. 59–71.

DONATI, C. et al. Microcystin-LR adsorption by powdered activated carbon. **Water Research**, v. 28, n. 8, p. 1735–1742, 1994.

GHAFARI, S. et al. Application of response surface methodology (RSM) to optimize coagulation–flocculation treatment of leachate using poly-aluminum chloride (PAC) and alum. **Journal of Hazardous Materials**, v. 163, n. 2–3, p. 650–656, abr. 2009.

GUYO, U. et al. Application of response surface methodology for Cd(II) adsorption on maize tassel-magnetite nanohybrid adsorbent. **Journal of Environmental Chemical Engineering**, v. 3, n. 4, p. 2472–2483, 2015.

GWENZI, W. et al. Biochar-based water treatment systems as a potential low-cost and sustainable technology for clean water provision. **Journal of Environmental Management**, v. 197, p. 732–749, 15 jul. 2017.

INYANG, M.; DICKENSON, E. The potential role of biochar in the removal of organic and microbial contaminants from potable and reuse water: A review. **Chemosphere**, v. 134, p. 232–240, 1 set. 2015.

LAWSON, J. **Design and Analysis of Experiments with R**. [s.l: s.n.].

LE MOAL, M. et al. Eutrophication: A new wine in an old bottle? **Science of the Total Environment**, v. 651, p. 1–11, 15 fev. 2019.

LEHMAN, P. W. et al. Impacts of the 2014 severe drought on the Microcystis bloom in San Francisco Estuary. **Harmful Algae**, v. 63, p. 94–108, 1 mar. 2017.

LI, D. C.; JIANG, H. The thermochemical conversion of non-lignocellulosic biomass to form biochar: A review on characterizations and mechanism elucidation. **Bioresource Technology**, v. 246, p. 57–68, 1 dez. 2017.

LI, J. et al. Comparative study for microcystin-LR sorption onto biochars produced from various plant- and animal-wastes at different pyrolysis temperatures: Influencing mechanisms of biochar properties. **Bioresource Technology**, v. 247, p. 794–803, jan. 2018.

LI, S. et al. Predicting biochar properties and functions based on feedstock and pyrolysis temperature: A review and data syntheses. **Journal of Cleaner Production**, v. 215, p. 890–902, 2019.

LINS, R. P. M. et al. Cyanobacteria in a eutrophicated reservoir in a semi-arid region in Brazil: dominance and microcystin events of blooms. **Revista Brasileira de Botanica**, v. 39, n. 2, p. 583–591, 1 jun. 2016.

LIU, C. et al. Synthesis, characterization and flocculation performance of a novel sodium alginate-based flocculant. **Carbohydrate Polymers**, v. 248, n. July, 2020.

LIU, Y. et al. Fouling control of PAC/UF process for treating algal-rich water. **Desalination**, v. 355, p. 75–82, 2015.

LÜRLING, M.; VAN OOSTERHOUT, F.; FAASSEN, E. Eutrophication and warming boost cyanobacterial biomass and microcystins. **Toxins**, v. 9, n. 2, 11 fev. 2017.

MA, C. et al. Enhancing integrated removal of Microcystis aeruginosa and adsorption of microcystins using chitosan-aluminum chloride combined coagulants: Effect of chemical dosing orders and coagulation mechanisms. **Colloids and Surfaces A: Physicochemical and Engineering Aspects**, v. 490, p. 258–267, 2016.

MOHAMED, T. A.; EL-TAYEB, N. S. M. Improving the Mechanical Properties of Acetal Homopolymer Material to Boost its Quality. **Journal of Management & Engineering Integration**, v. 7, n. 1, p. 50, 2014.

PAERL, H. W.; OTTEN, T. G. Harmful Cyanobacterial Blooms: Causes, Consequences, and Controls. **Microbial Ecology**, v. 65, n. 4, p. 995–1010, maio 2013.

PAERL, H. W.; OTTEN, T. G.; JOYNER, A. R. Moving towards adaptive management of cyanotoxin-impaired water bodies. **Microbial Biotechnology**, v. 9, n. 5, p. 641–651, 1 set. 2016.

PAERL, H. W.; PAUL, V. J. Climate change: Links to global expansion of harmful cyanobacteria. **Water Research**, v. 46, n. 5, p. 1349–1363, abr. 2012.

PEI, H.-Y. et al. The behaviors of Microcystis aeruginosa cells and extracellular microcystins during chitosan flocculation and flocs storage processes. **Bioresource Technology**, v. 151, p. 314–322, 2014.

PETER, E. L. et al. Total polyphenols and antihyperglycemic activity of aqueous fruits extract

of Abelmoschus esculentus: Modeling and optimization of extraction conditions. **PLoS ONE**, v. 16, n. 4 April, p. 1–16, 2021.

SHARMA, S.; MALIK, A.; SATYA, S. Application of response surface methodology (RSM) for optimization of nutrient supplementation for Cr (VI) removal by Aspergillus lentulus AML05. **Journal of Hazardous Materials**, v. 164, n. 2–3, p. 1198–1204, 2009.

WANG, B. et al. Removal of Microcystis aeruginosa and control of algal organic matter by Fe(II)/peroxymonosulfate pre-oxidation enhanced coagulation. **Chemical Engineering Journal**, v. 403, n. July 2020, p. 126381, 2021.

WEBER, K.; QUICKER, P. Properties of biochar. **Fuel**, v. 217, n. December 2017, p. 240–261, abr. 2018.

WELLS, M. L. et al. Harmful algal blooms and climate change: Learning from the past and present to forecast the future. **Harmful Algae**, v. 49, p. 68–93, 1 nov. 2015.

YIN, Q. et al. Biochar as an adsorbent for inorganic nitrogen and phosphorus removal from water: a review. **Environmental Science and Pollution Research**, v. 24, n. 34, p. 26297–26309, 1 dez. 2017.

SUPPLEMENTARY MATERIAL

Figure S1 – Diagnostic plots for the validation of the Logit colour removal model

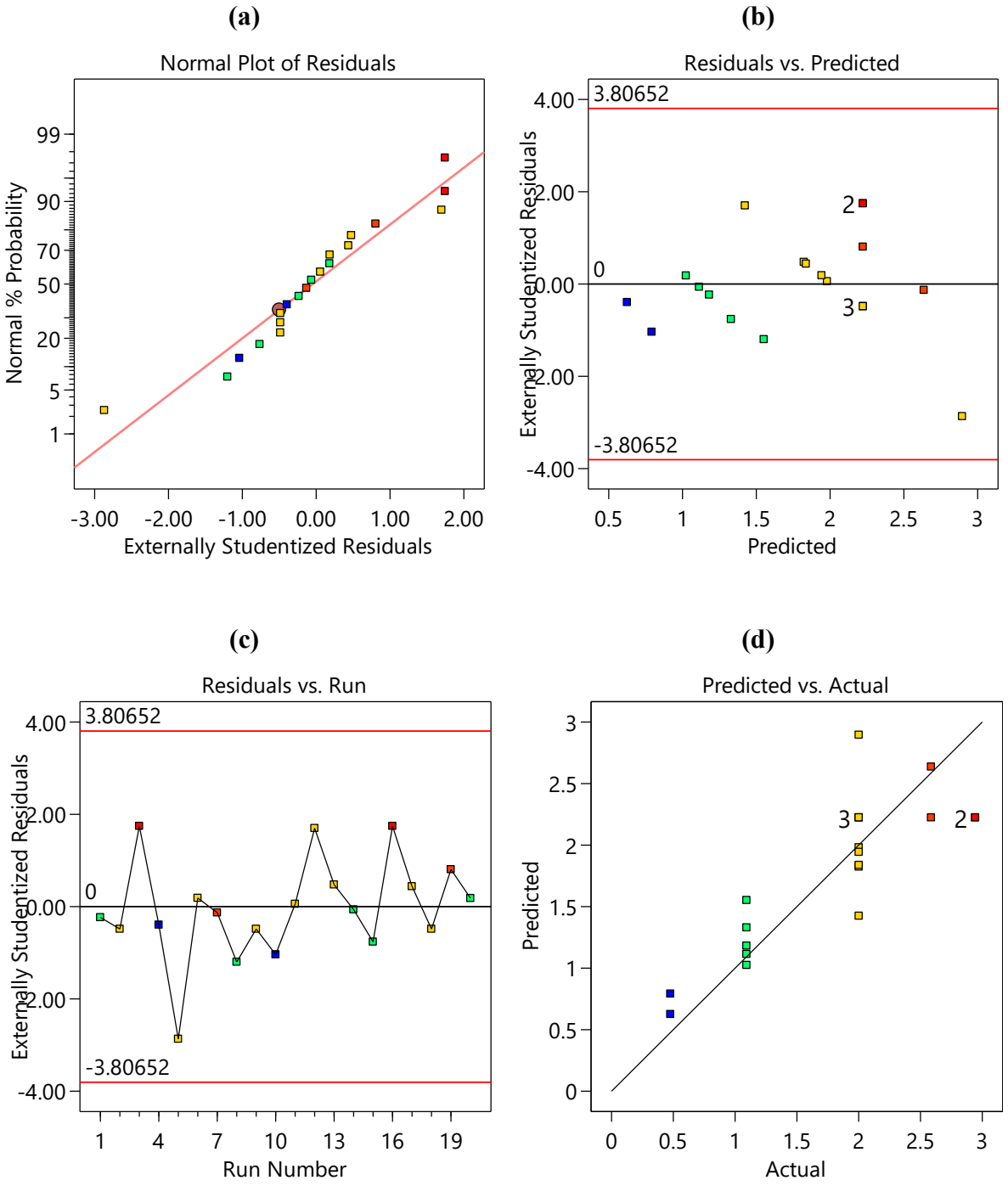

Figure S2 – Diagnostic plots for the validation of the Logit turbidity removal model

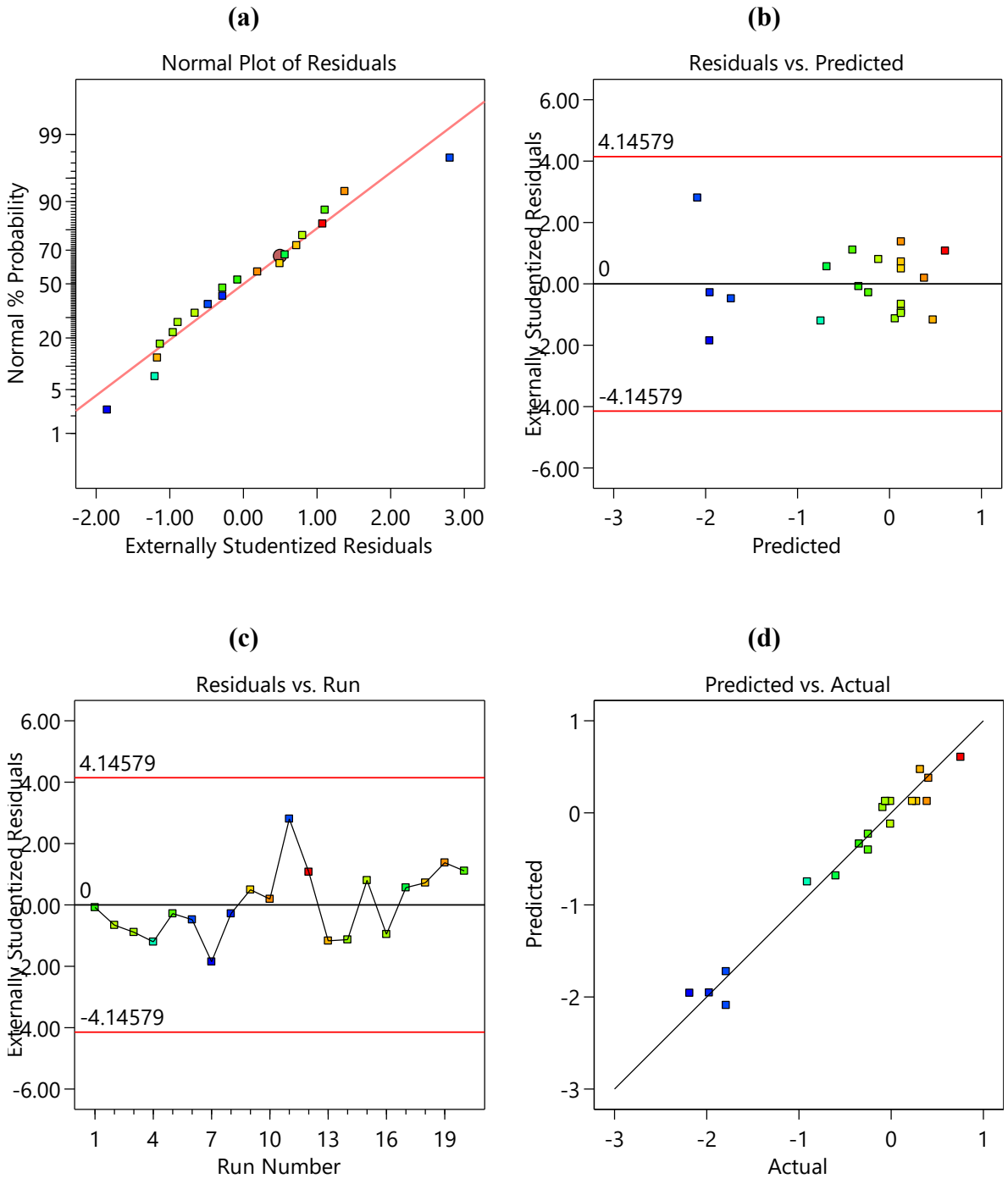

Figure S3 – Diagnostic plots for the validation of the Logit chlorophyll-*a* removal model

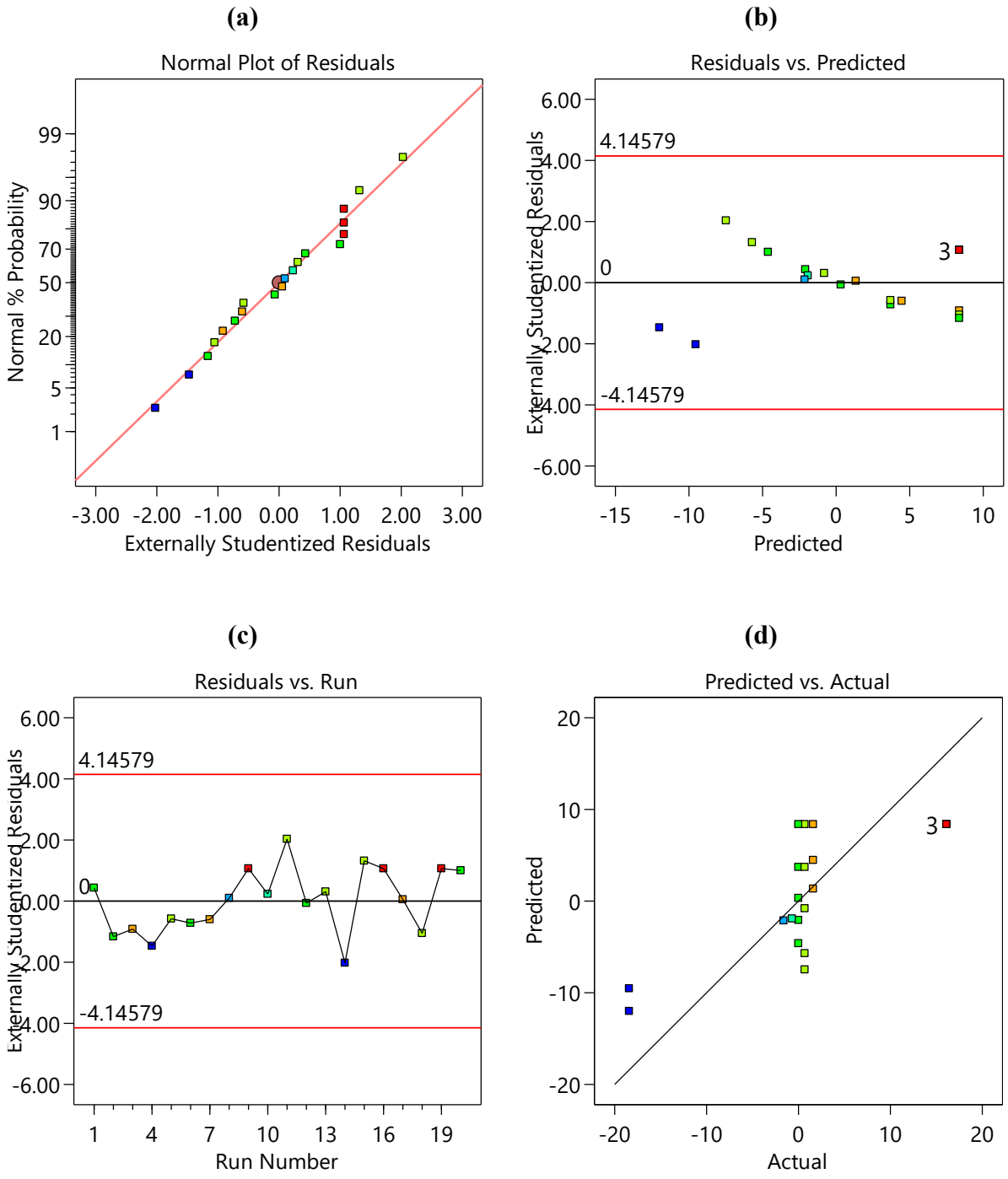

Figure S4 – Diagnostic plots for the validation of the Logit UV_{254} removal model

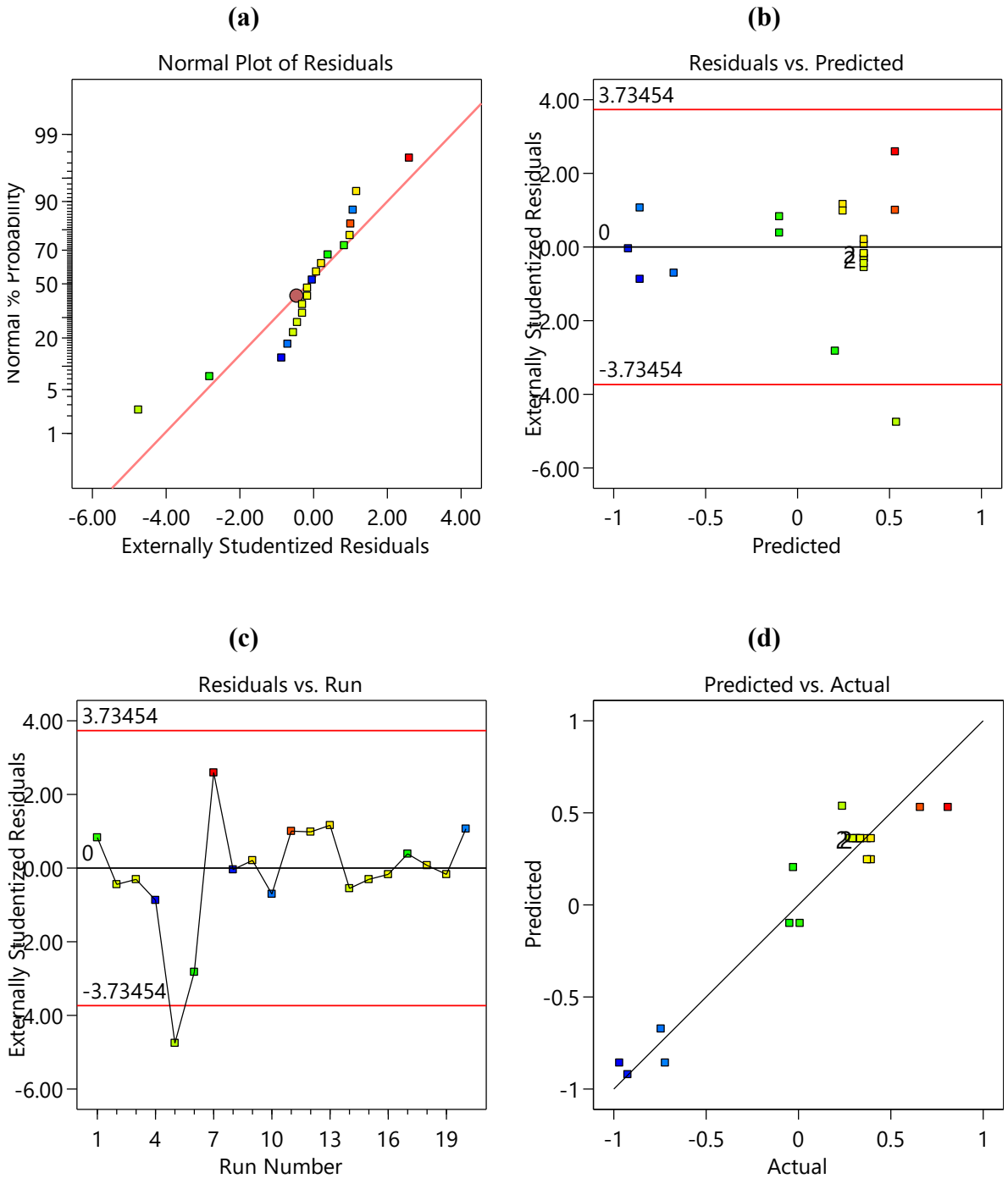

15 GENERAL CONCLUSIONS

When considered alone, the systematic review showed that properties such as surface area are not a good indicator of adsorption capacity. It is necessary to evaluate a combination of adsorbate, adsorbent and aqueous solution properties for the correct selection of PAC or biochar. Although activated carbon has been widely used for cyanotoxin removal, not enough data are available, and few studies have been performed for different toxins, as most focus on MC-LR. As for biochar, the knowledge gaps are even greater.

In the second part of this research, after the production and characterization of the biochar derived from DWT sludge, it was found that the increase in temperature negatively affected the biochar yield, which decreased from 37.5 to 33.5 % as the temperature increased from 450 to 600 °C. The dried sludge sample had a pH of 5.6 and as the pyrolysis temperature increased from 450 to 600 ºC, the pH of the biochar increased from 6.6 to 6.9. BC600, produced at a higher temperature, had a larger surface area (66.54 m^2/g) than BC450 (43.18 m^2/g). After chemical activation, the activated biochar (BC600A) showed a substantial increase in surface area, reaching 2,000 m^2/g. Furthermore, chemical activation resulted in a decrease in the zeta potential. The high mineral fraction in the sludge resulted in biochar rich in ash (61-71 %) and low in carbon (0.2-1.4 %), thus attributing more inorganic than organic characteristics to the material. The biochar produced at a higher temperature showed a more developed carbonaceous structure typical of adsorbent materials.

Finally, the application of biochar in the treatment process proved inefficient for the treatment of natural waters, having little contribution to the coagulation and adsorption process. Thus, the use of DWT sludge biochar should be studied further to better understand its characteristics and possible chemical or physical modifications that could improve its properties as an adsorbent.

GENERAL REFERENCES

ABBAS, T. et al. Recent advancements in the removal of cyanotoxins from water using conventional and modified adsorbents—a contemporary review. **Water (Switzerland)**, v. 12, n. 10, 1 out. 2020.

CARPENTER, S. R. et al. Nonpoint pollution of surface waters with phosphorus and nitrogen. **Ecological Applications**, v. 8, n. 3, p. 559–568, 1998.

CHOW, C. W. K. et al. The impact of conventional water treatment processes on cells of the cyanobacterium microcystis aeruginosa. **Water Research**, v. 33, n. 15, p. 3253–3262, 1999.

GWENZI, W. et al. Biochar-based water treatment systems as a potential low-cost and sustainable technology for clean water provision. **Journal of Environmental Management**, v. 197, p. 732–749, 15 jul. 2017.

HENDERSON, R. et al. Experiences of algae in UK waters: A treatment perspective. **Water and Environment Journal**, v. 22, n. 3, p. 184–192, 2008.

INYANG, M.; DICKENSON, E. The potential role of biochar in the removal of organic and microbial contaminants from potable and reuse water: A review. **Chemosphere**, v. 134, p. 232–240, 1 set. 2015.

OLIVEIRA, F. R. et al. Environmental application of biochar: Current status and perspectives. **Bioresource Technology**, v. 246, p. 110–122, dez. 2017.

PAERL, H. W.; OTTEN, T. G. Harmful Cyanobacterial Blooms: Causes, Consequences, and Controls. **Microbial Ecology**, v. 65, n. 4, p. 995–1010, maio 2013.

WURTSBAUGH, W. A.; PAERL, H. W.; DODDS, W. K. Nutrients, eutrophication and harmful algal blooms along the freshwater to marine continuum. **Wiley Interdisciplinary Reviews: Water**, v. 6, n. 5, set. 2019.